ISSN 1810-648X
E-ISSN 2537-6365

GHITU INSTITUTE OF ELECTRONIC
ENGINEERING AND NANOTECHNOLOGIES

INSTITUTE OF APPLIED PHYSICS

STATE UNIVERSITY OF MOLDOVA

PHYSICAL SOCIETY OF MOLDOVA

Moldavian Journal of the Physical Sciences

Issue dedicated to the memory of academician Vsevolod Moskalenko
(1928 – 2018)

Chisinau
2018

Volume 17
No. 1-2

Scientific journal **Moldavian Journal of the Physical Sciences** includes original scientific articles, communications and reviews concerning various problems of modern physics. The journal is published in English, its periodicity is 4 numbers a year, with circulation of 200 copies.

web: http://sfm.asm.md/moldphys/

GUIDELINES FOR AUTHORS

The "Moldavian Journal of Physical Sciences" appears quarterly and publishes in English papers referring to original scientific research in physics and related fields, including applications in electronics and technology, material engineering and device physics. A review paper for every issue is planned and short communications with hot news are encouraged.

Papers must be prefaced by a brief abstract in English up to 100 words. Single space of the rows in the manuscript is required.

Authors are invited to send two printed copies of their papers, as well as an electronic record on a $3^{1/4}$ inches diskette, or by e-mail, in English. The articles will be edited by using WORD for Windows. Chapters must be numbered by using Arabic figures, as follows:

3. Experimental results.
3.1. Results analysis.
3.2. Methods of calculus.

Formulae must be written very clearly and easy-to-read. Do not use non-explained abbreviations. Illustrations and diagrams must be realized on computer drafts (on images). All graphic and text objects must be of very good quality and easy to read. Figures included in the text are preferable.

Reference citations will be presented as follows: author's forename initial and last name, journal name, volume, page number, year (in parentheses), for example: F.A. Moldovan, S.P. Russu, Phys. Rev. Let. 85, 357, (2000). Complete title, publisher, city and year will be written for book's author's name and forename initial, for example: M. Teodorescu, Cooperation in science and technology with Eastern and European countries, Editura Tehnica, Bucuresti, vol. 1, 1992. References into the text will be made within square brackets, for example [7]; reference citation numbers must be made successively, as they appear into the text.

Manuscripts of regular papers should be limited up to 10 pages and will be signed by authors; they also must be marked "Ready to print". Reviews are limited up to 20 pages. Maximum 4 pages are admitted for short communications. One full page of the journal (size A4) contains 54 rows with 95 characters/row; font size - 12. Page set up: top, left, right – 2,5; bottom – 3,5 cm. The very manuscript which is marked "Ready to print" will be published within 6 months from sending.

The submitted papers must be reviewed by two independent reviewers. The papers must contain original work and have not submitted for publication to any other journal. The papers which have been published previously, as well those accepted to be published in other reviews, will be not be admitted by Editorial Board; the authors have to mention this situation.

Proofs will be sent to authors for checking. Corrections must be restricted to errors since modifications to the text may be charged to the author. The publishers reserve the right to adapt the presentation of an article to conform to our style. After their publishing in our journal, the manuscripts and corresponding illustrations become the property of Editorial Board and will not be returned to the authors. The same for the papers, which have not been admitted for publication. The publishing in our journal is made free of charge.

The papers sent for publishing are considered not secret. The authors only are responsible for this in front of their own institutes or employers. Authors have to mention their complete address and telephone, fax number and e-mail.

Papers from around the world can be sent to be published to the following address:

Ghitu Institute of Electronic Engineering and Nanotechnologies, 3/3 Academy St., MD 2028 Chisinau, the Republic of Moldova, tel. (00 37322) 73-70-92; E-mail: ursaki@yahoo.com, E-mail of responsible secretary: sofiadonu@yahoo.com

PREFACE

The contribution of Vsevolod Moskalenko to developing the theory of high-temperature superconductivity and other fields of condensed matter physics, as well as his personal achievements, are summarized by Prof. M. E. Palistrant and dr. I. D. Chebotari. Different aspects of his life, research activities, creation of a scientific school, and other activities are described by his brother, academician Sveatoslav Moskalenko, head of the Laboratory of Theoretic Physics at the Institute of Applied Physics, Moldova, and dr. Sergiu Cojocaru from the Department of Theoretical Physics at the Horia Hulubei National Institute of Physics and Nuclear Engineering, Romania.

Our objective has been to pay our tribute to the memory of brilliant scientist Vsevolod Moskalenko by selecting papers from two categories of contributions:

— The first category contains some papers written in co-authorship with his brother, academician Sveatoslav Moskalenko during the last years of his life.

— Other contributions are relevant because they were written by researchers from the group which he headed at the Institute of Applied Physics in Moldova, by authors from the Joint Institute of Nuclear Research in Dubna, where he played an important role in establishing strong relations of collaboration with scientists from Moldova, being the plenipotentiary representative of the Government of the Republic of Moldova at this institute during the period of time between 1992 and 2005, and by authors from the Institute for Theoretical Physics of the National Academy of Sciences of Ukraine, which is named after academician Bogolyubov, the personality who played an important role in the scientific life of Vsevolod Moskalenko.

We have also included "In memoriam" of Professor Konstantin Gudima, Professor Piotr Khadzhi, and Doctor Igor Dobynda — members of the team of Vsevolod Moskalenko, who sadly passed away this year.

With this special issue of the Moldavian Journal of the Physical Sciences, we hope to honor the memory of academician Vsevolod Moskalenko who contributed a lot and was a firm believer in the success of this journal.

V. Ursaki,
Editor-in-Chief

IN MEMORIAM OF ACADEMICIAN VSEVOLOD MOSKALENKO

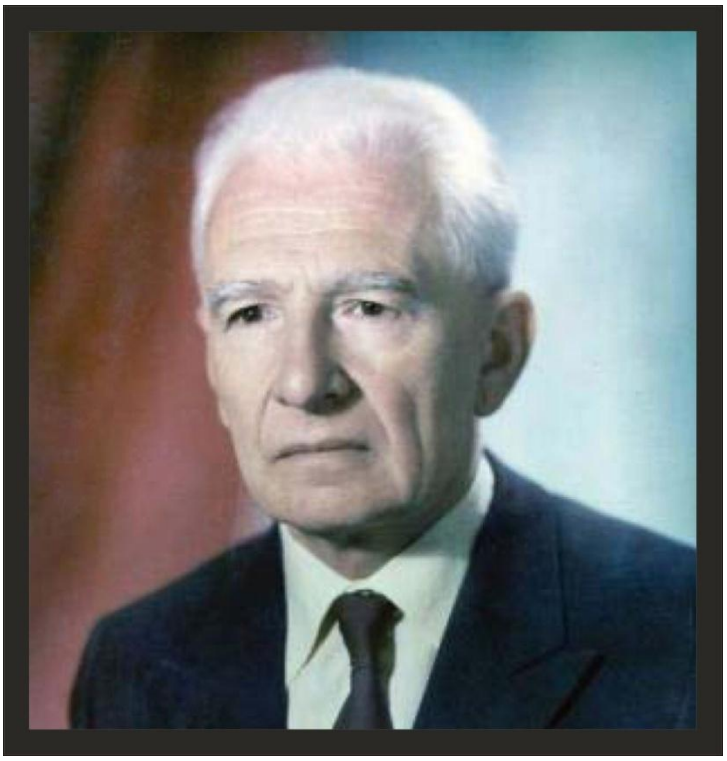

(September 26, 1928–April 2, 2018)

On the 2nd of April, 2018, the Moldovan and international scientific community lost an outstanding member of highest value and a person of great integrity—academician Vsevolod Moskalenko. For those who knew him, he will remain an example to look up to in many respects, while his scientific and public legacy accumulating over 60 years of dedicated work will remain a source of inspiration and a model to follow for many generations of physicists to come. Being one of the founders of the school of theoretical and mathematical physics in Moldova, Vsevolod Moskalenko was a teacher, a colleague, a leader, and a friend to many of us. Science was the passion of his entire life also because the uncompromising search for truth and beauty was one of the defining features of his personality. He was never concerned with looking for easy paths or ways to achieve a guaranteed success; on the contrary, he was always attracted by the hardest problems and was never discouraged by difficulties. It was his talent, solid education, will power, and hard work that every time drove him through the apparently unsurmountable complexity to reveal, in the end, the beauty hidden behind a scientific puzzle. For me, as a fresh applicant for postgraduate studentship about 35 years ago, the encounter with his style of work was an unforgettable experience right from the beginning. In the introductory discussion, he briefly told that, together with his team, they were studying a completely new type of disorder in magnetic systems, referred to as spin glasses, which can not be explained in terms of standard quantum statistics. I was told that there is no overall magnetization, but still the state seems to have some hidden long-range order in it, and that some researchers—Edwards and Anderson—proposed a "replica trick" that could allow grappling with this puzzle. Until I could get hold of any details in

this “before the Google” era and after many “from scratch” attempts to derive what this “trick” might be about, my curiosity was fully ignited. The years that followed were a journey full of hard work and new paradoxes in this fascinating field, during which Vsevolod Moskalenko led us by his own example and enthusiasm. He developed an original and rigorous field theoretic method for understanding the phenomena taking place in this fundamental state, which later found numerous interesting and unexpected applications. For instance, starting from the Hopfield model of the neural cell, it turned out to be important for understanding the mechanisms of associative memory and properties of neural networks, which later evolved into a distinct research field. It is yet another example of how the value of a deep mind can be appreciated even more with the passage of time.

Twin brothers Vsevolod and Sveatoslav Moskalenko were born on the 26th of September, 1928 in the village of Bravicea of the Orhei county of Romania (at present, the Republic of Moldova). The village is about 70 km away from Chisinau; by that time, it had a population of a few thousands and a primary school where the brothers studied in 1935–1939. Then, they studied in “B.P. Hasdeu” high school and later in “A. Russo” high school in Chisinau until 1944, when the school was evacuated to Craiova, where they continued their studies at “Carol I” National College (1944–1945). After World War II, they came back to Orhei, where they finished a secondary school with excellence in 1946. In summer of the same year, their fascination with natural sciences brought them to Chisinau State University and they became students of the Faculty of Physical and Mathematical Sciences. However, in that period, the joy of studies came with tremendous hardships for their family: they had already lost their father who was arrested in 1940 and died in the dungeons of NKVD in 1941; after the war, they suffered from poor living conditions and severe illnesses that posed a real threat to their physical existence. Still, the strength and independence of their character crystallized from the turmoil of this dramatic life experience.

After graduating from the Chisinau State University with excellency in 1951, Vsevolod Moskalenko worked at the university, first as an assistant and later as a lecturer; he taught regular and special courses in Theoretical Physics for the next 10 years (1951–1960). During this period, he continued the studies as a trainee and then as a postgraduate student (1957–1959) of famous academician N.N. Bogolubov and professor S.V. Tyablikov at Moscow State university and at Steklov Institute of Mathematics of the USSR Academy of Sciences. It was the time when the puzzle of superconductivity was being unraveled by the joint effort of the elite theorists including the scientific supervisors of the young postgraduate student. In 1958, shortly after the Nobel winning BCS theory of superconductivity and the insightful formulation by N.N. Bogolubov were published, Vsevolod Moskalenko submited his milestone work, in which, unlike the BCS, superconducting charge carriers belong to different energy bands, for publication. A year later, a similar work was submitted to Physical Review Letters by Suhl, Matthias, and Walker, and the two papers were published in 1959. In the same year, Vsevolod Moskalenko defended his candidate's dissertation at Steklov institute. The elegant theory of multiple-band superconductivity proposed by him was later developed by him together with several generations of his students and colleagues in Chisinau. In some important aspects, this theory predicted a behavior even qualitatively different from BCS (e.g., sensitivity to nonmagnetic impurities). Quite recently, after the discovery of novel materials, the theory has received a brilliant experimental confirmation; at present, it plays a key role in the upsurge of research on some priority topics, such as unconventional and high-Tc superconductors.

In 1961, Vsevolod Moskalenko became Head of the Department of Theoretical Physics of the newly-formed Institute of Physics and Mathematics of the Moldovan Academy of Sciences.

Being a member of the "Bogolyubov's school," Vsevolod Moskalenko built up what will later become a "school" of his name in Chisinau and thus established a strong relationship between the two schools. Their scientific collaboration continued actually until the last years of academician N.N. Bogolubov, when their common work on the existence of superconductivity in the Hubbard model was published in the Theoretical and Mathematical Physics journal (1991). In 1964–1966, Vsevolod Moskalenko carried out post-doctoral studies under supervision of N.N. Bogolubov at Moscow State University and then defended his doctoral dissertation in physics and mathematics at Steklov institute in 1967. These close contacts contributed to the broadening of collaboration in both scientific and organizational areas. With the natural growth of the Academy, the Department changed its name for the Department of Statistical Physics of Institute of Applied Physics. Moldova received support for training of young researchers in new areas, such as Elementary Particles Physics and Nuclear Physics, in connection with ongoing research at Joint Institute for Nuclear Research in Dubna (JINR, Russia). Numerous visits and direct collaborations with many renowned scientists, among which D.N. Zubarev, Y.A. Tserkovnikov, N.M. Plakida, E.E. Tareeva, and V.M. Loktev, and participation at conferences and seminars provided an invaluable boost to the development of theoretical physics in Moldova. Vsevolod Moskalenko became a member of the USSR Academy of Sciences Scientific Councils on Solid State Theory and Low Temperature Physics. In 1970 Vsevolod Moskalenko was elected corresponding-member of the Moldovan Academy of Sciences; in 1976, he became full member; in 1971 he received the title of Professor in Physics and Mathematics. In 1972 the bureau of the Mathematical Section of the USSR Academy of Sciences chaired by academician N.N. Bogolubov had a session in Chisinau in recognition of the achievements of Moldovan colleagues. Vsevolod Moskalenko used the authority he earned to promote international collaboration with important international scientific centers, such as JINR (Russia), National Institute of Physics and Nuclear Engineering (Romania), Duisburg University (Germany), North-Eastern University of China, International Center for Theoretical Physics in Trieste, and the University of Salerno (Italy). For over a decade (1990–2004) academician Vsevolod Moskalenko was the Plenipotentiary representative of the Republic of Moldova and a member of the Scientific Council of the JINR. In appreciation of his long-time contribution, he received the title of "Doctor Honoris Causa" of the Joint Institute for Nuclear Research (Russia, 2009).

His educational activity spread from the organization of regular scientific seminars at Institute of Applied Physics till direct involvement, at the school level, as Chairman of the Scientific Society of Schoolchildren "Viitorul." I have this experience of my own and remember well what an important role was played by the stimulating atmosphere created in those times for the upbringing of young researchers. It was at one of these seminars in the 1980s when we learned about the recent discovery of high-temperature superconductors. The exceptional importance of this discovery was immediately clear then. Still, up till present days, the problem of the mechanism of high-Tc phenomenon remains one of the central topics in physics, multiple-band superconductivity being one of the lines of thought. Nevertheless, Vsevolod Moskalenko initiated the exploration of the completely new paradigm requiring a deep revision of the basics of the standard condensed matter theory: strongly correlated electronic states and inapplicability of the single-particle picture of excitations and the concept of Fermi liquid. This courageous decision was motivated by the necessity to understand the anomalous properties of the new materials in their normal phase first. He developed an original and rigorous field-theoretic diagram perturbation method, which allowed him to implement this paradigm and study many aspects of these systems, such as magnetic and charge ordering, Mott–Hubbard metal–insulator transition, interaction with phonons, and some features of the superconducting transition.

Vsevolod Moskalenko was a scientific adviser for 20 doctoral and 5 doctor habilitation theses; he published over 200 scientific papers and 6 monographs in various domains of the Quantum Theory of Solids to which his major scientific achievements belong: theory of polaron, bipolaron; theory of low temperature superconductors with energy bands overlapping on the Fermi surface and superconducting alloys; coexistence of superconductivity CDW, SDW, and spin glass phases; methods of quantum Green's functions; theory of spin and quadrupole glasses; theory of high-Tc superconductivity and strongly correlated electron systems based on the new diagram technique with application to one- and three-band Hubbard Model, Periodic Anderson Model and Hubbard–Holstein electron–phonon systems; using this theory, he showed a possibility of a new mechanism of superconducting pairing for strong electron–phonon coupling due to exchange of phonon clouds between polarons. His lifelong merits were praised by highest national distinctions, such as the State Prize for Science and Technology of the SSRM (1981), Order of Honour and „Dimitrie Cantemir" Medal, Order of the Republic (1996), and honorary title "Om Emerit" ("Emeritus Person") of the Republic of Moldova.

Despite poor health and immense complexity of the scientific task, he continued to work on his new theory till the last days giving us an ultimate example of the victory of spirit over flesh. Academician Vsevolod Moskalenko, through his works and through his spiritual example, will remain part of the national heritage for the generations to come.

Dr. Sergiu Cojocaru,
Department of Theoretical Physics,
Horia Hulubei National Institute of Physics and Nuclear Engineering,
Romania

LEADER IN THEORETICAL AND MATHEMATICAL PHYSICS DEVELOPED IN THE REPUBLIC OF MOLDOVA

Together with my brother, Vsevolod Moskalenko, we graduated from the faculty of physics and mathematics of the Kishinev State University (KSU) in 1951. As one of the most eminent graduate students, Vsevolod Moskalenko was kept at the university to continue his improvement and work as an assistant in the field of theoretical physics, teaching the students and performing the practical courses. We studied the theoretical physics under the guidance of Professor Vladimir Malyarov, who arrived each week from Odessa by a biplane and delivered his lectures on quantum mechanics in a brilliant form in 1950.

However, we have written our diploma theses under the guidance of Professor Yurii Perlin, who began to work in KSU in the 1950/1951 academic year. We were the first diploma students; our theses were related to the theory of polarons in semiconductors. The polaron problem was an important topic in theoretical physics in that period of time as an example of an interaction of the electron with the quantum field. In that period of time, the papers by Bogoliubov and Tyablikov, by Landau and Pekar, by Feynman, Toyozawa, and other appeared. They attracted our attention; together with our colleagues Evghenii Pokatilov, who graduated from KSU in 1950, and Victor Kovarskii, who graduated from KSU in 1952, we have organized a seminar to discuss these papers.

The first results obtained by Vsevolod Moskalenko in the theory of polarons published in the fiftieth years were mentioned by H. Haken in his review article dedicated to the theory of polarons published abroad and rewritten in the Soviet Union. A decisive role in the scientific life of Vsevolod Moskalenko was played by the influence of the scientific school created by the outstanding theoretical physicist and mathematician N.N. Bogoliubov at M.V. Lomonosov Moscow State University (MSU) and V.A. Steklov Mathematical Institute of the Academy of Sciences of the USSR. A happy event in the Vsevolod Moskalenko's life happened in 1958–1959, when he was sent as a young promising researcher for two years to MSU to improve his qualification and perform his candidatus scientiarum thesis. It was an extraordinary period of time for theoretical physics, because one year earlier, in 1957, J. Bardeen, L.N. Cooper, and J.R. Schrieffer (BCS) formulated their microscopical theory of superconductivity. It was based on the idea of the Bose–Einstein Condensation (BEC) of Cooper pairs of electrons forming the bound, composed quasi-boson particles due to the electron–phonon interactions. Almost immediately, the BCS theory was reformulated by N.N. Bogoliubov using the coherent unitary transformation of the Hamiltonian in a similar way with his microscopical theory of superfluidity elaborated 10 years earlier in 1947. The difference consists in the use of the Bose operator description in the case of superfluidity and the Fermi operators in the case of superconductivity.

At the same time, N.N. Bogoliubov underlined the necessity to generalize the BCS theory taking into account the energy band structure of the real superconductors with many overlapping energy bands. This problem was solved by young researcher Vsevolod Moskalenko; in October of the same 1958 year, his paper was submitted to press. To better understand this unusual period in the development of physics, one can remember that, in the same 1958 year, in Moscow scientific school of academician L.D. Landau, young theoretical physicist A.A. Abrikosov elaborated his theory of vortices in superconductors, which were later referred to as Abrikosov filaments.

In the same period of time in Kiev the possibility to achieve the BEC of excitons and their superfluidity was suggested. This possibility was implemented experimentally much later.

Returning from Moscow to Kishinev, Vsevolod Moskalenko brought with him the best traditions of the academician N.N. Bogoliubov's scientific school, such as the high scientific level, high requirements to himself, and democracy in the personal contact with the colleagues, collaborators and doctorands. I remember that all of us taking parts in his seminars in the 1960s years began to study the methods of the quantum field theory in applications to the quantum statistics and to the condensed matter physics. These methods form the foundation of theoretical and mathematical physics; they are based on the perturbation theory, where the kinetic energy of the particles is supposed to be much greater than their interaction energy. All his scientific life Vsevolod Moskalenko worked in the first flight of the theoretical physics in Moldova and concentrated his efforts on the solution of many principal problems, such as the theory of superconductivity, the theory of spin glasses, and the theory of strongly correlated electron systems. He realized that, in the last case, the usual methods of theoretical physics cannot describe the new phenomena discovered in nature. And these efforts were consequently prolonged till the last years of his life. Just his interest in new and principal aspects of theoretical physics is reflected in our common study of the Chern–Simons theory and in its application to describe the interaction of a two-dimensional electron–hole system with quantum point vortices. Our paper will be published in the present issue.

Professor Vsevolod Moskalenko was elected a corresponding member of the Academy of Sciences of Moldova in 1970 and a full member in 1976. He was the founder of a Scientific School in the Theoretical and Mathematical Physics, in the frame of which, under his guidance, 20 candidatus scientiarum theses and 5 doctor habilitat theses were defended. More so, an independent daughter school was created under the guidance of Professor Maria Palistrant as a ramification of the main trunk of theoretical physics being dedicated to the multiband theory of superconductivity and related problems. In the frame of this school, 7 doctor of science theses were defended and 2 theses are under preparation.

Acad. Sveatoslav Moskalenko

ON SOME ACHIEVEMENTS OF MOLDOVAN PHYSICS AND PRIORITIES IN THE FORMATION OF MODERN DIRECTIONS OF THE CONDENSED MATTER THEORY

M. E. Palistrant and I. D. Cebotari

Institute of Applied Physics, Academiei str. 5,
Chisinau, MD-2028 Republic of Moldova

E-mail: chebotar.irina@gmail.com

(Received October 4, 2018)

Abstract

The work is dedicated to the activities of academician V.A. Moskalenko, a prominent Moldovan scientist. The main directions and some important results of his scientific activities are considered. The priority of V.A. Moskalenko in the construction of the two-band superconductivity model and in the development of a multiband theory of superconductivity, as well as his significant contribution to the solution of modern problems of condensed matter physics, is shown.

1. Introduction

Moldavan physical science has suffered a heavy loss: an outstanding world-class scientist, professor, academician Vsevolod Anatolyevich Moskalenko passed away in his ninetieth year. Today it is difficult to imagine the life of the scientists of the physical community of Moldova without ever bright and profound scientific works and speeches of this incredibly hardworking and purposeful scientist. We, the physicists of the Republic of Moldova, are deeply grieved and proud of our compatriot who managed to overcome incredible difficulties and prove a priority over world science in the development of a number of scientific directions of theoretical physics in Moldova, thereby upholding the importance of the Moldovan state and people.

In our opinion, it is of interest to briefly describe the formation of the personality of V.A. Moskalenko and the manifestation of the great efforts to achieve the set goals. We will tell about the difficulties of life in his youth, about the incredible courage and purposefulness at the beginning of his scientific activity and the achievements of this period, which still influence the development of research in certain areas of physics.

Of interest is the choice of the scientific direction after the discovery of the mechanism of superconductivity, which had remained a mystery for almost 50 years. The desire for cognition of the unknown and interesting, which was inherent in V.A. Moskalenko, here has played a role and moreover, leads researchers to the disclosure of the picture of the real world. The correctness of V.A. Moskalenko's approach in science led to the need for a detailed study of the presence of overlapping energy bands in superconducting systems and other features of the energy spectrum. As a result, a new and significant direction in the development of theoretical physics has sprung up and covered many countries of the world.

Let us show the role of ideas of V.A. Moskalenko and his disciples in the construction of the theory of high-temperature superconductivity, the essence of which cannot be understood

without taking into account the features of the energy spectrum, among which the idea of the existence of several overlapping electron and hole bands on the Fermi surface is on the first place. The theory developed by V. A. Moskalenko and his coworkers has become classical; to date, the priority of this theory in condensed matter physics has been proved. The priorities of the theory developed by Moldovan physicists in other fields of condensed matter physics are demonstrated, in particular, in the development of diagrammatic methods in the investigation of the role of electronic correlations in determining the properties of condensed matter. The universality of the activities of V.A. Moskalenko is briefly described in other current areas of development of theoretical physics as well.

2. Development of the Theory of Superconductivity on the Basis of a Two-Band Model

The first of the authors of this paper, almost all her working life from the student years, took part in numerous scientific researches and studies, being a coauthor of a number of research works written by V.A. Moskalenko, as well as the continuer of the development of the multiband theory of superconductivity. We will begin our description from those distant times when Moldova took the path of enlightenment and scientific research in a number of areas. These were difficult postwar years

In 1946, the Kishinev State University (now Moldova State University) was founded; it included several faculties for the study of natural sciences, particularly the Faculty of Physics and Mathematics, which did not have numerous students enrolled. However, among the students, there were quite capable and motivated young people, determined to learn and achieve high results. Several high-qualified specialists were invited, who established the educational process and, to some extent, the scientific research. In the process of studying, much attention was paid to self-reliant studies by studying the existing scientific problems using scientific literature. We will talk about theoretical physics. Along with the young employees, highly skilled specialists who arrived from other cities—Kiev, Leningrad, Odessa, etc.—also joined the work team. Thus, a base for the development of scientific research in theoretical physics was created.

Over time, V.A. Moskalenko became one of the leaders in the development of the theoretical physics in Moldova and headed the Department of Theoretical Physics of the Institute of Applied Physics of the Academy of Sciences of Moldova. At the beginning of his scientific career, his interests were related to the development of the theory of polarons and the optical properties of semiconductors. Despite the remoteness from the scientific centers, his works were relevant and significant.

Once, in one of the prestigious physics journals V.A. Moskalenko opened the work of academician N.N. Bogolyubov, studied it, and decided to go to Moscow to personally get to know Bogolyubov and his disciples. At that time, it was not easy. A determined character and purposefulness allowed V.A. Moskalenko to be in Moscow on an internship in a team of employees of world-famous academician (physicist and mathematician) N.N. Bogolyubov.

Scientific ties with outstanding physicists and professors, namely, S.V. Tyablikov, D.N. Zubarev, and other disciples of the school of academician N.N. Bogolyubov were quite close and maintained particularly with the disciples of V.A. Moskalenko.

Note that, in the late 1950s, the physical science was developed very rapidly. It is a question of a phenomenon of superconductivity. This phenomenon was discovered by Camerlene Ones in 1911 quite randomly when studying the properties of mercury at low temperatures. It was found that, as the temperature is lowered to the critical point ($T = T_c$), the resistance disappears and the motion of electrons in the crystal does not experience any obstacles. For

almost 50 years, scientists have been looking for a way to determine the mechanism of the origin of this phenomenon. There have been a lot of different studies, both theoretical and experimental. Finally, in 1957, the result was obtained; it was presented in the works of Bardeen, Cooper, and Schrieffer [1]. It was found that the mechanism of superconductivity is attributed to the formation of bound pairs of electrons with opposite impulses and spins due to the indirect attraction of electrons through the crystal lattice. This was a huge discovery, which generated many additional problems. It was impossible to stay away from this discovery and the problems associated with it. Vsevolod Anatol'evich Moskalenko, along with his previous domain of research (candidate's dissertation was almost ready), decided to go headlong into research of superconductivity.

Note that the theory of superconductivity constructed in 1957 was based on an ideal, isotropic model. The first works, which took into account the real properties of metals, belong to V.A. Moskalenko [2] and Suhl H., Matitias B.T. and Walker L.R. [3]. As follows from the references in these papers, the articles of Moskalenko came to the editorial office of the Fizika metallov i metallovedenie (Physics of Metals and Metallography) journal a year earlier than the works of the authors of [3] and were published several months earlier. In addition, paper [3] contains a model and a study of the behavior of the superconducting transition temperature, while papers [2] contain, along with the results of [3], a study of the behavior and other thermodynamic characteristics, in particular, heat capacity jump at the point $T = T_c$. These circumstances make it possible to consider that the priority in the creation of a two-band model and the application of the model belongs to V.A. Moskalenko.

Vsevolod Anatol'evich Moskalenko, on his return from Moscow to Chisinau, organized intensive research in the Department of Statistical Physics on the basis of proposed model for superconductors with overlapping energy bands. At first, the studies were carried out in the diagonal approximation in the indices of the bands. The model is as follows: the formation of Cooper pairs of electrons within one energy band and the transition of the pair as a whole to another band, which provides the appearance of intraband V_{nn} and the interband V_{mn} electron interactions, which lead to an additional attraction of electrons, which favors an increase in the superconducting transition temperature. There are two order parameters Δ_1 and Δ_2 in the two-band model.

The studies of the properties of two-band (multiband superconductors) carried out in Moldova attracted the attention of scientists from different countries, and a new tendency has formed in low-temperature physics: study of the properties of superconductors with an anisotropic energy spectrum. Along with the development of the theory, studies of materials exhibiting the properties inherent in multiband systems were conducted. The leading theoretical research in this new direction was the work carried out in Moldova under the leadership of V.A. Moskalenko.

It is of interest to note that the properties of superconductors with overlapping energy bands were found to be significantly different from the properties of single-band ones not only in terms of quantity, but also in terms of quality. For example, in two-band superconductors, high superconducting transition temperatures are possible not only in the attractive interaction between electrons, but also in the case of repulsion, depending on the relationship between the interaction constants of the electrons. In an impurity two-band superconductor, the Anderson theorem is not satisfied for $\Delta_1 \neq \Delta_2$ and the thermodynamic properties depend on the impurity concentration.

Using the two-band model and acceptable values of the coupling constants, one can obtain a high T_c, two energy gaps of $2\Delta_1 / T_c > 3.5$ and $2\Delta_1 / T_c < 3.5$, a positive curvature of the upper critical field near the superconducting transition temperature, etc. In the two-band model, it is possible to decrease T_c with increasing the disorder. Later, we considered more complicated

two-band and multiband models for the case of the phonon and nonphonon mechanism of superconductivity. Numerous new results and the history of the development of the theory of superconductivity of multiband superconductors are given, in particular, in [4, 5].

In 1986, another grand event occurred—the discovery of high-temperature superconductivity (HTSC) in oxide ceramics (T_c ~ 100 K). These compounds have a layered structure and have a rich set of physical properties. The following phase transitions are observed: magnetic, superconducting, and mixed states. The discovery of high-temperature superconductivity favorably affected the further development of the theory of multiband superconductors. A large number of results leading to qualitatively new relations between physical quantities and quite a good agreement between theory and experiment have been obtained. Analysis of the obtained results made it possible to publish a review article in the Journal of Advances in Physical Sciences (1991) [6]. According to a number of researchers, this paper contains the classical results of the theory of two-band superconductivity.

The great interest of researchers was caused by the discovery of the high-temperature intermetallic compound MgB_2 ($T_c \approx 40$ K). It seemed that all physicists involved in superconductivity switched to the studying the properties of this compound. It was found that, using the two-band model, one can describe all the observed anomalies of the physical characteristics of this substance. Physics journals were filled with papers in which the two-band theory of superconductivity was developed. We were amazed by the fact that our works of ten to twenty years ago were published as new and apparently as belonging to the new authors. Very often, no references to our research were cited. This attitude was the result of the collapse of the Soviet Union following a noticeable neglect for Soviet journals of physics and our scientific achievements. Within several years, we have achieved justice. It should be noted that a number of scientists from different countries of the world assisted V.A. Moskalenko in solving the problem of recognition of priority in the two-zone model (models in the theory of superconductivity) [7].

Finally, let us dwell on the last stage of the discovery of new superconductors. Since 2008, many papers presenting a new class of high-temperature superconducting compounds based on FeAs with the temperature of the superconducting transition of $T_c \approx 55$ K have been published. The Fermi surface intersects five bands arising from the *d*-states of Fe. An important role in these systems is played by the possibility of the emergence of a spin density wave state and a commensurate–incommensurate phase transition and the appearance of superconductivity.

In accordance with the statements of a number of scientists and the availability of published theoretical works, the properties of these high-temperature compounds should be described using the multiband theory of superconductivity. Research should be based on the theory of multiband superconductors described in our work [6], which represents the classical theory (M.V. Sadovsky, Usp. Fiz. Nauk 178, 1243 (2008)).

We can conclude that, in the Department of Statistical Physics of the Institute of Applied Physics of the Academy of Sciences of Moldova, as a result of research, a theory of the thermodynamic and electromagnetic properties of multiband superconductors has been developed; it's used to describe a large number of modern anisotropic systems.

The priority of the V. A. Moskalenko's multiband superconductivity model on a global scale, as well as the relevance of the theory as applied to modern multiband (real) superconductors, has been proved.

The two-band superconductor model was proposed long before the discovery of high-temperature superconductivity; research based on it was carried out by V. A. Moskalenko with employees and many scientists from other countries. After the experimental confirmation of the significant effect of the features of the densities of electronic states on the properties of

superconducting systems, the studies were substantially strengthened in view of the periodic discovery of new high-temperature compounds.

3. Study of Strongly Correlated Systems: Diagram Approach

An attempt to solve the problems that have arisen in the physics of superconductivity has broadened the scope of V.A. Moskalenko's scientific interests to the important domain of modern condensed matter physics, namely, the so-called physics of strongly correlated systems (SCS).

The fact is that transition metals, in compounds of which HTSC takes place (for example, copper oxide ceramics), comprise unfilled internal *d*- or *f*-shells. Coulomb repulsion of the electrons of these shells is strong (comparable to or exceeds the bandwidth). It was assumed that the strong Coulomb interaction of electrons can cause superconducting pairing. In addition, it could be assumed that, in HTSC, an important role is played by the interaction of electrons with lattice vibrations. Therefore, to study the HTSC phenomenon, it was necessary (a) to construct a theory that would take into account the energy of the strong Coulomb interaction and (b) to study the combined effect of strong electron interaction with one another and with phonons to elucidate the role of electron–phonon interactions.

By the time of discovery of HTSC, models taking into account strong correlations and features of the behavior of electrons in these systems had already been formulated. However, there was a need to reveal whether a superconducting phase exists in the systems described by these models. To this end, it was necessary to develop an alternative approach of quantum-statistical analysis of these systems, which would be self-consistent. This was due, in particular, to the fact that sometimes the use of various approximations and mathematical concepts that existed at that time led to some contradictory results obtained by different authors (for discussion, see, for example, [10]).

Therefore, V. A. Moskalenko considered that one of the primary tasks is the construction and development of methods for analyzing and calculating these systems. As noted by V.A. Moskalenko, the basis of these methods is the diagram technique and the Wick's theorem for statistical averages of T-products of operators [11].

Vsevolod Anatol'evich Moskalenko proposed the generalized Wick's theorem for strongly correlated electrons using the example of the one-band Hubbard model [11, 12]. According to this theorem, the averages of the T-product of electron operators in the interaction representation with the Hamiltonian H_0 can be represented as a sum that contains, in addition to the pair normal one-site products of operators corresponding to the usual Wick's theorem, irreducible one-site many-particle structures (Kubo cumulants).

On the basis of the generalized Wick's theorem for strongly correlated electrons along with other mathematical concepts, V. A. Moskalenko and co-workers constructed diagram techniques for the main models of strongly correlated systems, namely, the Hubbard and Anderson models (and their generalized versions). The developed diagram technique for strongly correlated electrons was also generalized for strongly correlated electron systems with strong interaction with phonons.

Let us list some of the results that this approach allowed us to obtain when studying the role of strong correlations in high-temperature superconductivity, the Mott metal–insulator transition, and other important issues of modern condensed matter physics.

First of all, this technique allowed us to investigate the possibility of the superconducting state in the systems described by the main SCS models. With it, systems of equations that

determine the superconducting state of the systems within these models were obtained, and the role of the strong Coulomb interaction in superconducting pairing was revealed. For some special cases in these models, equations that determine the temperature of the superconducting transition were obtained. Diagrammatic analysis of the Hubbard–Holstein, which takes into account, in addition to the strong interaction of electrons with each other, also the strongly electron-phonon interaction, allowed us to propose a new mechanism of superconductivity, which is based on the assumption of pairing of polarons by exchanging of phonon clouds [13]. On the basis of the developed diagram technique, V. A. Moskalenko also studied the thermodynamic properties of the systems described by the Anderson and Hubbard models [14–17]. For both models, the property of stationarity of the thermodynamic potential with respect to variations of the correlation function of the system was established. Interesting results were also obtained when considering the competing phases, such as the states of the spin-density wave of antiferromagnetism and superconductivity (due to correlations) [18] and many others.

The developed diagram technique for strongly correlated electron systems is an important result, first, from a technical point of view, since it allows us to construct a thermodynamic perturbation theory for the Green functions and correlation functions that contain important information about the macroscopic properties of the system. Second, being developed in order to clarify the properties of SCS, it has allowed V. A. Moskalenko and his colleagues to obtain important and interesting physical results in the study of SCS.

We note, in particular, as an example, the directions of theoretical research in the Academy of Sciences of Moldova.

(1) The theory of the thermodynamic and kinetic properties of two-band superconductors with variable density of charge carriers.
(2) Development of the theory of the thermodynamic properties of superconducting systems based on the Moskalenko's two-band model by means of generalizations, in particular, allowing to take into account all types of electron–phonon interactions, both intraband and inter-band, particularly between electrons of different zones, which also make it possible to describe the properties of two-layer systems with different layers and more complex modern structures.
(3) Development of the theory of superconductivity of liquefied systems (with small values of charge carrier density) in the Schafroth–Bose condensate scenario of local pairs.
(4) Development of diagram techniques for the study of strongly correlated systems using the model Hamiltonians of these systems
(5) Study of the role of strong correlation in high-temperature superconductivity and Mott metal–insulator transition, the thermodynamic and kinetic properties of the systems described by these models in the normal and superconducting phases.

4. Conclusions

In conclusion, we would like to note the constant striving of V.A. Moskalenko to increase the level of knowledge both of his own and of his disciples. To accomplish this goal, he made a lot of effort, which could not but affect the results in the issue of training of his scientific staff. In the Department of Statistical physics, about 30 candidatus scientiarum and habilitat theses were defended; in the Moskalenko's School, 5 doctor habilitat theses were defended.

It is necessary to mention the long-term activities of V.A. Moskalenko and his colleges aimed at the organization of the Department of Field Theory and Nuclear Matter at the Institute

of Applied Physics. We believed that it was necessary to have the most advanced scientific directions in the development of theoretical physics at the Institute of Applied Physics. Vsevolod Anatol'evich Moskalenko had to make a lot of effort and overcome many difficulties to solve this problem. Thanks to the persistence of V.A. and his assistants, this department was organized. This event promoted the Academy of Sciences to become a member of the large family of the countries belonging to JINR. The opportunity to be on the first line of research on various topics was opened.

Vsevolod Anatol'evich Moskalenko will remain forever in the memory of people who knew him, respected and loved him deeply. His research and the obtained results will be regarded as the foundations of the development of a stronghold of new ideas necessary for understanding the state of matter and practical applications.

Vsevolod Anatol'evich Moskalenko was not only a high-level scientist, but also a remarkable person. He will always be remembered as a very decent and delicate person with a gentle nature with people and, at the same time, firm in his convictions. We will always remember his kind laugh and smile. Being a talented and enthusiastic person, all his life he was doing what he loved, while remaining devoted to science. We lost a rare person, one of the titans of science, with whom the development of Moldavian theoretical physics began. He left behind a rich scientific heritage and a bright memory.

References

[1] J. Barden, L.N. Cooper, and L.R. Schrieffer, Phys. Rev. 106, 162 (1957); Phys. Rev. 108, 1175 (1957).
[2] V.A. Moskalenko, Fiz. Met. Metalloved. 8, 503 (1959); Phys. Met. Metalogr. 8, 25, (1959).
[3] H. Suhl, B.T. Matthias, and L.R. Walker, Phys. Rev. Lett. 3, 552 (1959).
[4] M.E. Palistrant, Condens. Matter Phys. 12, 677 (2009); arXiv: cond-mat/0309707 (2003).
[5] M.E. Palistrant and L.Z. Kon, Ukr. J. Phys. 55, 44 (2010).
[6] V.A. Moskalenko, M.E. Palistrant, and V.M. Vakalyuk, Usp. Fiz. Nauk. 161, 155 (1991); Phys. Usp. 34, 717 (1991).
[7] M.E. Palistrant, J. Supercond. Nov. Magn. 23, 1441 (2010).
[8] M.E. Palistrant and V.A. Ursu, Zh. Eksp. Teor. Fiz. 131, 59, (2007); J. Exp. Theor. Phys. 104, 51 (2007).
[9] M.E. Palistrant, I.D. Cebotari, and V.A. Ursu, Zh. Eksp. Teor. Fiz. 136, 272 (2009); J. Exp. Theor. Phys. 109, 227 (2009).
[10] N.N. Bogolyubov and V.A. Moskalenko, Teor. Mat. Fiz. 86, 16 (1991); Theor. Math. Phys. 86, 10, (1990).
[11] V.A. Moskalenko, Voprosy kvantovoy teorii kondensirovannykh sred [in Russian], Kishinev, Stiinta, 122 (1990) .
[12] V.A. Moskalenko and M.I. Vladimir, Teor. Mat. Fiz. 82, 428 (1990); Theor. Math. Phys. 82, 301 (1990).
[13] V.A. Moskalenko, P. Entel, M. Marinaro, and D.F. Digor, Zh. Eksp. Teor. Fiz. 124, 700 (2003).
[14] V.A. Moskalenko, P. Entel, L.A. Dohotaru, and R. Citro, Teor. Mat. Fiz 159, 162 (2009); Theor. Math. Phys. 159, 551 (2009).
[15] V.A. Moskalenko, L.A. Dohotaru, and R. Citro, Teor. Mat. Fiz. 162, 439 (2010); Theor. Math. Phys., 162, 366 (2010).

[16] V.A. Moskalenko, L.A. Dohotaru, and I.D. Cebotari, Zh. Eksp. Teor. Fiz. 138, 107 (2010); J. Exp. Theor. Phys. 111, 97 (2010).
[17] V.A. Moskalenko, L.A. Dohotaru, D.F. Digor, and I.D. Cebotari, Low Temp. Phys. 38, 1167 (2012).
[18] V.A. Moskalenko, P. Entel, D.F. Digor, and L.A. Dohotaru, Phase Transitions 78, 277 (2005).

IN MEMORIAM OF PROFESSOR PIOTR KHADZHI

(April 3, 1939 – August 3, 2018)

Professor of theoretical and mathematical physics, doctor habilitat in physics and mathematics, Piotr Ivanovich Khadzhi has been a permanent principal scientific collaborator for many years. In the last years, he was a consultant of the Institute of Applied Physics, in laboratory of theoretical physics; he was the founder of the scientific school in this field with vast multilateral applications, in the frame of which, under his guidance, 19 theses of doctor of sciences were defended. The list of disciples is attached below.

Professor Piotr Ivanovich Khadzhi was born in the Cairaclia village of the Taraclia district of the Republic of Moldova on April 3, 1939 and deceased unexpectedly on August 3, 2018 on the 80th year of his life. He was a son of a peasant, and the working peasantry was the medium from which he inherited, in his childhood, the habit and skill to work hard. He graduated from the Kishinev State University and had postuniversity studies at the Institute of Applied Physics of the Academy of Sciences of Moldova. He became a doctor of sciences in 1968 year and defended his doctor habilitat thesis in 1983 at Bogoliubov Institute of Theoretical Physics in Kiev at the Scientific Council headed by academician A.S. Davydov. Due to his multiple and outstanding achievements, Prof. P.I. Khadzhi became the leader of the researchers in the field of coherent nonlinear phenomena. The research areas include the coherent nonlinear optics of semiconductors involving high-density excitons and biexcitons, the propagation of electromagnetic waves in couplers and wave guides as well as of the matter waves in Bose–Einstein condensed atomic and molecular systems including the ultracold chemistry.

Professor P.I. Khadzhi was characterized by a capacity to work hard and the insatiable

interest in science. Unlike other colleagues in our laboratory of theoretical physics, he had a special interest in some fields of mathematics, such as special functions and integral calculations. For example, he introduced two new error functions and calculated a lot of new integrals containing special functions. This marvelous capacity enabled him to solve many problems encountered in our daily work and penetrate into many published papers reporting them very often at our laboratory seminar. To characterize the entire contribution of Prof. P.I. Khadzhi to the science, we can remember that he was the author of about 1500 scientific publications, including 6 monographs dedicated to the exciton–biexciton physics in semiconductors, and 2 textbooks. One of them contains the new integrals as was mentioned above and is widely used by the researches, whereas the second one contains the theory of oscillations, being written for students. The list of these monographs is attached below.

Some particular results obtained by Prof. P.I. Khadzhi and his coauthors will be enumerated bellow following the review article written on the occasion of his 70th birthday anniversary published in [1] and adding some new results obtained in the last decade. The results mentioned in [1] were published in the papers cited wherein. They concern the exciton–biexciton physics, which is more known for us and will be briefly represented below.

1. In discussing the polariton soliton formation, it was found that it is an aperiodic nonlinear process. In the first half of evolution, the light penetrating into a crystal is transformed into excitons. In the second half of the process, the energy accumulated in the crystal is returned back to the light, which thereby continues its propagation. Using the slowly varying amplitude approximation and taking into account the phase modulation, Khadzhi et al. [1] succeeded to obtain an exact solution describing the profile of the soliton wave packet. In addition, the authors determined the group velocity of the soliton wave packet and the dispersion relation between the frequency and the wave vector of the carrier wave. It was shown that, inside the polariton gap, a third polariton branch with an inverse dispersion law appeared.

2. In the theory of the exciton–photon nutation, Khadzhi et al. [1] have generalized the linear theory developed earlier by Davydov and Serikov taking into account the nonlinear effects related with high density of photons. It was shown that the nutation frequency increases monotonically with increasing photon density, in the case where the detuning between the exciton and photon frequencies equals to zero.

3. The photon-echo phenomenon has been first described by Khadzhi et al. avoiding the fixed field approximation. Typically, the echo response of the system to the successive action of two ultrashort pulses—first with the area $\pi/2$ and the second with area π—is described neglecting the inverse action of the system on the electromagnetic field. In the model exciton–biexciton system, the creation of the coherent photon field generated by the coherent excitons and biexcitons and coexisting with the external laser pulses was taken into account. The new property of the echo signal was revealed. For example, the polarization of the echo signal depends not only on the areas of the exciting pulses, but also on their initial densities.

4. Another aspect of the ultrashort laser pulses propagation in the crystals is the transient stage beginning with the penetration into the crystal and finishing with the formation of stationary wave packets. This stage is governed by the area theorem deduced in the case of two level atoms by McCall and Hahn supposing that, initially, all atoms are in the ground state. The area theorem

in the case of a multicomponent system with the participant being initially in the ground and excited states was deduced by Khadzhi et al. [1].

5. The light propagation along two directional couplers is a problem of technical physics and concerns the elaboration of the integrated-optics devices. Khadzhi et al. [1] have studied theoretically the light propagation under stationary conditions along two directional couplers with saturable non-linearity interacting between them. The process is described by two differential nonlinear equations describing the distribution along the axes of the couplers of the intensity of the light beam with the intensity of input in one coupler. The problem was solved by Khadzhi et al. [1] exactly in quadrature. It was shown that the properties of the intensity distribution along the axis of the waveguides can be explained studying the behavior of the potential energy of an effective nonlinear oscillator. The potential energy depends on two main parameters, such as the nonlinearity parameter a and the input of the first coupler Y_1. The critical values of a, which are referred to as a_c, correspond to the potential energy equal to zero. They are different at different values of Y_1 and determine the optical switches of the devices. The $a_c\left(Y_1\right)$ dependence is known as a bifurcation curve. If the input intensity is smaller than the critical value, when the potential energy is negative, then the intensity in waveguide 1 varies along the axis periodically. If the input intensity is slightly higher or smaller than the critical level, then the input power is almost entirely applied to one or other waveguide. A small variation in the input intensity around the switching (critical) value causes a sharp change in the output intensity. This effect can find application in all optical switchers, small signal amplifiers, optical transistors, and other devices. If parameter a is greater than a_c, the periodically varying intensity in the first coupler is above zero at any point of the axis.

6. Optical parametric oscillators based on exciton–polaritons and exciton–dipolaritons. Their dynamics and evolution.

Professor Khadzhi and coathors studied the nonstationary processes arising under the excitation of semiconductors by ultrashort laser pulses in the exciton range of spectrum where the exciton polaritons appear in a lot of papers [2–6]. Last years, these mixed exciton–photon states were studied in planar semiconductor microcavities with quantum wells embedded in them. A new class of quasi-two-dimensional particles with unique properties was formed. A brief report of his results will be based on [2, 6]. The dynamics of the parametric exciton–polariton oscillator in a microcavity, which is characterized by the periodic conversion of a pair of pump polaritons into polaritons of the signal and the idler modes and back, has been first theoretically studied by Khadzhi and Vasil'eva in [2, 3]. In addition to exciton–polaritons, a new quasiparticle, which is referred to as the dipolariton, was formed in coupled double quantum wells embedded in a microcavity and observed experimentally [7]. Unlike an exciton–polariton, a dipolariton is a superposition of a microcavity photon, a direct exciton, and of an indirect exciton. A direct exciton is a bound state of an electron–hole pair situated in the same quantum well, whereas an indirect exciton is formed by the binding of an electron and a hole located in the neighboring wells. In symmetric quantum wells, the appropriate electric field can ensure coupling between all three components. The coupling of a microcavity photon to direct and indirect excitons leads to the formation of eigenmodes with three dispersion branches referred to as the lower, middle, and upper dipolariton branches [8]. The description of polariton parametric oscillator was proposed in [9]; however, there have been no works in which the specific feature of the dynamics of the system of polaritons in a microcavity would be considered comprehensively. This task was

solved by Khadzhi et al. in [2, 3]. They studied the situation when polaritons are excited on the lower polariton branch at a "magic" angle and described the process of parametric scattering of two pump polaritons into the signal and the idler modes, as was first proposed in [9]. Using nonlinear equations containing coherent macroscopic waves, namely, pump, signal, and idler, the integrals of motion were deduced in quadrature. These equations were supplemented with the initial condition at the initial moment of time $\tau = 0$. It was shown that the exact solution can be represented as oscillations of a nonlinear oscillator with kinetic and potential energies and with amplitude $y(\tau)$. If the frequency detuning between the exciton and photon modes is zero, there exists only an aperiodic regime of the time evolution of the system and the increasing or decreasing character of the solution is specified by the time derivative in the initial moment $dy/dt\big|_{\tau=0}$. In the case $dy/dt\big|_{\tau=0}^{>0}$, all polaritons of the signal and idler modes are transformed in pair into pump polaritons, after which the evolution is completed. There is no inverse process, i.e., a decay of the pump polaritons in pairs into polaritons of the signal and idler modes, because only the induced processes of interaction between polaritons are taken into account. In a similar way, Khadzhi et al. studied the dynamics of the dipolariton excitations [4–6]. The parametric oscillator regime on a timescale shorter than the excitation relaxation time was also used. The system is pumped by a femtosecond laser pulse creating the initial population of coherent dipolaritons. After that, the system evolution is left to its own. First of all, the high density of dipolaritons is created in the middle branch of the dispersion law. As a result, dipolaritons of the pump experience parametric scattering accompanied by the generation of dipolaritons in the signal and idler modes. However, two scattering channels now exist. One is the scattering of a pair of pump dipolaritons with the formation of signal dipolaritons on the lower dipolariton branch as well as the idler dipolaritons on the upper dipolariton branch. Another possibility is the formation of the signal and idler dipolaritons on the same middle dipolariton branch. Both channels satisfy the energy and momentum conservation laws.

Khadzhi et al. [4–6] showed that, if pump dipolaritons are initially lacking in the middle branch and only the signal and idler dipolaritons are present, the evolution of the system accompanied by changes in the dipolariton densities is impossible. The system remains in its initial state. Khadzhi et al. considered some particular cases in which exact analytic solutions can be obtained. In the initial state, with the numbers of dipolaritons different from zero in the pump state, as well as in the signal and idler states, there are two aperiodic exact solutions similar to the case of polaritons described above. One of the solutions steadily decreases with time, and the signal mode becomes fully depleted of dipolaritons as they are converted into dipolaritons of the pump mode. The other solution increases with time, and the pump mode becomes fully depleted of dipolaritons as they are converted into dipolaritons of the signal and idler modes. The pump dipolaritons either increase steadily with time or decrease steadily approaching zero at long times.

7. Autler–Towness effects with participation of excitons and biexcitons revealed in the framework of the pump-probe technique.

Professor Khadzhi and his collaborators, in a series of papers, theoretically studied the optical properties of the semiconductors in the exciton spectral region and explained and predicted many effects revealed experimentally in the framework of the pump-probe technique. In this section the steady-state conditions will be discussed. The pump-probe technique is based on the use of two laser beams: an intense pump beam and a weak probe beam, which probes the changes in the optical properties of a crystal caused by the intense pump beam. Earlier Khadzhi

and Tkachenko [10] showed that the susceptibilities of the semiconductor in the exciton range of spectrum exhibit a bistable behavior with variations in the frequency and intensity of a pump pulse, if the elastic exciton–exciton interaction is taken in to account. In [11], Khadzhi and Nad'kin studied the susceptibilities of a $CuCl$ type crystal, where the model energy spectrum of the semiconductor consists of substantially nonequidistant excitonic and biexcitonic energy levels. In this case, the pump pulse photons can provide only optical exciton–biexciton conversion; however, they cannot be involved in the probing of the excitons due to large resonance detuning with respect to the exciton transition frequency. The susceptibility of the medium was found in all order of the perturbation theory in amplitude of the pulse field and in the first order of the perturbation theory in amplitude of the probe pulse field under steady-state conditions. Two excitonic states (quasi-levels) with frequencies $\omega_{\pm}$ appear under exposure to a pump field. The difference between them $\Omega = \omega_{+} - \omega_{-}$ is referred to as the Autler–Towness splitting. It determines the optical nutation frequency in a system of excitons and biexcitons in the M-band region. The dispersion relation of probe pulse photons in the presence of a pump field contains three polaritons-like branches. The middle branch covers the spectral range that is bounded by frequencies ω_{+} and ω_{-}; this interval expands as the pump intensity increases.

The upper polariton branch coincides with ω_{+} frequency at point $k = 0$ and tends to photon frequency at larger values of wave vector k, whereas the lower polariton branch begins with photon branch at low k values and tends to ω_{-} frequency at high k values. The absorption component of susceptibility χ'' as a function of resonance detuning was determined. The more general case was considered by Khadzhi et al. in [12], where, in addition to the previous version, the pump pulse, together with the probe pulse, create biexcitons directly in a two-photon quantum transition from the ground state of the crystal. In such a way, there are two pulses of resonance laser radiation with frequencies ω_1 and ω_2, respectively, incident on the medium. The first pulse with frequency ω_1 excites excitons from the ground state of the crystal; the second pulse with frequency ω_2 converts these excitons into biexcitons and, together with the first pulse, simultaneously generates biexcitons due to a two-photon quantum transition from the ground state directly in the biexciton state. Typically, in the case of Autler–Towness conditions, the biexciton level replica shifted downward by the photon energy of a powerful pulse lies in the range of the exciton level forming an energy-degenerate case. The energy spectrum of the system was obtained under steady-state conditions in the mean field approximation and in the limit of the given field of the second pulse. The last condition made it possible to reduce the number of equations of motion from four to three and linearize them. The obtained dispersion law contains three branches, as in the previous case considered above; however, it exhibits a much more complicated dependence on the constants of the exciton–photon interaction, the exciton–biexciton conversion, and the two-photon quantum transition from the ground state of the crystal to the biexciton state.

8. Generation and amplification of the terahertz radiation during resonant exciton formation in semiconductors.

Khadzhi et al. [12] have proposed a new mechanism of the generation and amplification of terahertz radiation in semiconductors based on quantum transitions between two exciton and biexciton states under the conditions of single-photon excitation of excitons from the ground state of the crystal. In their theoretical model, the resonant laser radiation with frequency ω_0

corresponding to an exciton transition is incident onto a semiconductor and excites many excitons from the ground state of the crystal. It was supposed that the exciton level (ex) is macro populated as well as the two exciton state (2ex) with double frequency $2\omega_0$. The biexciton state (biex) is situated below the two-exciton state and has the frequency Ω_m. The corresponding difference is determined mainly by the biexciton binding frequency; it equals to $(2\omega_0 - \Omega_m)$. Therefore, if a weak pulse of terahertz radiation with a frequency of $\omega_2 = (2\omega_0 - \Omega_m)$ enters the crystal concomitantly with the single-photon excitation producing the inversion population between the 2ex and biex levels, this radiation will be amplified due to the inversion. Two plane electromagnetic waves propagating in the crystal were considered: one of the waves has electric field amplitude E_1 and frequency ω_1 resonant to exciton transition frequency ω_0; the other wave has electric field amplitude E_2 and terahertz frequency ω_2 resonant to the two-exciton–biexciton transition frequency $(2\omega_0 - \Omega_m)$. Susceptibilities χ_1 and χ_2 of the medium in the regions of frequencies ω_1 and ω_2 were deduced; the conditions providing the amplification of the terahertz radiation at frequency ω_2 and the suppression of the pump radiation at frequency ω_1 were determined. The system exhibits bistability. It means that intensity I_2 of the terahertz wave is three-valued depending on intensity I_1 of the pump wave at a given frequency detuning and depending on the frequency detuning at a given intensity I_1. The same hysteresis-type dependences take place for the exciton density. The changes in the intensity or in the frequency of the pumping wave lead to bistability and the existence of domains with low and high densities of excitons and biexcitons in the crystal.

Other aspects of the multilateral activities of Prof. P.I. Khadzhi are related with the propagation of ultrashort light pulses through thin semiconductor films in the exciton range of spectrum [13] and with the dynamics of the optically stimulated atomic–molecular conversion [14]. The last two papers are completely reproduced below.

9. **Peculiarities of Supershort Light Pulses Transmission by Thin Semiconductor Film in Exciton Range of Spectrum [13]**.

Piotr Ivanovich Khadzhi, I.V. Beloussov, D.A. Markov, A.V. Corovai, and V.V. Vasiliev, taking into account the exciton–photon and elastic exciton–exciton interactions, studied the peculiarities of the transmission of supershort light pulses by thin semiconductor films. They predicted the appearance of a time-dependent phase modulation and dynamical red and blue shifts of the transmitted pulse. Their paper [13] is reproduced below.

1. Introduction

The studies of the unique optical properties of thin semiconductor films (TSF) induce a raised interest because of the great prospects of the practical applications. The nonlinear relation between the field of an electromagnetic wave propagating through a TSF and the polarization of the medium gives rise to a number of interesting physical effects both under the stationary and nonstationary excitation. It is very important that the TSF has the property of the optical bistability in the transmitted and reflected light wave without any additional device. The peculiarities of the nonstationary interaction of supershort pulses (SSP) of laser radiation with TSF were studied, which consists of two- and three-level atoms [13]. A number of new results were obtained in the investigation of the TSF transmission, taking into account the effects of exciton–photon interaction, the phenomenon of exciton dipole momentum saturation, the optical

exciton–biexciton conversion, and the single-pulse and two-pulse two-photon excitation of biexciton from the ground state of the crystal [13]. The new possibilities of ultraspeed control by the transmission (reflection) of TSF were predicted, which can have great prospects of their utilization in the optical information processing systems. Therefore, further investigation into the peculiarities of the TSF transmission (reflection) in the exciton range of spectrum at a high level of excitation is of high priority.

2. Basic Equations

In this section, we present the main results of the theoretical investigation of nonlinear optical properties of the TSF in the conditions of the generation of high-density excitons by the supershort pulse of the resonant laser radiation with the amplitude of the electric field, E_i, and the frequency, ω, being in resonance with the exciton self-frequency, ω_0, normally incidents on the TSF with the thickness, L, which is much smaller than the light wave length, λ, but much more than the exciton radius, a_0. In the frame of these conditions, the elastic exciton–exciton interaction is the main mechanism of nonlinearity. We consider the process of pulse transmission through the TSF, taking into account the exciton–photon and elastic exciton–exciton interactions. We suppose that only one macrofilled mode of the coherent excitons and photons exists. We handle the problem using the Maxwell equations for the field and the Heisenberg (material) equation for the amplitude of the exciton wave of polarization. We proceed from the Keldysh equation [13] for the amplitude, a, of the exciton wave

$$i\hbar\frac{\partial a}{\partial t} = -\hbar\left(\Delta + i\gamma\right)a + g\left|a\right|^2 a - \frac{d_{ex}}{\sqrt{v_0}}E^+, \tag{1}$$

where $\Delta = \omega - \omega_0$ is the resonance detuning, γ is the damping constant of the excitons, g is the constant of the elastic exciton–exciton interaction, d_{ex} is the exciton dipole momentum transition from the ground state of the crystal, v_0 is the volume of the unit cell of the crystal, and E^+ is the positive-frequency component of the electric field of the wave propagating through the TSF. The parameters d_{ex} and g contained in (1) are defined by the expressions

$$d_{ex} = \left(\varepsilon_b v_0 \hbar\omega_{LT} / 4\pi\right)^{1/2},\ g = \left(26/3\right)\pi I_{ex} a_0^3, \tag{2}$$

where ε_b is the background dielectric constant, a_0, ω_{LT}, and I_{ex} are the radius, longitudinal–transversal frequency, and the binding energy of the exciton respectively. The (1) for the bulk crystal corresponds to the mean field approximation, the applicability of which was considered in [13]. Following [13] the boundary conditions for the tangential components of the fields of the propagating pulses, we can obtain the electromagnetic relationship between the fields of incident, E_i, transmitted, E_t, and reflected, E_r, waves and the amplitude, a, of the exciton wave of polarization in the form

$$E_t^+ = E_i + i\frac{2\pi\omega L}{c}\frac{d_{ex}}{\sqrt{v_0}}a,\ E_t^+ = E_i + E_r^+, \tag{3}$$

where L is the film thickness and c is the light velocity in vacuum. We present the macroscopic amplitudes as the products of slowly varying in time envelopes and fast-oscillating exponential functions with the frequency ω. By introducing the normalized quantities

$$A = \sqrt{n_0}a,\ F_t^+ = F_t^+ / F_t^+ E_{eff},\ F_i = E_i / E_{eff},\ \tau = t/\tau_0,\ \delta = \Delta\tau_0,\ \Gamma = \tau_0\gamma, \tag{4}$$

we can rewrite the (1) and (3) in the form

$$i\frac{\partial a}{\partial t} = -(\delta + i\Gamma)A + |A|^2 A - iA - F_i, \tag{5}$$

$$F_t^+ = F_i + iA,\ F_r^+ = iA, \tag{6}$$

where the characteristic time parameter τ_0 of the TSF response, the effective field strength, E_{eff}, and the exciton density, n_0, are defined by the expressions

$$\tau_0^1 = 2\pi\omega L d_{ex}^2/(c\hbar\nu_0),\ n_0 = \hbar/(g\tau_0),\ E_{eff} = \hbar\sqrt{n_0\nu_0}/(d_{ex}\tau_0). \tag{7}$$

Let us estimate the values of parameters for CdS-like TSF with the thickness $L = 10^{-6}$ cm, using $\varepsilon_b = 9.3$, $\nu_0 = 1.25\times10^{-22}$ cm^{-3}, $a_0 = 2.8$ nm, $\hbar\omega_{LT} = 1.9$ meV, $I_{ex} = 29$ meV, and $\gamma = 10^{11}$ s^{-1} [13]. We have obtained $\Gamma = 5.7\times10^{-2}$, $\mathrm{d}_{ex} = 0.53\times10^{-18}$ erg$^{1/2}$cm$^{3/2}$, $g = 2.8\times10^{-32}$ erg cm^3, $\tau_0 = 5.7\times10^{-13}$ s, $n_0 = 6.3\times10^{16}$ cm^{-3}, and $E_{eff} = 2.8\times10^3$ V/cm, which corresponds to the intensity 10^3 W/cm^2.

Presenting the functions $A(\tau)$ and $F_t^+(\tau)$ as a sum of the real and imaginary parts, that is, $A = x + iy, F_t^+ = F + iG$ and supposing that the envelope of the incident pulse, F_i, is a real function of time, we can write the (5) and (6) in the form

$$\dot{x} = -(1+\Gamma)x - (\delta - z)y, \tag{8}$$

$$\dot{y} = -(1+\Gamma)y + (\delta - z)x + F_i, \tag{9}$$

$$F = F_i - y,\ G = x, \tag{10}$$

where $z = x^2 + y^2$ is the normalized density of excitons, for which we can obtain the equation too

$$\dot{z} = -2(1+\Gamma)z + 2F_i y. \tag{11}$$

We see that the amplitude of transmitted wave through TSF (as well as the amplitude of exciton polarization) is the phase-modulated function of time. In the linear approximation, the solution for the function $A(\tau)$ is the damped function of time

$$A = iF_0(1+\Gamma-i\delta)^{-1}\left\{1-\exp\left[-(1+\Gamma-i\delta)\tau\right]\right\}, \tag{12}$$

where the damping constant is equal to $1+\Gamma$. In (12), the exponentially damping factor is conserved even though $\Gamma = 0$, i.e., if the exciton state does not decay. This is due to the fact that the film is the open system and the emergence of the radiation presents the additional "dissipative" mechanism in the system of excitons. In the limit $\Gamma \ll 1$ $\left(\gamma \ll \tau_0^{-1}\right)$, the real dissipation due to the outflow of excitons from the coherent macrofilled mode to the incoherent one is not accomplished.

From (8)–(11), we obtain the dependence of the stationary density of excitons z_s on the field amplitude $F_i = F_0 = \mathrm{Const}$ of the rectangular incident pulse. The dependence is defined by the solution of the cubic equation

$$z_s\left[(z_s-\delta)^2 + (1+\Gamma)^2\right] = F_0^2. \tag{13}$$

For the detuning $\delta < \delta_c = \sqrt{3}(1+\Gamma)$ the density of excitons monotonously increases when the amplitude, F_0, of the incident pulse increases. The dependence in $z_s(F_0)$ this case is the nonlinear, but single-valued one. At high level of excitations, the dependence $z_s(F_0)$ is nonlinear,

multivalued and is characterized by the hysteresis when $\delta > \delta_c$. For the values of the field amplitude, $F_{\pm}$, the jumps appear in the behavior of the function $z_s(F_0)$ at $z = z_{\pm}$ where

$$z_{\pm} = \frac{1}{3}\left[2\delta \pm \sqrt{\delta^2 - 3(1+\Gamma)^2}\right], \tag{14}$$

$$F_{\pm}^2 = \frac{2}{27}\left[\delta\left(\delta^2 + 9(1+\Gamma)^2\right) \pm \left(\delta^2 - 3(1+\Gamma)^2\right)^{3/2}\right]. \tag{15}$$

For the critical resonance detuning $\delta = \delta_c = \sqrt{3}(1+\Gamma)$, we obtain $z_c = 2(1+\Gamma)/\sqrt{3}$ and $F_c = z_c^{3/2}$. The cyclic change of the amplitude, Fi, of incident pulse results in the jump-like change of the exciton density in film forming the hysteretic behavior for $F_+ < F_0 < F_-$. The shift of the exciton level for the increasing excitation intensity is the main physical reason for the hysteretic dependence $z(F_0)$. An investigation of these solutions concerning the stability upon the small deviation from the stationary values leads to a conclusion that the instability of the stationary state for z_c takes place in the range $z_- < z < z_+$, which corresponds to the middle part of the hysteretic curve $z_c(F_0)$. The system of (8)–(11) has three stationary solutions, two of which are the specific points such as stable node (for $\delta/3 < z < \delta$) or stable focus (for $z < \delta/3$ and $z > \delta$) and the third point is a saddle. The phase portrait of the dynamic system (8) and (9) in the region of the trivaluedness is presented on Fig. 1.

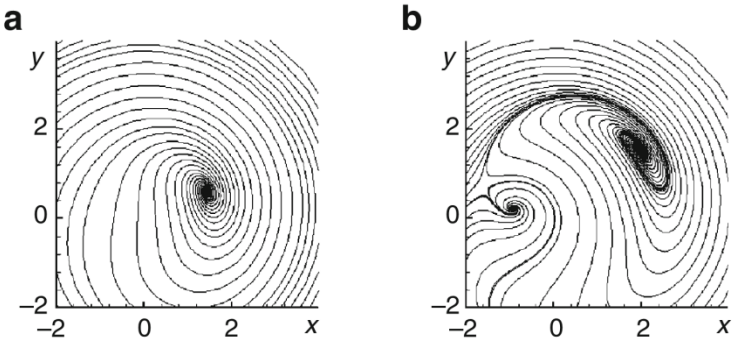

Fig. 1. The phase portrait of the dynamical system under the investigation for the detunings $\delta = 0$ (a) and $\delta = 5$ (b).

10. **Features of Stimulated Atomic–Molecular Conversion with the Formation of Heteronuclear Molecules in Bose–Einstein Condensates [14].**

P.I. Khadzhi and A.P. Zingan have investigated the dynamics of optically stimulated atomic–molecular conversion in a Bose–Einstein condensate, i.e., the periodic association of two unlike Bose atoms into a heteronuclear molecule followed by dissociation of the molecule into two atoms. It has been shown that the period and amplitude of the molecular density oscillations depend substantially on the initial particle densities and phase difference.

Substantial progress has been achieved in recent years in the experimental and theoretical investigation of the properties of atomic Bose–Einstein condensates. Currently, studies of the dynamics of coupled atomic–molecular condensates under conditions of Feshbach resonance or stimulated photoassociation of two atoms into a molecule are of special interest. According to [14], such processes may lead to a fundamentally new chemistry, so-called coherent superchemistry, in which stimulation of chemical reactions becomes possible. Atomic–molecular conversion treated as

the simplest parametric three-wave process is reduced to periodic association of two atoms into a molecule and back. The meanfield theory of parametric Raman scattering of two laser pulses considered as a single (onestage) process was proposed in [14], where the association of two identical atoms into a homonuclear molecule in the presence of two resonance laser pulses was studied. It was shown that conversion can proceed in both the periodic and aperiodic regimes so that the evolution of the system is essentially determined by the initial particle densities. Jing et al. [14] theoretically studied two-stage photoassociation of two unlike Bose atoms into a heteronuclear molecule under the action of two laser pulses. Seemingly, this process can be also considered as one-stage, because the common excited level of the molecule appears to be unpopulated.

So far, association into homonuclear molecules was observed for K_2, Li_2, Cs_2, Na_2, and Rb_2 [14]. The observation of not only homonuclear molecules but also heteronuclear ones, which are composed of unlike atoms, was a considerable success. In this case, atomic–molecular conversion in Fermi–Fermi, Bose–Bose, and Fermi–Bose mixtures of atoms with the formation of $^6Li^{40}K$, $^6Li^{23}Na$, $^7Li^{133}Cs$, $^{23}Na^{133}Cs$, $^{83}Rb^{133}Cs$, $^{39}K^{85}Rb$, $^{40}K^{87}Rb$, and $^{41}K^{87}Rb$ [14] heteronuclear molecules was observed. The majority of experiments were aimed at detecting diatomic homonuclear or heteronuclear molecules. However, the Cs_4 homonuclear tetramer [14] and $^{87}Rb^{40}K^6Li$ heteronuclear trimer [14] were recently observed. This indicates the possibility of the formation of even more complex molecules under conditions of the Bose–Einstein condensation.

The aim of this work is to study the features of optically stimulated atomic–molecular conversion with the formation of a heteronuclear molecule treated as a unified one-stage process. Let two unlike Bose-condensed atoms a_1 and a_2 with energies $\hbar\omega_{01}$ and $\hbar\omega_{02}$ be associated into the ground-state heteronuclear molecule b with energy $\hbar\Omega_0$ via molecular excited state E_u simultaneously absorbing and emitting optical photons c_1 and c_2 with energies $\hbar\omega_1$ and $\hbar\omega_2$, respectively (Fig. 1). This process can be represented as the reaction $a_1 + a_2 + c_1 \leftrightarrow b + c_2$, where a_1 and a_2 are two unlike, e.g., ^{41}K and ^{87}Rb, atoms and b is a $^{41}K\,^{87}Rb$ heteronuclear molecule.

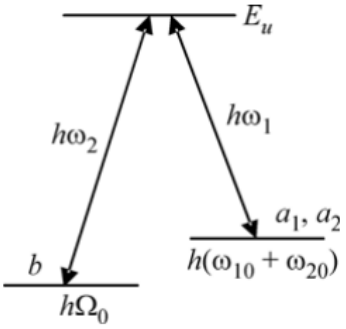

Fig. 1. Energy diagram and quantum transitions in the three-level Λ system.

The intermediate excited molecular state with energy E_u can be excluded by the adiabatic passage principle [14]. Note that the process under consideration is essentially optical Raman nutation under conditions of atomic–molecular conversion, which is the periodic density variation of atomic and molecular Bose–Einstein condensates under the action of two coherent resonant laser pulses accompanied by periodic amplification of one pulse and attenuation of the

other. According to [14], the population of the intermediate E_u level is vanishingly small. This allows us to describe the optically stimulated atomic–molecular conversion as a unified one-stage process. In this case, the interaction Hamiltonian H_{int} [14] that describes the unified stimulated atomic–molecular conversion can be generalized and expressed in the form

$$H_{\text{int}} = \hbar g\left(\hat{a}_1^{\dagger}\hat{a}_2^{\dagger}\hat{b}\hat{c}_1^{\dagger}\hat{c}_2 + \hat{a}_1\hat{a}_2\hat{b}^{\dagger}\hat{c}_1\hat{c}_2^{\dagger}\right), \tag{1}$$

where $\hat{a}_1$, $\hat{a}_2$ and $\hat{b}$ are the bosonic annihilation operators of the atomic and molecular states, respectively; $\hat{c}_1$ and $\hat{c}_2$ are the annihilation operators of photons; and g is the coupling constant. Using Eq. (1), one can easily obtain the set of Heisenberg equations for operators, $\hat{a}_1$, $\hat{a}_2$, $\hat{b}$, and $\hat{c}_2$. Averaging these equations and using the mean field approximation [14], we arrive at the set of nonlinear equations for the amplitudes (order parameters) of the matter field, $\left\langle \hat{a}_{1,2} \right\rangle = a_{1,2}$ and $\left\langle \hat{b} \right\rangle = b$, and the electromagnetic field, $\left\langle \hat{c}_{1,2} \right\rangle = c_{1,2}$,

$$i\dot{a}_k = \omega_{0k}a_k + ga_{3-k}^{*}bc_k^{*}c_{3-k},\ i\dot{b} = \Omega_0 b + ga_1a_2c_1c_2^{*},\ i\dot{c}_k = \omega_k c_k + ga_k^{*}a_{3-k}^{*}bc_{3-k}\ (k=1,2). \tag{2}$$

Introducing particle densities $n_{1,2} = \left|a_{1,2}\right|^2$, $N = \left|b\right|^2$, $f_{1,2} = \left|c_{1,2}\right|^2$ and the respective phases

$$a_k = \sqrt{n_k}e^{i\varphi_k},\ b = \sqrt{N}e^{i\psi},\ c_k = \sqrt{f_k}e^{i\psi_k}\ \ (k=1,2), \tag{3}$$

we can easily find from Eq. (2) four independent integrals of motion for the particle densities

$$n_1 + N = n_{10} + N_0,\ \ f_1 + N = f_{10} + N_0 \tag{4}$$

and reduce the entire set of equations (2) to a single nonlinear differential equation for the density of molecules N

$$\frac{dN}{dt} = \pm 2g\left\{N\left(N_0 + n_{10} - N\right)\times\left(N_0 + n_{20} - N\right)\left(N_0 + f_{10} - N\right)\left(N - N_0 + f_{20}\right) - \right.$$
$$\left. -\left[\frac{\Delta}{2g}\left(N - N_0\right) + \sqrt{N_0 n_{10} n_{20} f_{10} f_{20}}\cos\theta_0\right]^2\right\}^{1/2}, \tag{5}$$

where N_0, n_{10}, n_{20}, f_{20}, and f_{20} are the initial particle densities; ψ_0, $\varphi_{10,}$ φ_{20} and ψ_{20} are the respective phases; $\theta_0 = \psi_0 + \psi_{20} - \psi_{10} - \varphi_{10} - \varphi_{20}$ is the initial phase difference; and $\Delta = \omega_{01} + \omega_{02} - \Omega + \omega_1 - \omega_2$ is detuning from resonance. The general solution to Eq. (5) can be formally represented analytically as a generalized hyperelliptic integral, which cannot be expressed in terms of ordinary functions. Thus, further consideration is conducted with numerical methods. According to Eq. (5), the system dynamics is essentially determined by the initial particle densities, phase difference, and detuning. We further consider the evolution of the system only in the case of exact resonance by setting $\Delta = 0$ in Eq. (5). Then, it can be easily seen that the evolution of the system is independent of the initial phase difference if the initial density of at least one component is zero. In addition, the system does not evolve if any two of the initial particle densities are zero.

We first consider the evolution at the initial phase difference $\theta_0 = \pi/2$. According to Eq. (5), the system can evolve both periodically and aperiodically in this case depending on the relations between the initial particle densities. In the general case, if $N_0 \neq f_{20}$ and $n_{10} \neq n_{20} \neq f_{10}$, the system evolves periodically with the period essentially determined by the initial densities.

First, we represent the main results for $f_{20} > N_0$. The oscillation period T is given by the expression

$$T = \frac{1}{2g}\int_0^{N_0+n_m} \frac{1}{\sqrt{N\left(N_0+n_{10}-N\right)\left(N_0+n_{20}-N\right)}} \times \frac{1}{\sqrt{\left(N_0+f_{10}-N\right)\left(N-N_0+f_{20}\right)}}\, dN, \qquad (6)$$

where

$$n_m = \min\left(n_{10}, n_{20}, f_{10}\right), \qquad (7)$$

that is, n_m is the lowest of three initial densities in the parentheses. In this case, the oscillation amplitude is $A = N_0 + n_m$. Thus, with an arbitrary change in the ratio of the initial densities n_{10}, n_{20} and f_{10}, the lowest of them determines the oscillation amplitude. However, if the lowest density (e.g., n_{10}) coincides with the middle one (e.g., n_{20}), i.e., if they are ordered as $n_{10} = n_{20} < f_{10}$, the oscillation period T becomes infinite (Fig. 2). This implies that the oscillation period increases monotonically and the periodic evolution is transformed into aperiodic when n_{10} approaches n_{20} (Figs. 2, 3). Remarkably, the very direction of the aperiodic variation of the function $N(t)$ is determined by the sign of its derivative $dN/dt\big|_{t=0} \equiv N_0$ at the initial time. If $N_0 > 0$, the density of molecules increases monotonically and asymptotically approaches the value $N_0 + n_m$. If < the density of molecules decreases monotonically, vanishes at a certain time, and then increases monotonically and asymptotically approaches $N_0 + n_m$. If $N_0 < 0$, the density $N(t)$ of molecules decreases monotonically, vanishes at a certain time, and then increases monotonically and asymptotically approaches $N_0 + n_m$. Thus, at $n_{10} = n_{20}$ the function $N(t)$ at large times tends asymptotically to the limiting value $N_0 + n_m$ irrespective of the sign of N_0. This is because the association of atoms into molecules is induced by the photons of both pulses and the atoms themselves. In other words, the rate of variation of the molecular density is determined by the initial particle densities. When $n_{10} = n_{20}$, the density of atoms decreases during their association into molecules; thus, stimulation of the reaction weakens and stops when all atoms are converted into molecules. The opposite process, i.e., the dissociation of molecules into atoms, does not occur, because there are no more atoms and the respective stimulation by atoms is absent. When $n_{10} \neq n_{20}$, the process remains stimulated by atoms even after complete transformation of atoms of the first type due to the residual $n_{20} - n_{10}$ atoms of the second type, as follows from Eq. (2).

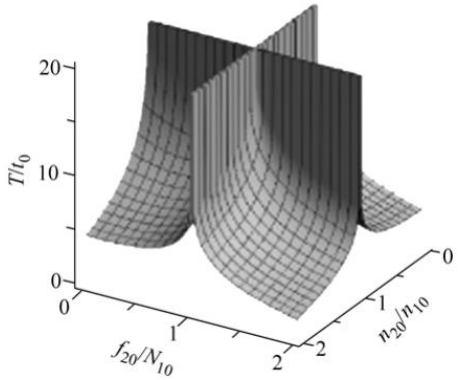

Fig. 2. Period of molecular density oscillations versus f_{20}/N_0 and n_{10}/n_{20} at $f_{10}/N_0 = 80$ and $n_{10}/N_0 = 2$.

As is seen in Figs. 2 and 3, the oscillating regime of atomic–molecular conversion takes place at $n_{10} \neq n_{20}$. In this case, the amplitude of the molecular density oscillations increases monotonically from zero to $N_0 + n_{10}$ with an increase in the ratio n_{10} / n_{20} from zero to unity and remains equal to $N_0 + n_{10}$ at $n_{10} / n_{20} > 1$ (Fig. 3). This result is independent of the direction of the initial variation of the molecular density (Fig. 3).

Under the condition $n_{10} < n_{20} = f_{10}$, the reaction is still periodic and the oscillation amplitude *A* remains equal to $N_0 + n_m$. The period of the molecular density oscillations changes continuously with f_{10} in the $f_{10} \geq n_{20}$ range. Note that the solutions of Eq. (5) with the plus and minus signs differ from each other by a constant phase determined by the initial particle densities, provided that all other conditions are identical.

Let us now consider the case $f_{20} = N_0$. In this case, only aperiodic evolution takes place at any relation between $n_{10}, n_{20},$ and f_{10} and the oscillation period becomes infinite (Fig. 2). If $n_{10} < n_{20} \leq f_{10}$, the (+) solution first increases monotonically, reaches a maximum value of $N_0 + n_{10}$, and then decreases monotonically down to zero, whereas the (–) solution decreases monotonically from N_0 down to zero. Consequently, both solutions vanish at large times; i.e., all initial molecules dissociate into atoms. If $n_{10} = n_{20} \leq f_{10}$, the evolution is still aperiodic but the (+) solution increases monotonically from N_0 to $N_0 + n_{10}$, while the (–) solution decreases monotonically from N_0 to zero. Thus, either complete dissociation of initial molecules or complete association of initial atoms is possible in this case depending on the initial direction of the change in molecular density.

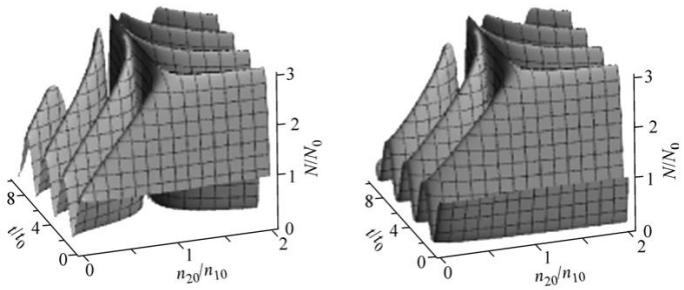

Fig. 3. Relative molecular density N / N_0 as a function of time and parameter at n_{20} / n_{10} and $f_{10} / \mathrm{N}_0 = f_{20} / N_0 = 50$ for the solution with the (left panel) plus and (right panel) minus signs.

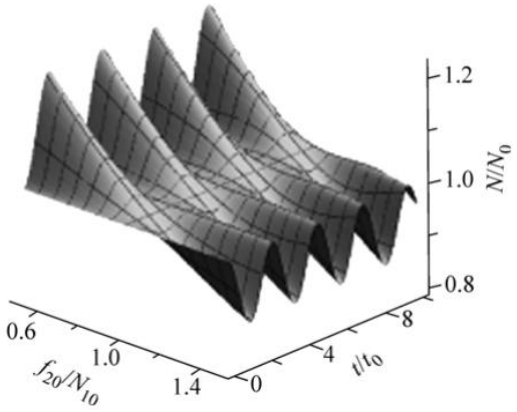

Fig. 4. Molecular density N / N_0 as a function of time and parameter f_{20} / N_0 at $f_{10} / N_0 = 3$ and $n_{10} / N_0 = n_{20} / N_0 = 50$.

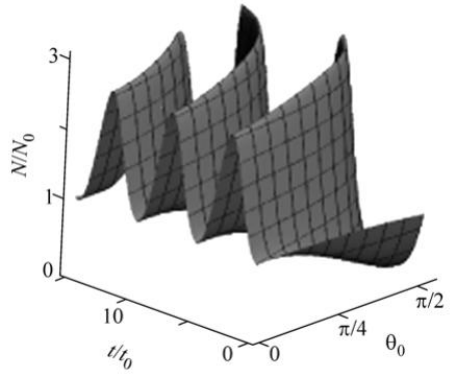

Fig. 5. Molecular density N / N_0 as a function of time and initial phase difference θ_0 at $f_{10} / N_0 = 2$, $f_{20} / N_0 = 1.1$ and $n_{10} / N_0 = n_{20} / N_0 = 50$.

Let us finally consider the case $f_{20} < N_0$. The oscillation period T in this case is given by the expression

$$T = \frac{1}{2g} \int_{N_0 - f_{20}}^{N_0 + n_m} \frac{1}{\sqrt{N\left(N_0 + n_{10} - N\right)\left(N_0 + n_{20} - N\right)}} \times \frac{1}{\sqrt{\left(N_0 + f_{10} - N\right)\left(N - N_0 + f_{20}\right)}} dN, \qquad (8)$$

where n_m is determined by Eq. (7) and the oscillation period is $A = n_m + f_{20}$. At $n_{10} < n_{20} \le f_{10}$, the evolution of the system is periodic. The molecular density changes periodically from $N_0 - f_{20}$ to $N_0 + n_{10}$ with the amplitude $n_{10} + f_{20}$. The oscillation period increases monotonically with n_{10} and becomes infinite at $n_{10} = n_{20}$. At $n_{10} > n_{20}$, the evolution of the system becomes periodic again, the molecular density oscillates with the amplitude, and the period decreases with an increase in n_{10} (Fig. 2). If $n_{10} = n_{20}$, the evolution is aperiodic. The (+) solution increases monotonically from N_0 and asymptotically approaches $N_0 + n_{10}$. The (–) solution first decreases monotonically from N_0, reaches a minimum density of $N_0 - f_{20}$ at a certain time, and then increases monotonically and asymptotically approaches $N_0 + n_{10}$.

In the case $\theta_0 = 0$, there are no aperiodic evolution regimes that take place at $\theta = \pi/2$. However, a new regime of stability with finite densities of all particles appears at $1/N_0 + 1/f_{20} = 1/n_{10} + 1/n_{20} + 1/f_{10}$. In this case, the total energy of the equivalent nonlinear oscillator is exactly equal to its minimum potential energy at $N = N_0 \neq 0$. In addition, the (+) and (–) solutions of Eq. (5) coincide, because the value $N = N_0$ at the initial time appears only on one slope of the potential energy profile.

The evolution of the molecular density at $\theta_0 = 0$ is shown in Fig. 4. Clearly, the oscillation amplitude first decreases monotonically, reaches zero, and then increases with an increase in the parameter f_{20}/N_0.

Last, we present the calculation results of the system dynamics as a function of the initial phase difference θ_0 at fixed initial particle densities obtained by numerical integration of Eq. (5). As is seen in Fig. 5, the system evolves periodically with the oscillation amplitude and period depending on the initial phase difference.

Thus, the dynamics of atomic–molecular conversion is essentially determined not only by the initial particle densities but also by the initial phase difference θ_0, which allows phase control of the process.

In conclusion, we estimate the period of particle density oscillations. Comparing Hamiltonian (1) with Hamiltonian (2) from [14], we can obtain the relation $g = \chi/\hbar\sqrt{f_{10}f_{20}}$, where $\chi = 8\times10^{-7}$ $m^{3/2}s^{-1}$ [14]. For particle densities on the order of 10^{14} cm^{-3}, this yields an oscillation period of about $10^{-3} - 10^{-4}$ s.

References

[1] S.A. Moskalenko, Mold. J. Phys. Sci. 8, 1, 114 (2009).
[2] P.I. Khadzhi and O.F. Vasil'eva, Phys. Solid State 53, 6, 1283 (2011).
[3] P.I. Khadhzi and O.F. Vasil'eva, Opt. Spectrosc. 111, 5, 814 (2011).
[4] P.I. Khadhzi and O.F. Vasil'eva, JETP Lett. 102, 9, 581 (2015).
[5] P.I. Khadhzi, O.F. Vasil'eva, and I.V. Belousov, Opt. Spectrosc. 120, 5, 760, (2016).
[6] P.I. Khadhzi, O.F. Vasil'eva, and I.V. Belousov, JETP 126, 2, 147 (2018).
[7] P. Cristofolini et al., Science 336,704 (2012).
[8] A.V. Nalitov, D. D. Solnyshkov, N. A. Gippius, and G. Malpuech, Arxiv: 1410.2812, (2014).
[9] I.A. Shelykh et al., Phys. Rev. B: Condens. Matter 76, 155308, (2007).
[10] P.I. Khadzhi and D.V. Tkacenko, Fiz. Tverd. Tela (St. Petersburg) 40, 934 (1998) [Phys. Solid State 40, 860 (1998)].
[11] P.I. Khadzhi and L.Yu. Nad'kin, Phys. Solid State 47, 12, 2237 (2005).
[12] P.I. Khadzhi, L.Yu. Nad'kin, and D.A. Markov, Phys. Solid State 60, 4, 663 (2018).
[13] P.I. Khadzhi, I.V. Belousov, D.A. Markov, A.V. Korovai, and V.V. Vasiliev, in Nanoscale Phenomena: Fundamentals and Applications, Nanoscience, and Technology, H. Hahn et al. (eds), Springer-Verlag, Berlin, Heidelberg, chapter 4, 2009 and references wherein.
[14] P.I. Khadzhi and A.P. Zingan, JETP Lett. 92, 7, 444 (2010) and references wherein.

List of monographs written by Prof. P.I. Khadzhi himself and with coauthors

1. P.I. Khadzhi, Funktsiya veroyatnosti, RIO AN MSSR, Kishinev, 398, 1971.
2. S.A. Moskalenko, A.I. Bobrysheva, A.V. Lelyakov, M.F. Miglej, P.I. Khadzhi, and M.I. Shmiglyuk, Vzaimodeistvie eksitonov v poluprovodnikakh, RIO AN MSSR, Kishinev, Shtiintsa, 211, 1974.
3. P.I. Khadzhi, Kinetika rekombinatsionnogo izlucheniya eksitonov i bieksitonov v poluprovodnikakh, Kishinev, Shtiintsa, 243, 1977.
4. S.A. Moskalenko, P.I. Khadzhi, and A.Kh. Rotaru, Solitony i nutatsiya v eksitonnoi oblasti spektra, Kishinev, Shtiintsa, 195, 1980.
5. P.I. Khadzhi, Nelineinye opticheskie processy v sisteme eksitonov i bieksitonov v poluprovodnikakh, Kishinev, Shtiintsa, 213, 1985.
6. P.I. Khadzhi and G.D. Shibarshina, Opticheskaya bistabil'nost' v sisteme kogerentnykh eksitonov i bieksitonov v poluprovodnikakh, Kishinev, Shtiintsa, 120, 1988.
7. P.I. Khadzhi, Izbrannye zadachi po teorii kolebanii, Tiraspol', RIO PGKU, 1996.

List of doctor dissertations prepared and defended under the guidance of Prof. P.I. Khadzhi himself and with coadvisors

1. C.G. Petrascu together with S.A. Moskalenko
2. A.S. Rusu together with S.A. Moskalenko
3. S.S. Rusu together with S.A. Moskalenko
4. S.N. Belkin together with S.A. Moskalenko
5. E.S. Kiseliova together with E.P. Pocatilov
6. G.D. Shibarshina together with S.A. Moskalenko
7. Lu.D. Slavov
8. O.F. Pasecinic
9. S.L. Gaivan
10. L.P. Glazova (scientific consultant)
11. K.D. Lyakhomskaia
12. A.M. Rusanov together with E.P. Sineawskii
13. A.V. Corovai
14. O.V. Corovai
15. D.V. Tkachenko
16. D.A. Markov
17. L.Yu. Nad'kin
18. A.P. Zingan
19. O.F. Vasil'eva.

S.A. Moskalenko and I.V. Podlesny

IN MEMORIAM OF KONSTANTIN GUDIMA

(September 9, 1942—March 8, 2018)

This year, in March, the Moldavian scientific community suffered a great loss in the person of Konstantin Gudima. He was a scientist with world-wide reputation known in the field of the theory of nuclear reactions. He has made an inestimable contribution to the development of theoretical nuclear physics of the Republic of Moldova.

I was lucky to work together with this marvelous man during recent five decades. I met K. Gudima 50 years ago, in February 1968. At that time, I was just sent to Dubna Scientific Research Institute of Nuclear Physics—affiliate of the Moscow State University—to continue my study at the University. It was just in the first days of my stay in Dubna when I got acquainted

with the young family of Gudima—Konstantin and his wife Mariya. At that time, he was a postgraduate student of the Joint Institute for Nuclear Research (JINR).

Since then, our lives have been bound together for a long time. Actually, we lived our whole life side by side. We worked in the same field of science and tackled the same scientific problems. For the last 15 years, we worked sitting in the same room. Our friendship became even stronger due to close relationships between our families.

Konstantin Gudima was born on September 9, 1942 in the village of Byrnova, Oknitsa region, Moldova. In 1959 he entered the faculty of physics and mathematics of the Kishinev State University (at present, Moldova State University); in 1964 he graduated from it. In 1965 he started his work as a laboratory assistant at the Institute of Mathematics of the Academy of Sciences of Moldova. This year he was sent for specialization in the field of the theory of atomic nuclear and elementary particles to the Dubna affiliate of the Moscow State University. It was the beginning of his scientific career in the team of well-known Russian scientist Vladilen Sergeevich Barashenkov. That school of physicist theoreticians has laid the foundation of a new direction of fundamental and applied nuclear physics, namely, computer modeling of interactions between the particles at intermediate energies and nuclei with atomic nuclei and macroscopic targets. The proposed models made it possible to identify the mechanisms of those interactions and reveal new fundamental effects; the generated codes were used as the basis for generators of events of complex transport codes to calculate the interaction of radiation with matter. In 1969, upon completion of the work at the JINR in Dubna (in the period of 1965—1968, there was a break for forced military service) Konstantin Gudima publicly defended a doctoral dissertation with specialization in "Physics of Atomic Nucleus and Elementary Particles." Having an academic rank, the young scientist returns to the Academy of Sciences of Moldova, to the Institute of Applied Physics (IAP), being appointed to a post of a senior scientific worker (1971). In 1975, a Laboratory of Theory of the Atomic Nucleus and Elementary Particles was organized in the IAP. Konstantin Gudima remained to be the chief of this laboratory till 1993, when the Department of Statistical Physics headed by acad. V. Moskalenko was combined with the Laboratory of Theory of the Atomic Nucleus and Elementary Particles to form the Laboratory of Statistical Nuclear Physics of the IAP (2011–2015); Konstantin became a deputy assistant of acad. V.A. Moskalenko. Since 2015, after the reorganization—integration of physicist theoreticians—Konstantin was a leading researcher in the Laboratory of Theoretical Physics of IAP. His entire scientific work was devoted to studying the mechanisms of nuclear reactions of intermediate and relativistic energies initiated by elementary particles and heavy ions.

For over 50 years of fruitful scientific work, Konstantin Gudima collaborated with leading researchers from various authoritative nuclear centers of Russia, France, Germany, and the USA, where the global projects were developed on new levels of modern physics: the Higgs boson, the origin of exotic dark matter, supersymmetry, antimatter, quarks, and gluons. Having experience in this field, Konstantin took part in the development of calculation programs used for the modeling of spectra, in which new effects could be revealed, in particular, nuclear transitions of nuclear matter into quark–gluon state at densities and temperatures which significantly surpass the values of a normal state of the nuclear matter. Some of the studies were focused on the formation of hypernuclei and nuclear fragments, which were predicted by theory and supported by experiments with collisions of particles and heavy ions with atomic nuclei at high energies, together with studies of the Frankfurt Institute for Advanced Studies (FIAS) in Germany. The generators of nuclear events (calculation codes) developed by Konstantin Gudima were effectively brought into use in the Los Alamos National Laboratories and Fermi Laboratories of Accelerators in Batavia, the USA, as well as at the JINR in Dubna. Along with the theoretical

studies in the field of nuclear reactions, K. Gudima participated in a number of international projects; among them, the project of MultiPurpose Detector (MPD) for the NICA collider in Dubna, BM&N (studies of Baryonic Matter at Nuclotron) and "E&T–RAW" (Energy and Transmutation of RadioActive Waste) at the JINR.

The research results were published in more than 300 top international journals. Konstantin Gudima took part in the training of over 20 specialists in nuclear physics both at the IAP in Chisinau and the JINR in Dubna.

The models of nuclear reactions proposed and developed by our colleague, which are cited and known as CEM (Cascade-Exciton Model) and QGSM (Quark-Gluon String Model), are extensively used for analysis, calculation, and interpretation of phenomena occurring during collisions of elementary particles and heavy ions with atomic nuclei at high energies.

The year 2017, when Konstantin Gidima celebrated his 75^{th} jubilee, was especially fruitful for him, since he published seven papers in specialized international journals: two in Phys. Rev., one paper written also for this journal was published in arxiv-nucl-th, and four appeared in journal EPJ Web of Conferences as reports presented at international conferences. In 2017, for a series of works "Kinetic Models of Nuclear Reactions CEM (Cascade Exciton Model) and LAQGSM (LosAlamos QuardGluonString Model)—A Theoretical Instrument for Studying the Mechanism of Nuclear Reactions Initiated by Elementary Particles and Heavy Ions at Intermediate and Relativistic Energies," Konstantin Gudima was awarded with the annual premium of the IAP for high achievements in studies in the field of theoretical nuclear physics. On the occasion of 75^{th} anniversary and 50-year scientific activities, Konstantin Gudima was awarded with the medal "Meritul Scientific."

Our dear colleague Konstantin Gudima was a real friend, world-known scientist, devoted researcher. Kind memory of him will remain forever in our hearts.

Mircha Baznat,
leading researcher

DOCTOR IGOR DOBYNDE THE DEVOTED KNIGHT OF SCIENCE

Igor Dobynde graduated from the Technical University of Moldova in 1977. After that, for some years, he improved his skills at the M.V. Lomonosov Moscow State University, at the chair of the physics of semiconductors guided by Prof. V.S. Dneprovskii. After returning to Kishinev, he worked at the Institute of Applied Physics of the Academy of Sciences of Moldova with specialization in the field of picosecond optical spectroscopy of semiconductors. These investigations were conducted using special equipment containing an Agat strike-camera and providing the registration of the time evolution of the luminescence process at a picosecond time resolution. These measurements require a high precision in the optical and mechanical parts of the installation and a continuous improvement to maintain the optical–kinetic complex in the working state. Only the exceptional devotion to science demonstrated by Igor Dobynde for about 40 years made it possible to provide these conditions. Another exceptional feature of his scientific style was high requirements for the verity of scientific results; he subjected his results to multiple verifications. It is no wonder that Igor Dobynde defended his doctor of physics thesis much latter than his colleagues of the same age did. However, as a recompense of his exigency, the honorable official opponents estimated his doctoral thesis as exceeding the usual requirements addressed to the candidatus scientiarum degree two- or threefold. Last years, he intended to enlarge these results and present them as a doctor habilitat thesis.

The entire scientific life of Dr. Igor Dobynde was dedicated to the investigations of the optical properties of semiconductors under a high level of laser excitation. The mean scientific results concern the kinetic processes with participation of high density of nonequilibrium charge carriers (NCCs). These processes are developing in a short and ultrashort interval of time (hundreds of picoseconds).

The theoretical interpretation of the obtain results was performed in collaboration with Prof. Igor Beloussov and in multiple discussions with Prof. Piotr Khadzhi and with the participants at the seminars of the laboratory.

The phononless Auger recombination processes were revealed. They take place, for example, when two indirect excitons accumulated at the electron valley minima situated at the opposite points at the boundary of the Brillouin zone take part in radiative recombination. The emitted photon appears as a result of the annihilation of one indirect exciton from one valley accompanied by the transformation of the second indirect exciton from the opposite valley into the direct exciton at the Γ point of the Brillouin zone.

Another impressive result was a considerable shift—by 25 meV—of the forbidden energy band gap edge after the ultrashort laser excitation of a semiconductor. It takes place due to the formation of the electron–hole plasma from the NCC. It leads to the lowering of the energy per one electron–hole pair in the frame of plasma and disappears in an interval of time of about 50 ps after excitation together with the annihilation of plasma. The observed phenomenon was proposed for implementation as an optical breech-block. Time-resolved spectroscopy permitted Dr. Dobynde, who began with his work at the M.V. Lomonosov Moscow State University and continued at the Institute of Applied Physics, to reveal a spectacular process of the relaxation of the NCC between the levels of the size quantization in the system of quantum dots excited by an ultrashort laser pulse. The charged carriers excited initially on the upper levels of the size quantization and step-by-step changed their occupation numbers gradually lowering their positions on the energy scale. The Pauli principle interdicts the excitation of the new carriers on the occupied energy levels, leading to high transparency without absorption of light propagating in this spectral region. It permits the absorption of light with frequencies corresponding to the transitions on the nonoccupied energy levels, leading to small transparency in this case.

Acad. Sveatoslav Moskalenko,
Prof. Igor Beloussov,
Dr. Igor Podlesny,
Vladimir Pavlenko,
Ion Zubac

A TWO-DIMENSIONAL ELECTRON–HOLE SYSTEM UNDER CONDITIONS OF FRACTIONAL QUANTUM HALL EFFECTS

S. A. Moskalenko and V. A. Moskalenko

Institute of Applied Physics, str. Academiei 5, Chisinau, MD-2028 Republic of Moldova
E-mail: exciton@phys.asm.md

(Received June 25, 2018)

Abstract

It has been shown that the Chern–Simons (C–S) gauge field created by quantum point vortices under conditions of fractional quantum Hall effects (FQHEs) leads to the formation of composite electrons and holes with equal integer numbers of quantum point vortices attached to each particle. The coherent superposition of the velocities of these vortices leads to the formation of the C–S vector potential, which depends on the difference between density operators $\hat{\rho}_e$ of the electrons and $\hat{\rho}_h$ of the holes. The C–S vector potential generates an effective magnetic field acting on the particles in addition to the external magnetic field. In the mean field approximation, when the average densities of electrons and holes coincide, the effective C–S magnetic and electric fields vanish and the Landau quantization of the composite particles with the bare electron and hole effective masses take place only under the action of the external magnetic field.

1. Introduction

Jackiw and Pi [1] have constructed a nonrelativistic field theory for a two-dimensional (2D) *N*-body system of point particles with C–S interactions. The C–S gauge field is created by the quantum point vortices located at each charged particle.

The C–S theory, which was developed by Jackiw and Pi [1] and widely used in the theory of fractional quantum Hall effects (FQHEs) [2–4], was applied to describe a 2D coplanar electron–hole system in a perpendicular magnetic field interacting with quantum point vortices [5, 6]. The motions of each electron and hole are accompanied by an integer number of quantum point vortices; these numbers are the same for electrons and for holes. The coherent summation of the angles formed with the in-plane x axis by the reference vectors between the positions of the given point and the points where the charged particles are situated, being weighted by the particle density operator, gives rise to phase operator $\hat{\omega}(\vec{r})$ of the C–S field. The field gradient $\vec{a}(r) = \vec{\nabla}\hat{\omega}(\vec{r})$ determines the vector-potential, whereas the time derivative $\frac{d\hat{\omega}}{cdt}$ generates the scalar potential. The C–S vector potential is a coherent superposition of the vortex velocities also weighted with the density operators of the point electrical charges. The quantum point vortices are localized only at the points where the charged particles do exist. Their vorticities are singular being different from zero only at these points. The C–S vector potential $\hat{\vec{a}}(\vec{r})$ generates an effective magnetic field, which is created by the electron and hole vortices and depends on the difference of their density operators $\hat{\rho}_e(\vec{r})$ and $\hat{\rho}_h(\vec{r})$ as follows: $\hat{\rho}(\vec{r}) = \hat{\rho}_e(\vec{r}) - \hat{\rho}_h(\vec{r})$. In our

studies [5, 6] we have shown that the Landau quantization of the composite electrons and holes takes place with the effective masses of the bare electrons and holes mostly under the action of the external magnetic field, when the average values of density operators $\langle\hat{\rho}_e(r)\rangle$ and $\langle\hat{\rho}_h(\vec{r})\rangle$ coincide $\left(\langle\hat{\rho}(\vec{r})\rangle=0\right)$.

In [5, 6], the C–S interaction was introduced in the Hamiltonian of the 2D layer containing the periodic lattice potential and the Coulomb electron–electron interaction in the presence of an external perpendicular magnetic field. A two-band model with the electrons filling the conduction and the valence band was considered. The exclusion of the periodic lattice potential and the possibility of introducing the motions of electrons and holes with effective masses in the presence of the C–S gauge field were demonstrated. In this study, on the basis of the previous findings, we are starting from the Hamiltonian in the electron–hole representation introducing the C–S gauge field with the unitary transformation. The paper is organized as follows. In section 2, the starting Hamiltonian in the electron–hole representation is introduced. In the third section, the C–S gauge field is introduced and the Schrödinger equations for the operators describing the composite particles are deduced. The fourth section contains the conclusions.

2. Hamiltonian of the Electron-Hole System

The Hamiltonian of the bare electrons and holes under the action of a strong perpendicular magnetic field, interacting between them by the Coulomb interaction, is expressed in terms of electron and hole field operators $\hat{\psi}_e^{0^+}(\vec{r}),\hat{\psi}_e^0(\vec{r}),\hat{\psi}_h^{0^+}(\vec{r})$ and $\hat{\psi}_h^0(\vec{r})$, and consist of the kinetic and Coulomb parts $\hat{H}^0=\hat{K}^0+\hat{H}_{Coul}^0$, where

$$\hat{K}^0=\frac{\hbar^2}{2m_e}\int d^2\vec{r}\,'\psi_e^{0+}(\vec{r}\,')\left(-i\vec{\nabla}'+\frac{e}{\hbar c}\vec{A}(\vec{r}\,')\right)^2\hat{\psi}_e^0(\vec{r}\,')+$$
$$+\frac{\hbar^2}{2m_h}\int d^2\vec{r}\,'\hat{\psi}_h^{0+}(\vec{r}\,')\left(-i\vec{\nabla}'-\frac{e}{\hbar c}\vec{A}(\vec{r}\,')\right)^2\hat{\psi}_h^0(\vec{r}\,'). \tag{1}$$

Here, $\vec{A}(\vec{r})$ is the vector potential created by the external magnetic field perpendicular to the layer. It obeys to the condition $\vec{\nabla}\cdot\vec{A}(\vec{r})=0$ and, in the Landau gauge, has the form $\vec{A}(\vec{r})=(-By,0,0),$, where B is the magnetic field strength. The Coulomb interaction Hamiltonian $\hat{H}_{Coul}^0$ between the bare electrons and holes has the form

$$\hat{H}_{coul}^0=\frac{1}{2}\int d^2\vec{r}\,'\int d^2\vec{r}\,''V_{Coul}(\vec{r}\,'-\vec{r}\,'')\hat{\psi}_e^{0^+}(\vec{r}\,')\hat{\psi}_e^{0^+}(\vec{r}\,'')\hat{\psi}_e^0(\vec{r}\,'')$$
$$\hat{\psi}_e^0(\vec{r}\,')+\frac{1}{2}\int d^2\vec{r}\,''V_{Coul}(\vec{r}\,'-\vec{r}\,'')\hat{\psi}_h^{0^+}(\vec{r}\,')\hat{\psi}_h^{0^+}(\vec{r}\,'')\hat{\psi}_h^0(\vec{r}\,'')\hat{\psi}_h^0(\vec{r}\,')- \tag{2}$$
$$-\int d^2\vec{r}\,'\int d^2\vec{r}\,''V_{Coul}(\vec{r}\,'-\vec{r}\,'')\hat{\psi}_e^{0^+}(\vec{r}\,')\hat{\psi}_h^{0^+}(\vec{r}\,'')\hat{\psi}_h^0(\vec{r}\,'')\hat{\psi}_e^0(\vec{r}\,').$$

The interaction potential $V_{Coul}(\vec{r})$ in a 2D system can be represented as follows:

$$V_{Coul}\left(\vec{r}\right)=\sum_{\vec{Q}}V_{\vec{Q}}e^{i\vec{Q}\vec{r}},V_{\vec{Q}}=\frac{2\pi e^2}{\varepsilon_0 S\left|\vec{Q}\right|} \tag{3}$$

Here, ε_0 is the dielectric constant and S is the layer surface area. Along with coefficient $V_{\vec{Q}}$, another expression containing the magnetic length l_0 will be used below, namely

$$W\left(\vec{Q}\right)=V_{\vec{Q}}e^{-\frac{Q^2l_0^2}{2}},l_0^2=\frac{\hbar c}{eB}. \tag{4}$$

The densities of the bare electron and hole numbers are introduced as follows:

$$\begin{aligned}&\hat{\rho}_e^0\left(\vec{r}\right)=\hat{\psi}_e^{0^+}\left(\vec{r}\right)\hat{\psi}_e^0\left(\vec{r}\right);\ \hat{\rho}_h^0\left(\vec{r}\right)=\psi_h^{0^+}\left(\vec{r}\right)\psi_h^0\left(\vec{r}\right)\\&\hat{\rho}^0\left(\vec{r}\right)=\hat{\rho}_e^0\left(\vec{r}\right)-\hat{\rho}_h^0\left(\vec{r}\right);\ \hat{\rho}_i^{0^+}\left(\vec{r}\right)=\hat{\rho}_i^0\left(\vec{r}\right);\ \hat{\rho}_i^0\left(\vec{Q}=0\right)=\hat{N}_i,\ i=e,h\\&\hat{\rho}_i^0\left(\vec{Q}\right)=\int d^2\vec{r}\,'\hat{\rho}_i^0\left(\vec{r}\right)e^{i\vec{Q}\vec{r}};\ \hat{\rho}_i^{0^+}\left(\vec{Q}\right)=\hat{\rho}_i^0\left(-\vec{Q}\right).\end{aligned} \tag{5}$$

The bare field operators in the absence of the quantum point vortices, which will be introduced latter, obey the Fermi commutation relations

$$\begin{aligned}&\hat{\psi}_i^0\left(\vec{r}\right)\hat{\psi}_j^{0^+}\left(\vec{r}\,'\right)+\hat{\psi}_j^{0^+}\left(\vec{r}\,'\right)\hat{\psi}_i^0\left(\vec{r}\right)=\delta_{i,j}\delta^2\left(\vec{r}-\vec{r}\,'\right),\\&\hat{\psi}_i^0\left(\vec{r}\right)\hat{\psi}_j^0\left(\vec{r}\,'\right)+\hat{\psi}_j^0\left(\vec{r}\,'\right)\hat{\psi}_i^0\left(r\right)=0,\ i,j=e,h.\end{aligned} \tag{6}$$

The Coulomb interaction Hamiltonian $\hat{H}_{Coul}^0$ can be transcribed as follows:

$$\begin{aligned}\hat{H}_{Coul}^0=&\frac{1}{2}\sum_{\vec{Q}}V_{\vec{Q}}\left[\hat{\rho}_e^0\left(\vec{Q}\right)\hat{\rho}_e\left(-\vec{Q}\right)-\hat{N}_e\right]+\\&+\frac{1}{2}\sum_{\vec{Q}}V_{\vec{Q}}\left[\hat{\rho}_h^0\left(\vec{Q}\right)\hat{\rho}_h^0\left(-\vec{Q}\right)-\hat{N}_h\right]-\sum_{\vec{Q}}V_{\vec{Q}}\hat{\rho}_e^0\left(\vec{Q}\right)\hat{\rho}_h^0\left(-\vec{Q}\right).\end{aligned} \tag{7}$$

The Schrödinger equations for operators $\hat{\psi}_e^0\left(\vec{r}\right)$ and $\hat{\psi}_h^0\left(\vec{r}\right)$ have the form

$$\begin{aligned}&i\hbar\frac{d\hat{\psi}_e^0\left(\vec{r}\right)}{dt}=\left[\hat{\psi}_e^0\left(\vec{r}\right),\hat{H}^0\right]=\frac{\hbar^2}{2m_e}\left(-i\vec{\nabla}+\frac{e}{\hbar c}\vec{A}\left(\vec{r}\right)\right)^2\hat{\psi}_e^0\left(\vec{r}\right)+\\&+\int d^2\vec{r}\,'V_{Coul}\left(\vec{r}-\vec{r}\,'\right)\hat{\rho}^0\left(\vec{r}\,'\right)\hat{\psi}_e^0\left(\vec{r}\right);\\&i\hbar\frac{d\hat{\psi}_h^0\left(\vec{r}\right)}{dt}=\left[\hat{\psi}_h^0\left(\vec{r}\right),\hat{H}^0\right]=\frac{\hbar^2}{2m_h}\left(-i\vec{\nabla}-\frac{e}{\hbar c}\vec{A}\left(\vec{r}\right)\right)^2\hat{\psi}_h^0\left(\vec{r}\right)-\\&-\int d^2\vec{r}\,'V_{Coul}\left(\vec{r}-\vec{r}\,'\right)\hat{\rho}^0\left(\vec{r}\,'\right)\psi_h^0\left(\vec{r}\right);\\&i\hbar\frac{d\hat{\psi}_e^{0^+}\left(\vec{r}\right)}{dt}=-\frac{\hbar^2}{2m_c}\left(i\vec{\nabla}+\frac{e}{\hbar^e}\vec{A}\left(\vec{r}\right)\right)^2\hat{\psi}_h^{0^+}\left(\vec{r}\right)-\int d^2\vec{r}\,'V_{Coul}\left(\vec{r}-\vec{r}\,'\right)\\&\hat{\psi}_e^{0^+}\left(\vec{r}\right)\hat{\rho}^0\left(\vec{r}\,'\right);\ \hat{\rho}^0\left(\vec{r}\,'\right)=\hat{\rho}_e^0\left(\vec{r}\,'\right)-\hat{\rho}_h^0\left(\vec{r}\,'\right);\\&\frac{i\hbar d\hat{\psi}_h^{0^+}\left(\vec{r}\right)}{dt}=-\frac{\hbar^2}{2m_h}\left(i\vec{\nabla}-\frac{e}{\hbar c}\vec{A}\left(\vec{r}\right)\right)^2\hat{\psi}_h^{0^+}\left(\vec{r}\right)+\\&+\int d^2\vec{r}\,'V_{Coul}\left(\vec{r}-\vec{r}\,'\right)\hat{\psi}_h^{0^+}\left(\vec{r}\right)\hat{\rho}^0\left(\vec{r}\,'\right).\end{aligned} \tag{8}$$

On the basis of these equations of motion, time derivatives $\frac{d}{dt}\hat{\rho}_i^0(\vec{r})$ were determined and the continuity equations were derived:

$$\frac{d}{dt}\hat{\rho}_i^0(\vec{r}) = \frac{d}{dt}\left(\hat{\psi}_i^{0^+}(\vec{r})\hat{\psi}_i^0(\vec{r})\right) = -\vec{\nabla}\cdot\vec{J}_i^0(\vec{r}),\ i = e,h.$$
$$\vec{J}_e^0(\vec{r}) = \frac{\hbar}{2m_e i}\left(\hat{\psi}_e^{0^+}(\vec{r})\vec{\nabla}\hat{\psi}_e^0(\vec{r}) - \vec{\nabla}\hat{\psi}_e^{0^+}(\vec{r})\cdot\hat{\psi}_e^0(r)\right) + \frac{e}{m_e c}\vec{A}(\vec{r})\hat{\rho}_e^0(\vec{r}) \quad (9)$$
$$\vec{J}_h^0(\vec{r}) = \frac{\hbar}{2m_h i}\left(\hat{\psi}_h^{0^+}(\vec{r})\vec{\nabla}\hat{\psi}_h^0(\vec{r}) - \nabla\hat{\psi}_h^{0^+}(\vec{r})\cdot\hat{\psi}_h^0(\vec{r})\right) - \frac{e}{m_h e}\vec{A}(\vec{r})\hat{\rho}_h^0(\vec{r}).$$

To deduce formulas (8) and (9), the following commutation relations were used:

$$\left[\hat{\psi}_i^0(\vec{r}), \hat{\rho}_i^0(\vec{r}')\right] = \delta^2(\vec{r}-\vec{r}')\hat{\psi}_i^0(\vec{r}')$$
$$\left[\hat{\psi}_i^{0^+}(\vec{r}), \hat{\rho}_i^0(\vec{r}')\right] = -\delta^2(\vec{r}-\vec{r}')\hat{\psi}_i^{0^+}(\vec{r}') \quad (10)$$
$$\left[\hat{\rho}_i^0(\vec{r}), \hat{\rho}_j^0(\vec{r}')\right] = 0;\ \left[\hat{\rho}_i^0(\vec{r}), \hat{H}_{Coul}^0\right] = 0;\ i, j = e, h$$

3. Chern–Simons Gauge Field

The effect of 2D quantum point vortices will be introduced in terms of the C–S theory using the unitary transformation from the bare electron and hole operators $\hat{\psi}_i^{0^+}(\vec{r}), \hat{\psi}_i^0(\vec{r})$ to the new dressed electron and hole field operators $\hat{\psi}_i^+(\vec{r}), \hat{\psi}_i(\vec{r})$ as follows:

$$\hat{\psi}_e^0(\vec{r}) = \hat{U}(\vec{r})\hat{\psi}_e(\vec{r}), \hat{\psi}_e^{0^+}(\vec{r}) = \hat{\psi}_e^+(\vec{r})\hat{U}^+(\vec{r})$$
$$\hat{\psi}_h^0(\vec{r}) = \hat{U}^+(\vec{r})\hat{\psi}_h(\vec{r}), \psi_h^{0^+}(\vec{r}) = \hat{\psi}_h^+(\vec{r})\hat{U}(\vec{r}) \quad (11)$$
$$\hat{U}^+(\vec{r})\cdot\hat{U}(\vec{r}) = 1$$

They lead to the equalities of the bare and dressed density operators as follows:

$$\hat{\rho}_i(\vec{r}) = \hat{\psi}_i^+(\vec{r})\hat{\psi}_i(\vec{r}) = \hat{\rho}_i^0(\vec{r}) = \hat{\psi}_I^{0^+}(\vec{r})\psi_i^0(\vec{r}),\ i = e,h$$
$$\hat{\rho}(\vec{r}) = \hat{\rho}_e(\vec{r}) - \hat{\rho}_h(\vec{r}) = \hat{\rho}^0(\vec{r}) = \hat{\rho}_e^0(\vec{r}) - \hat{\rho}_h^0(\vec{r}) \quad (12)$$
$$\left[\hat{\rho}(r), \hat{\rho}(r')\right] = 0\ \hat{\rho}_i^+(\vec{r}) = \hat{\rho}_i(\vec{r});\ \hat{\rho}^+(\vec{r}) = \hat{\rho}(\vec{r})$$

Unitary transformation operator $\hat{U}(\vec{r})$ was discussed in detail by Jackiw and Pi in [1]; we are completely following their explanations. In the two-component electron–hole system, we introduced it in the form

$$\hat{U}(\vec{r}) = e^{\frac{ie}{\hbar c}\hat{\omega}(\vec{r})};\ \hat{\omega}(\vec{r}) = \frac{-\phi e}{\alpha}\int d^2\vec{r}\,'\theta(\vec{r}-\vec{r}')\hat{\rho}(\vec{r}'),$$
$$\hat{\rho}(\vec{r}') = \hat{\rho}_e(\vec{r}') - \hat{\rho}_h(\vec{r}') = \hat{\rho}^0(\vec{r}') = \hat{\rho}_e^0(\vec{r}') - \vec{\rho}_h^0(\vec{r}'). \quad (13)$$

The phase operator and the unitary transformation contain factor ϕ with integer values $\phi = 1, 2, 3...$ and a fine structure constant $\alpha = \frac{e^2}{\hbar c} = \frac{1}{137}$.

Function $\theta(\vec{r}-\vec{r}')$ is determined as the angle formed by the 2D vector $\vec{r}-\vec{r}'$ with the x axis lying in the plane of the layer. It is determined by the analytic formula

$$\Theta(\vec{r}-\vec{r}')=\arctan\left(\frac{y-y'}{x-x'}\right);\ \Theta(\vec{r}'-\vec{r})=\Theta(\vec{r}-\vec{r}')+\pi \tag{14}$$

Function $\Theta(\vec{r}-\vec{r}')$ is multivalued being determined with the precision of 2π. Jackiw and Pi paid special attention to calculations of phase operator $\hat{\omega}(\vec{r})$ and derivatives of it; these very instructive considerations will be reproduced later. In spite of these precautionary measures, unitary operator $\hat{U}(\vec{r})$ and the dressed operators are single valued due to the integer values of the factor $\phi=1,2,3...$ Only these cases will be discussed.

The new dressed operators are introduced as follows:

$$\begin{aligned}&\hat{\psi}_e(\vec{r})=\hat{U}^+(\vec{r})\hat{\psi}_e^0(\vec{r}),\ \hat{\psi}_e^+(\vec{r})=\hat{\psi}_e^{0^+}(\vec{r})\hat{U}(\vec{r}),\\&\hat{\psi}_h(\vec{r})=U(\vec{r})\hat{\psi}_h^0(\vec{r}),\ \hat{\psi}_h^+(\vec{r})=\hat{\psi}_h^{0^+}(\vec{r})U^+(\vec{r}).\end{aligned} \tag{15}$$

As will be shown later, their statistics in general case differ from the Fermi statistics of the bare electron and hole operators $\hat{\psi}_i^{0^+}(\vec{r}),\hat{\psi}_i^0(\vec{r})$. In the case of odd integer values $\phi=1,3,5...$ the dressed operators $\hat{\psi}_i^+(\vec{r}),\ \hat{\psi}_i(\vec{r})$ obey the Bose statistics, whereas in the case of even integer values $\phi=0,2,4,....$ their statistics is Fermi. Nevertheless, the commutation relations of the all dressed operators with density operators $\hat{\rho}_i(\vec{r})$ are the same as described by formulas (10).

It is evident from formulas (15) that, in the case of the electrons and the holes, the unitary transformation operations were effectuated using different Hermitian conjugated operators $\hat{U}(\vec{r})$ and $\hat{U}^+(\vec{r})$. The origin of this difference results from the definition of the hole field operator as the Hermitian conjugated field operator of the valence electron. Let us introduce the bare and dressed hole operators in the form

$$\hat{\psi}_h^0(\vec{r})=\psi_{ve}^{0^+}(\vec{r}),\ \hat{\psi}_h(\vec{r})=\psi_{ve}^+(\vec{r}) \tag{16}$$

where $\hat{\psi}_{ve}^0(r)$ and $\hat{\psi}_{ve}^{0^+}$ are the valence parts of the full bare electron operators $\hat{\psi}_e^0(r)$ and $\hat{\psi}_e^{0^+}(\vec{r})$. We will take into account the relation between the $\hat{\psi}_{ve}^0(\vec{r})$ and $\hat{\psi}_{ve}(r)$ as for the electron operators in the form $\hat{\psi}_{ve}^+(\vec{r})=\hat{\psi}_{ve}^{0^+}(\vec{r})\hat{U}(\vec{r})$; in this case, we will arrive to the necessity to use the form $\hat{\psi}_h(\vec{r})=\hat{\psi}_h^0(\vec{r})\hat{U}(\vec{r})$ instead of the form $\hat{\psi}_h(\vec{r})=\hat{U}(r)\hat{\psi}_h^0(\vec{r})$ accepted in the basic variant (11) and (15). In fact, the difference between them is not so significant because operators $\hat{U}(\vec{r})$ and $\hat{\psi}_h^0(\vec{r})$ can be transposed with the precision of the numerical phase factor derived below. In both versions, equality $\hat{\rho}_h(\vec{r})=\hat{\rho}_h^0(\vec{r})$ can be proved exactly on the basis of the relations derived below. Taking into account commutation relations (10) of the field operators with the density operators, one can obtain the transposition relations

$$\begin{aligned}
\hat{\psi}_e(\vec{r})e^{\pm\frac{ie}{\hbar c}\hat{\omega}(\vec{r}')} &= e^{\mp i\phi\theta(\vec{r}'-\vec{r})}e^{\pm\frac{ie}{\hbar c}\hat{\omega}(\vec{r}')}\hat{\psi}_e(\vec{r}),\\
\hat{\psi}_e^+(\vec{r})e^{\pm\frac{ie}{\hbar c}\hat{\omega}(\vec{r}')} &= e^{\pm i\phi\theta(\vec{r}'-\vec{r})}e^{\pm\frac{ie}{\hbar c}\hat{\omega}(\vec{r}')}\hat{\psi}_e^+(\vec{r}),\\
\hat{\psi}_h(\vec{r})e^{\pm\frac{ie}{\hbar c}\hat{\omega}(\vec{r}')} &= e^{\pm i\phi\theta(\vec{r}'-\vec{r})}e^{\pm\frac{ie}{\hbar c}\hat{\omega}(\vec{r}')}\hat{\psi}_h(\vec{r}),\\
\psi_h^+(\vec{r})e^{\pm\frac{ie}{\hbar c}\hat{\omega}(\vec{r}')} &= e^{\mp i\phi\theta(\vec{r}'-\vec{r})}e^{\pm\frac{ie}{\hbar c}\hat{\omega}(\vec{r}')}\hat{\psi}_h^+(\vec{r}).
\end{aligned} \tag{17}$$

The same relations are true in the case of the bare field operators, because the phase operator $\hat{\omega}(\vec{r})$ can be expressed in equal manner through the bare or dressed density operators $\hat{\rho}(\vec{r}) = \hat{\rho}^0(\vec{r})$, and commutation relations (10) are also the same in the both cases. Unitary transformations (11) and (15) guarantee the symmetrical description on equal footing of the electrons and the holes in the two-component system.

To deduce the Schrödinger equations for dressed field operators $\hat{\psi}_e(\vec{r})$ and $\hat{\psi}_h(\vec{r})$, the time derivatives of the unitary operators are required:

$$\begin{aligned}
i\hbar\frac{d}{dt}\hat{\psi}_e(\vec{r}) &= i\hbar\frac{d}{dt}\left(\hat{U}^+(r)\hat{\psi}_e^0(\vec{r})\right) = \frac{i\hbar d\hat{U}^+(\vec{r})}{dt}\cdot\hat{\psi}_e^0(\vec{r}) + \hat{U}^+(\vec{r})\frac{i\hbar d\hat{\psi}_e^0(r)}{dt}\\
i\hbar\frac{d}{dt}\hat{\psi}_h(\vec{r}) &= i\hbar\frac{d}{dt}\left(\hat{U}(\vec{r})\hat{\psi}_h^0(\vec{r})\right) = \frac{i\hbar d\hat{U}(\vec{r})}{dt}\cdot\psi_h^0(\vec{r}) + \hat{U}(\vec{r})i\hbar\frac{d}{dt}\hat{\psi}_h^0(\vec{r})
\end{aligned} \tag{18}$$

Jackiw and Pi [1] emphasized that it is necessary to take into account that the operator $\frac{d\hat{\omega}(r)}{dt}$ does not commute with operator $\hat{\omega}(\vec{r})$. Their commutator $\hat{L}(\vec{r})$ will be calculated later; however, the properties of it listed below

$$\begin{aligned}
&\left[\frac{d\hat{\omega}(\vec{r})}{dt}, \hat{\omega}(\vec{r})\right] = -i\cdot\hat{L}(\vec{r}),\ \mathrm{L}^+(r) = \hat{L}(\vec{r});\ \left[\hat{L}(\vec{r}), \hat{\rho}(\vec{r}')\right] = 0\\
&\left[\hat{L}(r), \hat{\omega}(\vec{r}')\right] = 0
\end{aligned} \tag{19}$$

will be used to determine the time derivates of the unitary transformation operators as follows [4, 5]:

$$\begin{aligned}
&\frac{d}{dt}\hat{U}(\vec{r}) = \frac{d}{dt}e^{\frac{ie}{\hbar c}\hat{\omega}(\vec{r})} = [\frac{ie}{\hbar c}\frac{d\hat{\omega}(\vec{r})}{dt} + \frac{i\hat{L}(\vec{r})}{2}(\frac{ie}{\hbar c})^2]\hat{U}(\vec{r}) = \hat{U}(\vec{r})[\frac{ie}{\hbar c}\frac{d\hat{\omega}(\vec{r})}{dt} - \frac{i\hat{L}(\vec{r})}{2}(\frac{ie}{\hbar c})^2];\\
&\frac{d}{dt}\hat{U}^+(\vec{r}) = \frac{d}{dt}e^{-\frac{ie}{\hbar c}\hat{\omega}(\vec{r})} = [-\frac{ie}{\hbar c}\frac{d\hat{\omega}(\vec{r})}{dt} + \frac{i\hat{L}(\vec{r})}{2}(\frac{-ie}{\hbar c})^2]\hat{U}^+(\vec{r}) = \hat{U}^+(\vec{r})[-\frac{ie}{\hbar c}\frac{d\hat{\omega}(\vec{r})}{dt} - \frac{i\hat{L}(\vec{r})}{2}(\frac{-ie}{\hbar c})^2].
\end{aligned} \tag{20}$$

They lead to the required derivatives

$$\begin{aligned}
i\hbar\frac{d\hat{U}(\vec{r})}{dt} &= \left[-\frac{e}{c}\frac{d\hat{\omega}(\vec{r})}{dt} + \frac{e^2}{2\hbar c^2}\hat{L}(\vec{r})\right]\hat{U}(\vec{r}),\\
i\hbar\frac{dU^+(\vec{r})}{dt} &= \left[\frac{e}{c}\frac{d\hat{\omega}(\vec{r})}{dt} + \frac{e^2}{2\hbar c^2}\hat{L}(\vec{r})\right]U^+(\vec{r}).
\end{aligned} \tag{21}$$

The calculations of operator $\hat{L}(\vec{r})$ is considerably simplified working with the bare field operators as follows:

$$-i\hat{L}(\vec{r})=\left[\frac{d\hat{\omega}(\vec{r})}{dt},\hat{\omega}(\vec{r})\right]=\left(\frac{\phi e}{\alpha}\right)^2\int d^2\vec{r}\,'\int d^2\vec{r}\,''\theta(\vec{r}-\vec{r}\,').$$

$$\theta(\vec{r}-\vec{r}\,'')\left\{\left[\frac{d\hat{\rho}_e^0(\vec{r}\,')}{dt},\hat{\rho}_e^0(\vec{r}\,'')\right]+\left[\frac{d\hat{\rho}_h^0(\vec{r}\,')}{dt},\hat{\rho}_h^0(\vec{r}\,'')\right]\right\}=$$

$$=-\left(\frac{\phi e}{\alpha}\right)^2\int d^2\vec{r}\,'\int d^2\vec{r}\,''\theta(\vec{r}-\vec{r}\,')\theta(\vec{r}-\vec{r}\,'')\left\{\left[\vec{\nabla}'\vec{J}_e^0(\vec{r}\,'),\hat{\rho}_e^0(\vec{r}\,'')\right]+\left[\vec{\nabla}'\vec{J}_h^0(\vec{r}\,'),\hat{\rho}_h^0(\vec{r}\,'')\right]\right\}= \tag{22}$$

$$=\left(\frac{\phi e}{\alpha}\right)^2\int d^2\vec{r}\,'\int d^2\vec{r}\,''\vec{\nabla}'\theta(\vec{r}-\vec{r}\,')\theta(\vec{r}-\vec{r}\,'')\times\left\{\left[\vec{J}_e^0(\vec{r}\,'),\hat{\rho}_e^0(\vec{r}\,'')\right]+\left[\vec{J}_h^0(\vec{r}\,'),\hat{\rho}_h^0(\vec{r}\,'')\right]\right\}.$$

Taking into account expressions (9) for current densities $\vec{J}_e^0(r')$ and $\vec{J}_h^0(r')$ and commutativity $\left[\hat{\rho}_c^0(r'),\rho_i^0(\vec{r}\,'')\right]=0$, expression (22) can be transcribed as follows:

$$\hat{L}(\vec{r})=\left(\frac{\phi e}{\alpha}\right)^2\frac{\hbar}{2m_e}\hat{M}_e(\vec{r})+\left(\frac{\phi e}{\alpha}\right)^2\frac{\hbar}{2m_h}\hat{M}_h(\vec{r}),$$

$$\hat{M}_i(\vec{r})=\int d^2\vec{r}\,'\int d^2\vec{r}\,''\vec{\nabla}'\theta(\vec{r}-\vec{r}\,')\theta(\vec{r}-\vec{r}\,'')\left\{\left[\hat{\psi}_i^{0^+}(\vec{r}\,')\vec{\nabla}'\hat{\psi}_i^0(\vec{r}\,'),\hat{\rho}_i^0(\vec{r}\,'')\right]- \tag{23}$$

$$-\left[\vec{\nabla}'\hat{\psi}_i^{0^+}(\vec{r}\,')\hat{\psi}_i^0(\vec{r}\,'),\hat{\rho}_i^0(\vec{r}\,'')\right]\right\},\ i=e,h.$$

Using commutation relations (10), one can write

$$\left[\hat{\psi}_i^{0^+}(\vec{r}\,')\vec{\nabla}'\hat{\psi}_i^0(\vec{r}\,'),\hat{\rho}_i^0(\vec{r}\,'')\right]=\hat{\psi}_i^{0^+}(\vec{r}\,')\vec{\nabla}'\left(\delta^2(\vec{r}\,'-\vec{r}\,'')\hat{\psi}_i^0(\vec{r}\,'')\right)-$$

$$-\delta^2(\vec{r}\,'-\vec{r}\,'')\psi_i^{0^+}(\vec{r}\,'')\vec{\nabla}'\hat{\psi}_i^0(\vec{r}\,'), \tag{24}$$

$$\left[\vec{\nabla}'\hat{\psi}_i^{0^+}(\vec{r}\,')\hat{\psi}_i^0(\vec{r}\,'),\hat{\rho}_i^0(\vec{r}\,'')\right]=-\vec{\nabla}'\left(\delta^2(\vec{r}\,'-\vec{r}\,'')\hat{\psi}_i^{0^+}(\vec{r}\,'')\right)\times$$

$$\times\psi_i^0(\vec{r}\,')+\vec{\nabla}'\hat{\psi}_i^{0^+}(\vec{r}\,')\delta^2(\vec{r}\,'-\vec{r}\,'')\hat{\psi}_i^0(\vec{r}\,''),\ i=e,h.$$

We can now calculate integrals $\hat{M}_i(\vec{r})$ as follows:

$$\hat{M}_i(\vec{r}) = -\int d^2\vec{r}\,'\vec{\nabla}\,'\theta(\vec{r}-\vec{r}\,')\theta(\vec{r}-\vec{r}\,')\hat{\psi}_i^{0^+}(\vec{r}\,')\vec{\nabla}\,'\psi_i^0(\vec{r}\,') -$$
$$-\int d^2\vec{r}\,'\vec{\nabla}\,'\theta(\vec{r}-\vec{r}\,')\theta(\vec{r}-\vec{r}\,')\vec{\nabla}\,'\psi_i^{0^+}(\vec{r}\,')\psi_i^0(\vec{r}\,') +$$
$$+\int d^2\vec{r}\,''\int d^2\vec{r}\,'\vec{\nabla}\,'\theta(\vec{r}-\vec{r}\,')\theta(\vec{r}-\vec{r}\,'')\psi_i^{0^+}(\vec{r}\,')\vec{\nabla}\,'\left(\delta^2(\vec{r}\,'-\vec{r}\,'')\hat{\psi}_i^0(\vec{r}\,'')\right) +$$
$$+\int d^2\vec{r}\,''\int d^2\vec{r}\,'\vec{\nabla}\,'\theta(\vec{r}-\vec{r}\,')\theta(\vec{r}-\vec{r}\,'')\vec{\nabla}\,'\left(\delta^2(\vec{r}\,'-\vec{r}\,'')\hat{\psi}_i^{0^+}(\vec{r}\,'')\right)\psi_i^0(\vec{r}\,') =$$
$$= -\int d^2\vec{r}\,'\vec{\nabla}\,'\theta(\vec{r}-\vec{r}\,')\theta(\vec{r}-\vec{r}\,')\vec{\nabla}\,'\hat{\rho}_i^0(\vec{r}\,') + \int d^2\vec{r}\,''\theta(\vec{r}-\vec{r}\,'')\cdot\int d^2\vec{r}\,'\cdot \tag{25}$$
$$\cdot\vec{\nabla}\,'\theta(\vec{r}-\vec{r}\,')\left[\hat{\psi}_i^{0^+}(\vec{r}\,')\vec{\nabla}\,'\left(\delta^{(2)}(\vec{r}\,'-\vec{r}\,'')\psi_i^0(\vec{r}\,'')\right) + \vec{\nabla}\,'\left(\delta^{(2)}(\vec{r}\,'-\vec{r}\,'')\cdot\psi_i^{0^+}(\vec{r}\,'')\right)\psi_i^0(\vec{r}\,')\right] =$$
$$= \int d^2\vec{r}\,'\vec{\nabla}'\left(\vec{\nabla}\,'\theta(\vec{r}-\vec{r}\,')\theta(\vec{r}-\vec{r}\,')\right)\cdot\hat{\rho}_i^0(\vec{r}) + \int d^2\vec{r}\,''\theta(\vec{r}-\vec{r}\,'')$$
$$\left[\int d^2\vec{r}\,'\vec{\nabla}\,'\theta(\vec{r}-\vec{r}\,')\hat{\psi}_i^{0^+}(\vec{r}\,')\vec{\nabla}\,'\left(\delta^{(2)}(\vec{r}\,'-\vec{r}\,'')\cdot\hat{\psi}_i^0(\vec{r}\,'')\right) +\right.$$
$$\left.+\int d^2\vec{r}\,'\vec{\nabla}\,'\theta(\vec{r}-\vec{r}\,')\vec{\nabla}\,'\left(\delta^2(\vec{r}\,'-\vec{r}\,'')\hat{\psi}_i^{0^+}(\vec{r}\,'')\right)\psi_i^0(\vec{r}\,')\right].$$

Here, we should take into account the equality $\Delta'\theta(\vec{r}-\vec{r}\,') = 0$, which simplifies the next calculation:

$$M_i(\vec{r}) = \int d^2\vec{r}\,'\left(\vec{\nabla}\,'\theta(\vec{r}-\vec{r}\,')\right)^2\hat{\rho}_i^0(\vec{r}\,') - \int d^2\vec{r}\,'\int d^2\vec{r}\,''\theta(\vec{r}-\vec{r}\,'')\vec{\nabla}\,'\theta(\vec{r}-\vec{r}\,')\cdot$$
$$\cdot\vec{\nabla}\,'\hat{\psi}_i^0(\vec{r}\,')\hat{\psi}_i^0(\vec{r}\,'')\delta^2(\vec{r}\,'-\vec{r}\,'') - \int d^2\vec{r}\,'\int d^2\vec{r}\,''\theta(\vec{r}-\vec{r}\,')\vec{\nabla}\,'\theta(\vec{r}-\vec{r}\,')\hat{\psi}_i^{0^+}(\vec{r}\,'')\cdot \tag{26}$$
$$\cdot\vec{\nabla}\,'\hat{\psi}_i^0(\vec{r}\,')\delta^2(\vec{r}\,'-\vec{r}\,'') = 2\int d^2\vec{r}\,'\left(\vec{\nabla}\,'\theta(\vec{r}-\vec{r}\,')\right)^2\hat{\rho}_i^0(\vec{r}\,'),\ i = e,h.$$
$$\hat{L}(\vec{r}) = \left(\frac{\phi e}{\alpha}\right)^2\hbar\left[\frac{1}{m_e}\int d^2\vec{r}\,'\left(\vec{\nabla}\,'\theta(\vec{r}-\vec{r}\,')\right)^2\hat{\rho}_e^0(\vec{r}\,') + \frac{1}{m_h}\int d^2\vec{r}\,'\left(\vec{\nabla}\,'\theta(\vec{r}-\vec{r}\,')\right)^2\hat{\rho}_h^0(\vec{r}\,')\right] \tag{27}$$
$$\left[\hat{L}(\vec{r}),\hat{\omega}(\vec{r}\,')\right] = 0;\ \left[\hat{L}(\vec{r}),\hat{\rho}(\vec{r}\,')\right] = 0;\ \hat{L}^+(r) = \hat{L}(\vec{r}).$$

To derive the Schrödinger equation for dressed field operators $\hat{\psi}_i(\vec{r})$ following formulas (17), it is necessary to determine expressions $\hat{U}^+(\vec{r})i\hbar\frac{d\hat{\psi}_e^0(\vec{r})}{dt}$ and $\hat{U}(\vec{r})i\hbar\frac{d\psi_h^0(\vec{r})}{dt}$. To this end, the equalities [1] were used below:

$$\hat{U}^+(\vec{r})(-i\vec{\nabla} + \frac{e}{\hbar c}\vec{A}(\vec{r}))^2\hat{\psi}_e^0(\vec{r}) = (-i\vec{\nabla} + \frac{e}{\hbar c}\vec{A}(\vec{r}) + \frac{e}{\hbar c}\vec{a}(\vec{r}))^2\hat{\psi}_e(\vec{r}),$$
$$\hat{U}(\vec{r})(-i\vec{\nabla} - \frac{e}{\hbar c}\vec{A}(\vec{r}))^2\hat{\psi}_h^0(\vec{r}) = (-i\vec{\nabla} - \frac{e}{\hbar c}\vec{A}(\vec{r}) - \frac{e}{\hbar c}\vec{a}(\vec{r}))^2\hat{\psi}_h(\vec{r}), \tag{28}$$
$$\hat{\psi}_e(\vec{r}) = \hat{U}^+(\vec{r})\hat{\psi}_e^0(\vec{r});\quad \hat{\psi}_h(\vec{r}) = \hat{U}(\vec{r})\hat{\psi}_h^0(\vec{r}).$$

Here, $\hat{\vec{a}}(\vec{r})$ is the C–S vector-potential determined by the definition

$$\hat{\vec{a}}(\vec{r}) = \vec{\nabla}\hat{\omega}(\vec{r}) = -\frac{\phi e}{\alpha}\int d^2\vec{r}\,'\vec{\nabla}\theta(\vec{r}-\vec{r}\,')\hat{\rho}(\vec{r}\,'). \tag{29}$$

Jackiw and Pi [1] in their fundamental studies of the C–S theory paid attention to the expression of type (29) to discussing the possibility of moving the gradient with respect to $\vec{r}$ out of the integral on variable $\vec{r}\,'$.

They mentioned that, in the general case, operator $\vec{U}(\vec{r})$ is singular, because $\theta(\vec{r}-\vec{r}\,')$ is a multivalued function and the integration over 2D $\vec{r}\,'$ plane requires the cut in $\vec{r}\,'$ beginning in $\vec{r}$. However, in the nonrelativistic quantum mechanics, the particles are points and the matter density operator $\hat{\rho}(\vec{r})$ is localized at these points being a superposition of δ-functions. This fact plays a crucial role in the calculations involving the C–S gauge field. It makes it possible to interchange the integration and the differentiation in the definition (29) of the C–S vector-potential. Jackiw and Pi [1] emphasized that the presence of the density operator $\hat{\rho}(\vec{r})$ with δ-function eigenvalues in the integral leads to an exceptional situation, when the $\vec{r}$ gradient can be moved outside the integral with impunity. In [1], some peculiarities of the 2D space were enumerated, such as

$$curl = \vec{\nabla}\times = \vec{e}_x\frac{\partial}{\partial y} - \vec{e}_y\frac{\partial}{\partial x};\ \vec{\nabla} = \vec{e}_x\frac{\partial}{\partial x} + \vec{e}_y\frac{\partial}{\partial y}$$

$$\vec{\nabla}\theta(\vec{r}-\vec{r}\,') = -\vec{\nabla}\times\ln|\vec{r}-\vec{r}\,'|;\ \vec{\nabla}\times\theta(\vec{r}-\vec{r}\,') = \vec{\nabla}\ln|\vec{r}-\vec{r}\,'|$$

$$\Delta\theta(\vec{r}-\vec{r}\,') = 0;\ \Delta\ln|\vec{r}-\vec{r}\,'| = 2\pi\delta^{(2)}(\vec{r}-\vec{r}\,') \tag{30}$$

$$\vec{\nabla}\cdot\vec{a}(\vec{r}) = 0;\ curl\hat{\vec{a}}(\vec{r}) = \vec{\nabla}\times\vec{a}(\vec{r}) = \hat{b}(\vec{r}) = \vec{\nabla}\times\frac{\phi e}{\alpha}\int d^2\vec{r}\,'\hat{\rho}(\vec{r}\,')\vec{\nabla}\times\ln|\vec{r}-\vec{r}\,'| =$$

$$= \frac{\phi e}{\alpha}\int d^2\vec{r}\,'\hat{\rho}(\vec{r}\,')\Delta\ln|\vec{r}-\vec{r}\,'| = \frac{2\pi\phi e}{\alpha}\hat{\rho}(\vec{r}).$$

The curl $\hat{\vec{a}}(\vec{r})$ determines the effective magnetic field strength $\hat{b}(\vec{r})$ created by the vortices. In the two-component electron–hole system it equals to

$$\hat{b}(\vec{r}) = curl\hat{\vec{a}}(\vec{r}) = \frac{2\pi\phi e}{\alpha}\hat{\rho}(\vec{r}) = \frac{2\pi\phi e}{\alpha}\left(\hat{\rho}_e(\vec{r}) - \hat{\rho}_h(\vec{r})\right) \tag{31}$$

In the mean field approximation, where the average values $\langle\hat{\rho}_e(\vec{r})\rangle$ and $\langle\hat{\rho}_h(\vec{r})\rangle$ coincide, the effective magnetic field strength $\langle\hat{b}(\vec{r})\rangle$ created by the quantum point vortices vanishes.

The gradient of the multivalued function $\theta(\vec{r})$ being considered alone, without density operator, gives rise to velocity field $\vec{V}(\vec{r})$ with singular vorticity $\Omega(\vec{r})$. In fact,

$$\vec{V}(\vec{r}) = \frac{-k}{2\pi}\vec{\nabla}\theta(\vec{r}) = \frac{k}{2\pi}\vec{\nabla}\times\ln(\vec{r}) = \frac{-k}{2\pi}\left(\frac{-\vec{e}_x y + \vec{e}_y x}{\vec{r}^{\,2}}\right)$$

$$\Omega(\vec{r}) = curl\vec{V}(\vec{r}) = \vec{\nabla}\times\vec{V}(\vec{r}) = \frac{k}{2\pi}\Delta\ln\vec{r} = k\delta^{(2)}(\vec{r}). \tag{32}$$

The C–S vector potential $\hat{\vec{a}}(\vec{r})$ arises due to the summation of velocities $\vec{V}(\vec{r})$ created by all vortices attached to the electrons and holes at these points of the 2D space, where the densities of the charges $\hat{\rho}_i(\vec{r})$ are different from zero. The electrons and holes with the attached quantum point vortices form composite particles. They have been first introduced in physics by Wilczek [6], yet in a slightly different way. The contemporary interpretation of the composite particles structure was proposed by Read [3]. The statistical properties of the dressed field operators describing the composite electrons and holes will be discussed below. As mentioned earlier, the bare electron and hole field operators obey the Fermi statistics, whereas the dressed field

operators will obey the Fermi or Bose statistics depending on the parity of the integer values of factor ϕ. To obey the Fermi or Bose statistics, the dressed field operators should satisfy the following requirements:

$$\begin{aligned}&\hat{\psi}_i(\vec{r})\hat{\psi}_j^+(\vec{r}\,')\pm\hat{\psi}_j^+(\vec{r}\,')\hat{\psi}_i(\vec{r})=\delta_{i,j}\delta^{(2)}(\vec{r}-\vec{r}\,')\\&\hat{\psi}_i(\vec{r})\hat{\psi}_j^+(\vec{r}\,')\pm\hat{\psi}_j^+(\vec{r}\,')\hat{\psi}_i(\vec{r})=0;\ i,j=e,h\end{aligned}\tag{33}$$

Here, the upper and lower signs concern to Fermi or to Bose statistics, respectively. We will determine the integer values of factor ϕ, which are compatible with requirements (33) using the electron field operators $\hat{\psi}_e(r)=U^+(r)\hat{\psi}_e^0(\vec{r})$ and $\hat{\psi}_e^+(\vec{r})=\hat{\psi}_e^{0^+}(r)\hat{U}(\vec{r})$ as a particular example. Substituting them into the first equation (33) and taking into account the transposition relations (17), we will find

$$\begin{aligned}&\hat{U}^+(\vec{r})\hat{\psi}_e^0(\vec{r})\hat{\psi}_e^{0^+}(\vec{r}\,')\hat{U}(\vec{r}\,')\pm\psi_e^{0^+}(\vec{r}\,')\hat{U}(\vec{r}\,')\hat{U}^+(\vec{r})\hat{\psi}_e^0(\vec{r})=\\&=e^{i\phi\cdot\theta(0)}\left[\hat{U}^+(\vec{r})\hat{\psi}_e^0(\vec{r})\hat{U}(\vec{r}\,')\hat{\psi}_e^{0^+}(\vec{r}\,')\pm\hat{U}(\vec{r}\,')\hat{\psi}_e^{0^+}(\vec{r}\,')\hat{U}^+(\vec{r})\hat{\psi}_e^0(\vec{r})\right]=\\&=e^{i\phi\theta(0)}\left[e^{-i\phi\theta(\vec{r}\,'-\vec{r})}\hat{U}^+(\vec{r})\hat{U}(\vec{r}\,')\hat{\psi}_e^0(\vec{r})\hat{\psi}_e^{0^+}(\vec{r}\,')\pm e^{-i\phi\theta(\vec{r}-\vec{r}\,')}\hat{U}(\vec{r}\,')\hat{U}^+(\vec{r})\hat{\psi}_e^{0^+}(\vec{r}\,')\hat{\psi}_e^0(\vec{r})\right]=\delta^2(\vec{r}-\vec{r}\,')\end{aligned}$$

(34)

Due to the commutativity $\hat{U}(\vec{r}\,')\hat{U}^+(r)=\hat{U}^+(\vec{r})\hat{U}(\vec{r}\,')$ and the relation $\theta(\vec{r}-\vec{r}\,')=\theta(\vec{r}\,'-\vec{r})-\pi$, requirement (34) can be transcribed as follows:

$$\begin{aligned}&\hat{\psi}_e(\vec{r})\hat{\psi}_e^+(\vec{r}\,')\pm\hat{\psi}_e^+(\vec{r}\,')\hat{\psi}(\vec{r})=e^{i\phi(\theta(0)-\theta(\vec{r}\,'-\vec{r}))}\hat{U}^+(\vec{r})\hat{U}(\vec{r}\,')\times\\&\times\left[\hat{\psi}_e^0(\vec{r})\hat{\psi}_e^{0^+}(\vec{r}\,')\pm e^{i\phi\pi}\hat{\psi}_e^{0^+}(\vec{r}\,')\hat{\psi}_e^0(\vec{r})\right]=\delta^{(2)}(\vec{r}-\vec{r}\,')\end{aligned}\tag{35}$$

The requirement can be satisfied, if

$$\pm e^{i\phi\pi}=1,\ \cos\phi\pi=\pm1;\ \begin{bmatrix}F\\B\end{bmatrix}\tag{36}$$

The same conditions take place for the second equation (33) as well as for the hole field operators. It means that dressed field operators $\hat{\psi}_i(\vec{r})$ with unitary transformations $\hat{U}(\vec{r})$, $\hat{U}^+(\vec{r})$ and with even integer values $\phi=0,2,4...$ obey the Fermi statistics, whereas in the case of the odd integer values $\phi=1,3,5,...$, they obey the Bose statistics.

The composite particles composed of a bare electron or a hole with an odd integer number ϕ of attached quantum point vortices are bosons, whereas in the case of an even integer number ϕ of attached vortices, they are fermions.

Combining expressions (8), (18), (21), and (28), we will obtain the Schrödinger equations for the dressed field operators

$$i\hbar\frac{d}{dt}\hat{\psi}_e(\vec{r})=\frac{\hbar^2}{2m_e}[-i\vec{\nabla}+\frac{e}{\hbar c}\vec{A}(\vec{r})+\frac{e}{\hbar c}\hat{\vec{a}}(\vec{r})]^2\hat{\psi}_e(\vec{r})+\int d^2\vec{r}\,'V_{Coul}(\vec{r}-\vec{r}\,')\hat{\rho}(\vec{r}\,')\hat{\psi}_e(\vec{r})+$$

$$+\frac{e}{c}\frac{d\hat{\omega}(\vec{r})}{dt}\hat{\psi}_e(\vec{r})+\frac{e^2}{2\hbar c^2}\hat{L}(\vec{r})\hat{\psi}_e(\vec{r});$$

$$i\hbar\frac{d}{dt}\hat{\psi}_h(\vec{r})=\frac{\hbar^2}{2m_h}[-i\vec{\nabla}-\frac{e}{\hbar c}\vec{A}(\vec{r})-\frac{e}{\hbar c}\hat{\vec{a}}(\vec{r})]^2\hat{\psi}_h(\vec{r})-\int d^2\vec{r}\,'V_{Coul}(\vec{r}-\vec{r}\,')\hat{\rho}(\vec{r}\,')\hat{\psi}_h(\vec{r})-$$

$$-\frac{e}{c}\frac{d\hat{\omega}(\vec{r})}{dt}\hat{\psi}_h(\vec{r})+\frac{e^2}{2\hbar c^2}\hat{L}(\vec{r})\hat{\psi}_h(\vec{r}); \qquad (37)$$

$$\frac{e^2}{2\hbar c^2}\hat{L}(\vec{r})=\frac{\hbar^2\phi^2}{2m_e}\int d^2\vec{r}\,'\frac{\hat{\rho}_e(\vec{r}\,')}{|\vec{r}-\vec{r}\,'|^2}+\frac{\hbar^2\phi^2}{2m_h}\int d^2\vec{r}\,'\frac{\hat{\rho}_h(\vec{r}\,')}{|\vec{r}-\vec{r}\,'|^2};$$

$$\hat{\rho}(\vec{r})=\hat{\rho}_e(\vec{r})-\hat{\rho}_h(\vec{r}); \quad \hat{\omega}(\vec{r})=-\frac{\phi e}{\alpha}\int d^2\vec{r}\,'\theta(\vec{r}-\vec{r}\,')\hat{\rho}(\vec{r}\,'); \qquad \hat{\vec{a}}(\vec{r})=\vec{\nabla}\hat{\omega}(\vec{r}).$$

It is evident that the composite electrons and holes have effective masses m_e and m_h and undergo the Landau quantization under the action of an external magnetic field and an effective magnetic field created by the vortices. It is a self-consistence in the system because the Landau quantization determines the quantum states of the composite particles; these quantum states, in turn, determine the value of the effective magnetic field. The electric charges of the composite particles are the same as those of the bare components and determine their Coulomb interactions and the interactions with the effective vector and scalar potentials created by the vortices. The kinetic energy of the vortices created with the participation of electrons and holes is also present in the Schrödinger equations.

4. Conclusions

The C–S gauge field created by quantum point vortices attached to electrons and holes situated on the lowest Landau levels under conditions of FQHEs gives rise to the vector and scalar potentials. The C–S vector potential generates an effective magnetic field depending on the difference between the density operators of electrons and holes in the way: $\hat{\rho}(\vec{r})=\hat{\rho}_e(\vec{r})-\hat{\rho}_h(\vec{r})$. In the mean field approximation, when this difference vanishes, the C–S effective magnetic and electric fields also vanish. In this case, the Landau quantization of the composite particles takes place under the action only of the external magnetic field. The effective masses of the composite particles are the same as those of the bare ones.

References

[1] R. Jackiw and S.-Y. Pi, Phys. Rev. D 42, 3500 (1990).
[2] B.I. Halperin, P.A. Lee, and N. Read, Phys. Rev. B 47, 7312 (1993).
[3] N. Read, Phys. Rev. B 58, 16262 (1998).
[4] F. Wilczek, Phys. Rev. Lett. 48, 1144 (1982); 49, 957 (1982).
[5] S.A. Moskalenko and V.A. Moskalenko, Mold. J. Phys. Sci. 16 (3–4), 133 (2017).
[6] S.A. Moskalenko, V.A. Moskalenko, D.F. Digor, and Ig.A. Leleacov, Mold. J. Phys. Sci. 16 (3–4), 173 (2017).

TWO-DIMENSIONAL PARA-, ORTHO-, AND BI-MAGNETOEXCITONS INTERACTING WITH QUANTUM POINT VORTICES

S. A. Moskalenko[1], V. A. Moskalenko[1], P. I. Khadzhi[1], I. V. Podlesny[1], M. A. Liberman[2], and I. A. Zubac[1]

[1]*Institute of Applied Physics, Academy of Sciences of Moldova, Academiei str. 5, Chisinau, MD-2028 Republic of Moldova*
[2]*Nordic Institute for Theoretical Physics (NORDITA) KTH and Stockholm University, Roslagstullsbacken 23, Stockholm, SE-106 91 Sweden*
E-mail: exciton@phys.asm.md

Abstract

The theory of two-dimensional (2D) magnetoexcitons was enlarged taking into account the electron–hole (e–h) exchange Coulomb interaction, which appears when the conduction and valence electrons belong partially to both bands. This Coulomb exchange interaction leads to the linear dispersion law of para-magnetoexcitons. Spectral properties and the new luminescence band, which arise owing to the existence of the metastable bound state, are discussed. The thermodynamic properties and the Bose–Einstein condensation conditions for para- and ortho-magnetoexcitons are described. Taking into account the vector potential of the Chern–Simons gauge field the anisotropy of the 2D magnetoexciton magnetic mass was revealed.

1. Introduction

The properties of 2D magnetoexcitons are as follows. The Lorentz force determines the Landau quantization (LQ) of electrons and holes separately. Their LQ states are determined by the cyclotron energies, the radii of the orbits, and the gyration points around which the oscillations take place. The gyration points depend on the wave vectors of the particles. The cyclotron energies depend on the particle effective masses, whereas the radii of the orbits are determined by the magnetic length and do not depend on the effective masses at all. This property is referred to as the hidden symmetry [1].

The structure of the magnetoexciton is shown in Fig. 1. It looks as an electric dipole with arm $\vec{d} = \left[\vec{k} \times \vec{z}\right] l_0^2$ oriented perpendicular to the center-of-mass wave vector $\vec{k}$ and with length $d = kl_0^2$, where l_0 is the magnetic length.

If wave vector $\vec{k}$ is zero, then two electron clouds are overposed and, because of the equal radii of the orbits, these magnetoexcitons with $\vec{k} = 0$ look as completely neutral compound particles. The magnetoexcitons with wave vectors $\vec{k} = 0$ form an ideal Bose gas [2].

The molecule formation from these two magnetoexcitons will now be discussed. Two magnetoexcitons being confined on the 2D layer on the finite limited size determined by the wave function of their relative motion can form the bound states of the molecular type, as shown in Fig. 2. The distance between two magnetoexcitons in the frame of the bound state and their wave vectors are interdependent due to the Heisenberg uncertainty relation. It means that these dipoles

have changing arms, which cannot be considered either rigid or constant. More so, the smaller the dipole arm, the greater the distance between them.

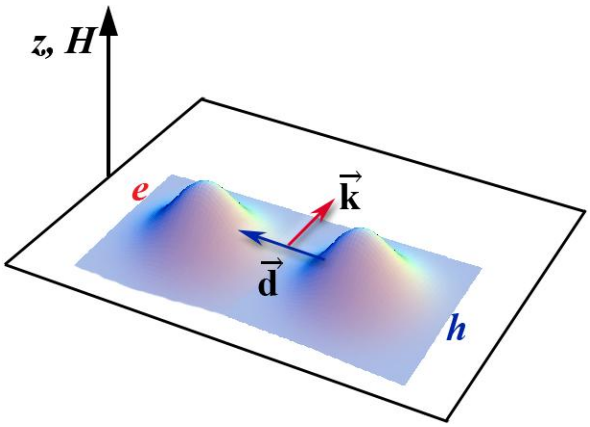

Fig. 1. Electric dipole model of the magnetoexciton with $\vec{k} \neq 0$.

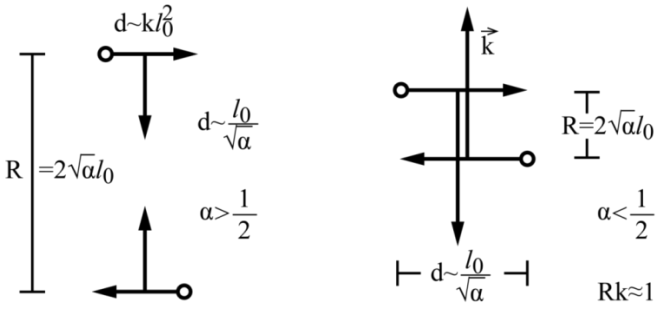

Fig. 2. Bound state of two magnetoexcitons with variational wave functions $\varphi_2(k) \sim (kl_0)^2 e^{-\alpha(kl_0)^2}$.

It is significant that we deal with the molecule in the rest with a wave vector of $\vec{k} = 0$. It means that, in our case, the electric dipoles have wave vectors with opposite directions and antiparallel dipole moments. Because of the full neutrality of the magnetoexcitons with $\vec{k} = 0$, the wave function of the relative motion should have the maximum outside the point $\vec{k} = 0$; that is, in the momentum space representation, it should be on the ring, as shown in Fig. 3.

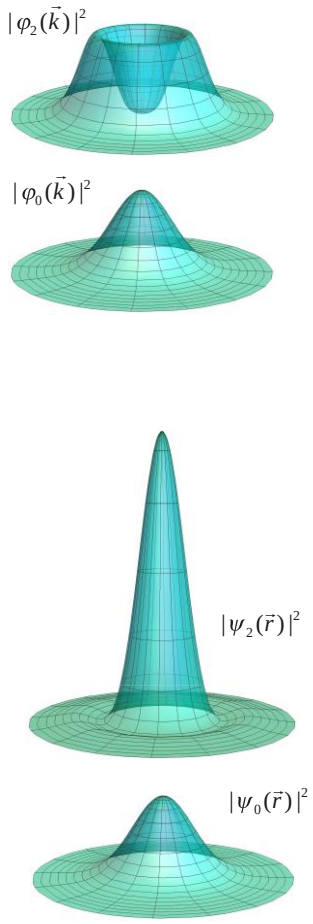

Fig. 3. Variational wave functions $\varphi_n(k)$ describing the bound states (a) in momentum representation $\varphi_0(k) \sim e^{-\alpha(kl_0)^2}$, $\varphi_2(k) \sim (kl_0)^2 e^{-\alpha(kl_0)^2}$ and (b) in real space representation $\psi_0(r) \sim \exp[-r^2/(4\alpha l_0^2)]$, $\psi_2(r) \sim \left(1-r^2/(4\alpha l_0^2)\right)\exp[-r^2/(4\alpha l_0^2)]$.

The functions have variational parameter α, which will minimize the Coulomb interaction of the particles involved in the molecule formation. The spin structure of four particles, namely, two electrons and two holes, can be chosen in four ways. The most interesting case was the combination of the spin of two electrons in singlet or triplet forms. In addition, the spin structures of two holes were organized in singlet or triplet forms. The spin structures of four particles can be of the triplet–triplet or singlet–singlet types. The mixed versions are forbidden due to the hidden symmetry. As one can see from Fig. 4, other possibilities are due to the correlations of the spins of the electron and the hole in the frame of each exciton, what gives rise to ortho and para spin states.

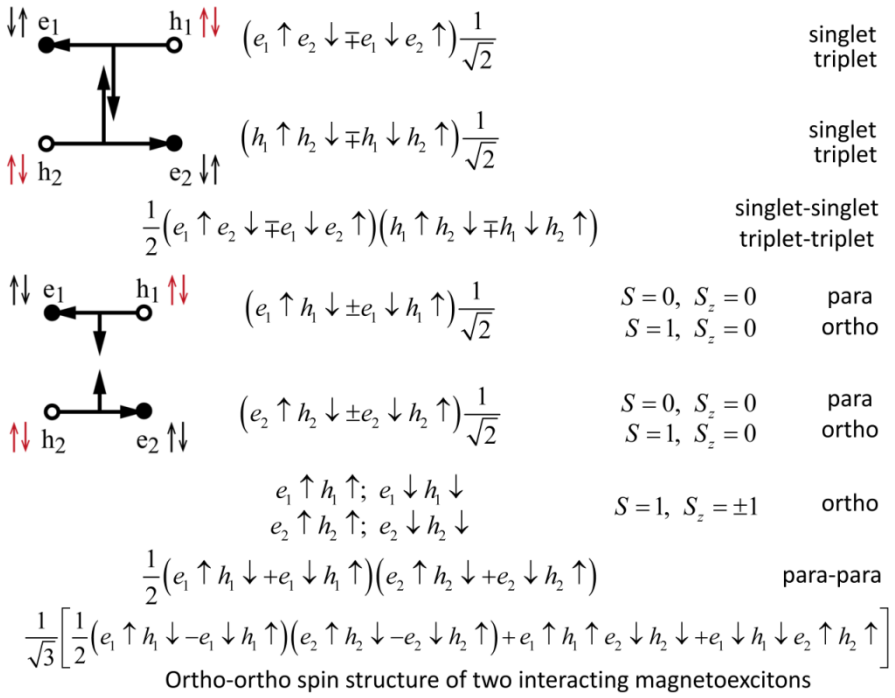

Fig. 4. Spin structure of two magnetoexcitons.

Four different spin structures were studied, and the Coulomb interaction integrals were calculated. The encountered Feynman diagrams containing the solid electron lines and the dashed hole lines can have an odd number of intersections, or an even number of intersections, or none intersections. All of them (Fig. 5) can be grouped in two main terms with spins structure parameter η, which takes four different values, namely, $+1$, -1, $+1/2$, $-1/2$:

$$E_{Bimex}=\frac{\left\langle\psi_{Bimex}(0,\eta)\middle|H_{Coul}^{LLL}\middle|\psi_{Bimex}(0,\eta)\right\rangle}{\left\langle\psi_{Bimex}(0,\eta)\middle|\psi_{Bimex}(0,\eta)\right\rangle};$$

$$\left\langle\psi_{Bimex}(0,\eta)\middle|H_{Coul}^{LLL}\middle|\psi_{Bimex}(0,\eta)\right\rangle=\left\langle\begin{matrix}\text{Feynman diagrams}\\ \text{without intersections or}\\ \text{with even numbers}\\ \text{of intersections}\end{matrix}\right\rangle+\eta\left\langle\begin{matrix}\text{Feynman diagrams with}\\ \text{odd numbers}\\ \text{of intersections}\end{matrix}\right\rangle;$$

$$\left\langle\psi_{Bimex}(0,\eta)\middle|\psi_{Bimex}(0,\eta)\right\rangle=2\left(1-\eta L_n(\alpha)\right),\ \text{where}$$

$\eta=1$ triplet–triplet spin structures of 2e+2h,

$\eta=-1$ singlet–singlet spin structures of 2e+2h,

$\eta=\frac{1}{2}$ ortho–ortho magnetoexcitons,

$\eta=-\frac{1}{2}$ para–para magnetoexcitons. (1)

The exact analytical calculations were performed because the binding energy was expected to be small or absent at all.

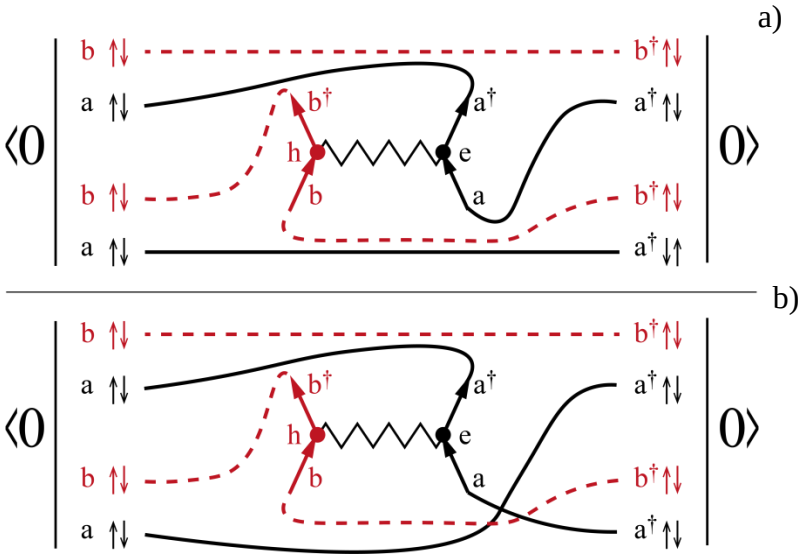

Fig. 5. Feynman diagrams describing the Coulomb electron–hole (e–h) interactions in the frame of the metastable bound state of two magnetoexcitons: (a) the case without intersections and (b) the case with one intersection.

The determined total energy of the Coulomb interaction as a function of variational parameter α is shown in Fig. 6.

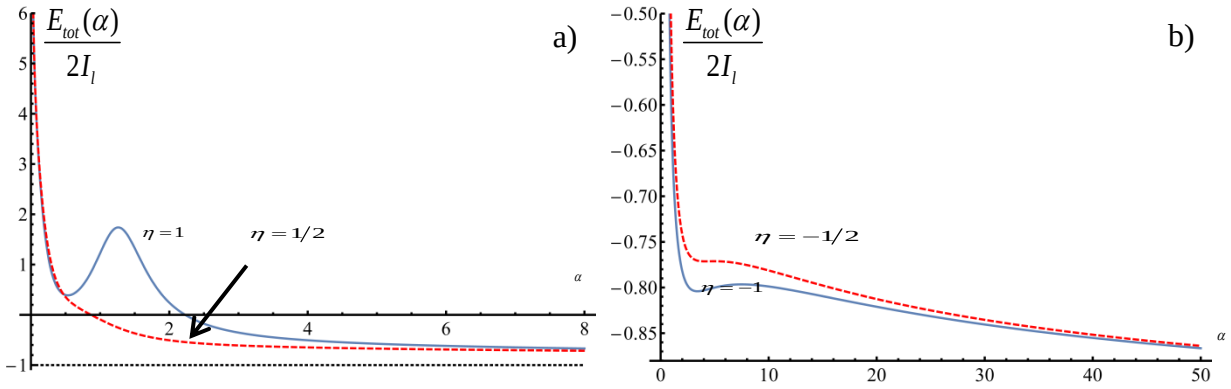

Fig. 6. Total energies of two bound 2D magnetoexcitons with wave vectors $\vec{k}$ and $-\vec{k}$, with different spin structures $\eta = \pm 1, \pm 1/2$ and with the variational wave function $\varphi_2(k)$ as a function of parameter α: (a) the case $\eta = 1,\ 1/2$ and (b) the case $\eta = -1, -1/2$. The total energies are normalized to the value $2I_l$, where I_l is the ionization potential of a free magnetoexciton with wave vector $\vec{k} = 0$.

The energy of two free magnetoexcitons with $k = 0$ is represented by the -1 line. At any α value, stable bound states are absent. All the states are unstable as regards the dissociation in two free magnetoexcitons with $k = 0$. However, despite this fact, in the triplet–triplet spin configuration, a metastable bound state with a considerable energy barrier of the order of two ionization potentials of two free magnetoexcitons was revealed. If we used the dipole–dipole

interaction, we could not meet with the metastable bound state. Two antiparallel 2D dipole moments repeal each other, and their interaction energy is positive, whereas two parallel 2D dipoles attract each other. It is evident from the formulas below:

$$V_{\vec{d}_1\vec{d}_2} = \frac{e^2}{\varepsilon_0}\left[\frac{\vec{d}_1\cdot\vec{d}_2}{R^3} - \frac{3(\vec{d}_1\cdot\vec{R})(\vec{d}_2\cdot\vec{R})}{R^5}\right];$$

$$V_{\substack{(\uparrow\uparrow)\\(\uparrow\downarrow)}}(R) = \pm\frac{e^2d^2}{\varepsilon_0 R^3}\left(1-3\cos^2\varphi\right) \simeq \mp\frac{e^2d^2}{2R^3\varepsilon_0}; \qquad \overline{\cos^2\varphi} = \frac{1}{2}. \tag{2}$$

Despite these properties of the dipole–dipole interaction, which can give only a rough picture of the Coulomb interaction in the frame of confined particles, the metastable bound state can exist.

2. Tunneling and the New Luminescence Band

The tunneling properties and the new luminescence band arising due to the existence of the metastable bound state will now be discussed using Fig. 7, where an effective rectangular barrier with height *U*–*E* and with length l_b was introduced.

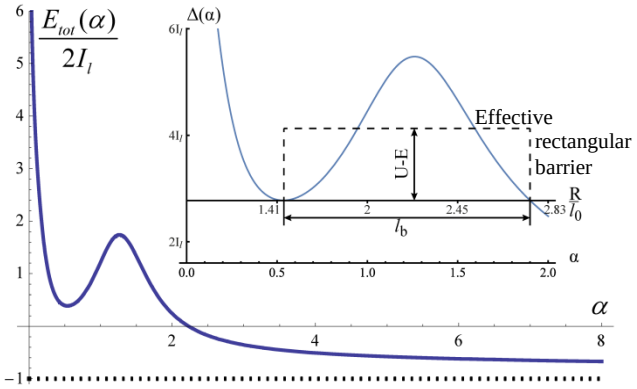

Fig. 7. Tunneling property of the metastable bound state.

The coefficient of the transparency of the energy barrier was estimated as 4%:

$$T = e^{-\frac{2}{\hbar}\sqrt{2M(U-E)}l_b} \sim e^{-3.2} \sim 10^{-1.4} \approx 0.04. \tag{3}$$

It does not depend on magnetic field strength *B*. The lifetime of the hypothetical particle confined in the trap behind the barrier can be estimated using the theory of the α-decay [3]. It is supposed that the hypothetical particle has the mass equal to one half of the magnetic mass *M*(*B*) of the magnetoexciton. It performs N_{bl} blows on the back of the barrier trying to escape from the trap and evade tunneling through the barrier. The number of the blows was estimated as follows:

$$N_{bl} \sim \frac{\mathrm{v}_0}{2r_0} \sim \frac{\hbar}{2Mr_0^2} \sim \frac{10^{13}}{\mathrm{sec}}, \tag{4}$$

where r_0 is the radius of the trap.

This number multiplied by the transparency coefficient gives rise to the probability of tunneling

$$P = N_{bl}T \simeq \frac{1}{\tau} \tag{5}$$

and life time τ in the metastable state. It equals to a few picoseconds: $\tau \sim 2.5$ ps. This life time is sufficient to permit the measurement of the radiative recombination process, when one magnetoexciton annihilates with the emission of the cavity photon, if the system is embedded into microcavity, leaving the second exciton in the state of para-magnetoexciton. This process is shown in Fig. 8.

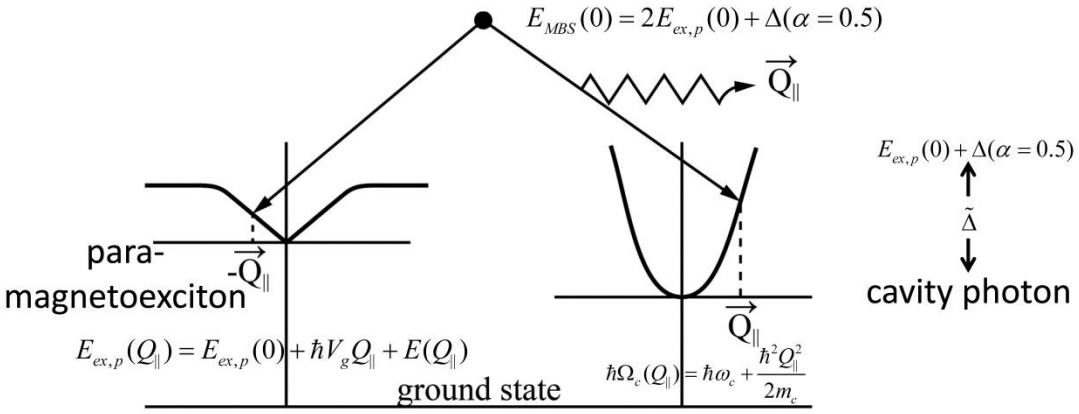

Fig. 8. Radiative recombination of the metastable bound state.

It is the conversion of the metastable state in the para-magnetoexciton. The probability of the conversion was estimated at about $10^8 - 10^{10}$ sec^{-1}:

$$P(\omega_c) = \frac{4e^2 m_c \,|\, \vec{e}_c \cdot \vec{p}_{c-v} \,|^2}{\pi c m_0^2 \hbar^2} e^{-\frac{2\tilde{\Delta} m_c l_0^2}{\hbar^2}} \approx 10^8 - 10^{10} \frac{1}{\text{sec}}, \tag{6}$$

where

$$m_c = 10^{-5} m_0, \quad l_0 \sim 10^{-6} \text{ cm}, \quad | \, p_{c-v} \, | \sim 10^{-20} - 10^{-19} \frac{\text{g cm}}{\text{sec}}, \quad \tilde{\Delta} = E_{ex,p}(0) + \Delta(\alpha = 0.5) - \hbar\omega_c. \tag{7}$$

The probability has a sharp, almost dropping dependence at the high energy side of the band due to the linear dispersion law of the para-magnetoexciton (see Fig. 9).

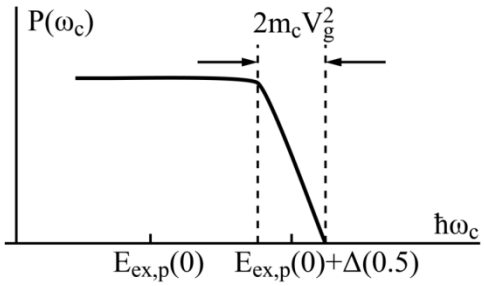

Fig. 9. Probability of the radiative recombination process.

The new luminescence band is shown in Fig. 10. It is located on the high energy side as regards the exciton luminescence line, because the molecular metastable state has the positive energy.

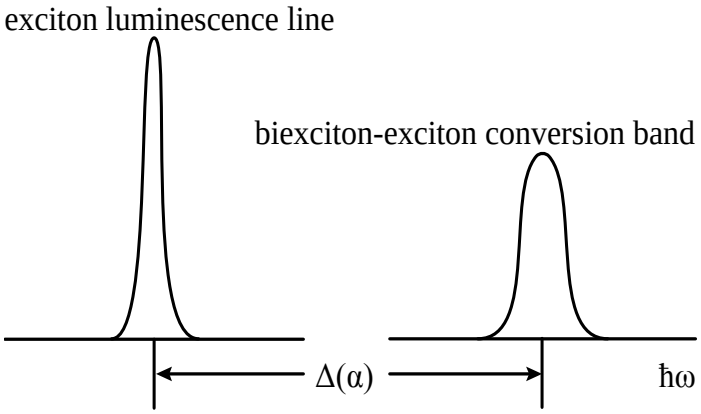

Fig. 10. Luminescence band of the metastable bound state due to radiative recombination with the emission of the photon and with the creation of the para-magnetoexciton. The new luminescence M band is situated at higher frequencies than the frequencies of the para-magnetoexciton luminescence line.

3. Thermodynamics of Para-Magnetoexcitons

To date, it has been known that magnetoexcitons are characterized by the quadratic dispersion law with magnetic mass $M(B)$ increasing with an increase in magnetic field strength B. We have found that the exchange Coulomb e–h interaction, being taken into account supplementary to the direct interaction, leads to the anisotropic linear dispersion law referred to as the anisotropic Dirac cone. It is shown in Fig. 11.

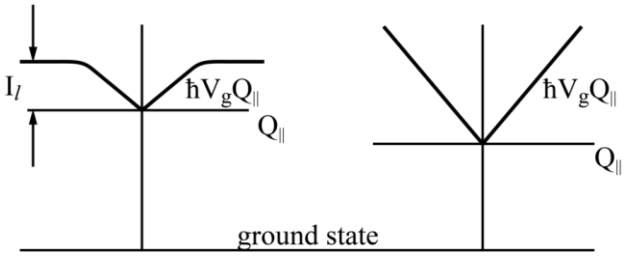

Fig. 11. Anisotropic Dirac cone-like dispersion law of the para-magnetoexciton with linear polarization at the same direction of the wave vector.

The group velocity is present only in the case of para-exciton $(\xi = 1)$ and is absent in the case of ortho-exciton $(\xi = -1)$; it is proportional to oscillator strength f_{ex} of the exciton transition. It means that the anisotropic linear dispersion law appears only in the case of the dipole-active, bright para-magnetoexciton line. The group velocity increases with increasing magnetic field strength:

$$E_{ex,p}(Q_\parallel) = E_{ex,p}(0) + \hbar V_g Q_\parallel + E(Q_\parallel),$$

$$k_B T_c = \left[\frac{2\pi\hbar^2 V_g^2 \sigma}{g_2(1)} \right]^{1/2},$$

$$V_g = \frac{(1+\xi)}{2} \frac{e^2}{\varepsilon_0 \hbar} \left| \frac{\vec{\rho}_{c-v}}{l_0} \right|^2 \sim B; \quad \xi = \begin{cases} +1, \text{ para} \\ -1, \text{ ortho} \end{cases}, \tag{8}$$

where

$$\left|\vec{\rho}_{c-v}\right|^2 \sim f_{ex} \frac{\pi\hbar}{4 m_0 \omega_{ex}} \left(\frac{a_{ex}}{a_0} \right)^3, \tag{9}$$

and resulted in

$$V_g = \frac{1+\xi}{2} f_{ex} \left(\frac{a_{ex}}{a_0} \right)^3 \frac{\pi e^2}{4 m_0 \varepsilon_0 \omega_{ex}} \frac{1}{l_0^2}, \tag{10}$$

where f_{ex} is the exciton oscillator strength, $\vec{\rho}_{c-v}$ is the inter-band matrix element of the coordinate, ω_{ex} and a_{ex} are the exciton frequency and radius correspondingly, and a_0 is the lattice constant.

The range of the wave vectors, where the linear dispersion takes place is sufficiently large: $k < 1/l_0$. As a consequence, the Bose–Einstein condensation (BEC) conditions for para- and ortho-magnetoexcitons are completely different.

It is well known that the 2D Bose gas with the quadratic dispersion law situated on infinite area S has the BEC temperature equal to zero according to the Hohenberg theorem [4]. To obtain the BEC of cavity exciton polaritons at nonzero temperatures, it was necessary to confine them on the light spot formed by a laser beam on the surface of the quantum well embedded into a microcavity. The experimental physicists' ingenuity succeeded to avoid the Hohenberg theorem.

In the case of the isotropic Dirac cone dispersion law the critical temperature T_c is proportional to group velocity V_g and to the square root of the magnetoexciton density σ. At $V_g = 10^4$ cm/sec and $\sigma = 10^{12}$ cm^{-2}, the critical temperature is 1 K. The BEC of para-magnetoexcitons on the state $k = 0$ will be possibly implemented without confining them on the spot.

With the isotropic linear dispersion law, the capacity to accommodate the noncondensed particles in the range of small wave vectors is limited; that is, it is not infinite as was earlier. The BEC of magnetoexcitons on the single-particle state with considerable wave vectors $kl_0 \sim 3-4$ at temperature T=0 was investigated in [5]. In this case, we have the magnetoexcitons with parallel

wave vectors and with dipole moments which attract each other. The attraction in the system is an adversary to the BEC. Nevertheless, taking into account the correlation energy and the polarizability of the Bose condensate as a whole using the coherent excited states, it was shown that the metastable Bose–Einstein (BE) condensation at $T=0$ does exist [5]. It is shown in Fig. 12.

Another property of the BEC of magnetoexcitons is the requirement for filling factors ν of the lowest Landau level. They should not exceed the fractional value $1/3\left(\nu \le 1/3\right)$. At this limit, we meet the phenomena encountered in the case of one component 2D electron gas (OC2DEG) under conditions of the fractional quantum Hall effects (FQHEs). As was outlined by Stormer [6], the fascinating properties discovered in the FQHEs arise from the strongly correlated motion of many electrons. It is not fission that leads to fractionally charged quasiparticles, but the interplay of many electrons that "collaborate" and create the bizarre objects (see Fig. 13). For example, the electrons absorb magnetic flux quanta seemingly eliminating the external magnetic field.

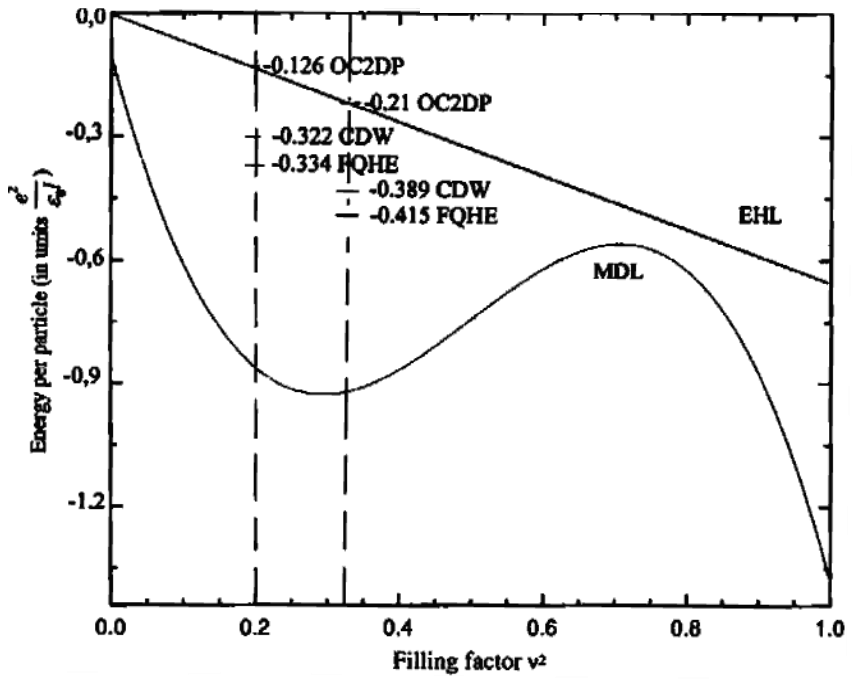

Fig. 12. Energies per particle in units $e^2/(l_0\varepsilon)$ in four different ground states of the OC2DEG and the 2D e–h system, such as: incompressible quantum liquid (IQL) arising under condition of FQHE, charge density wave (CDW), one-component two-dimensional plasma (OC2DP) with the properties similar to those of the e–h liquid (EHL) and the metastable dielectric liquid (MDL) phase formed by BEC 2D magnetoexcitons [5].

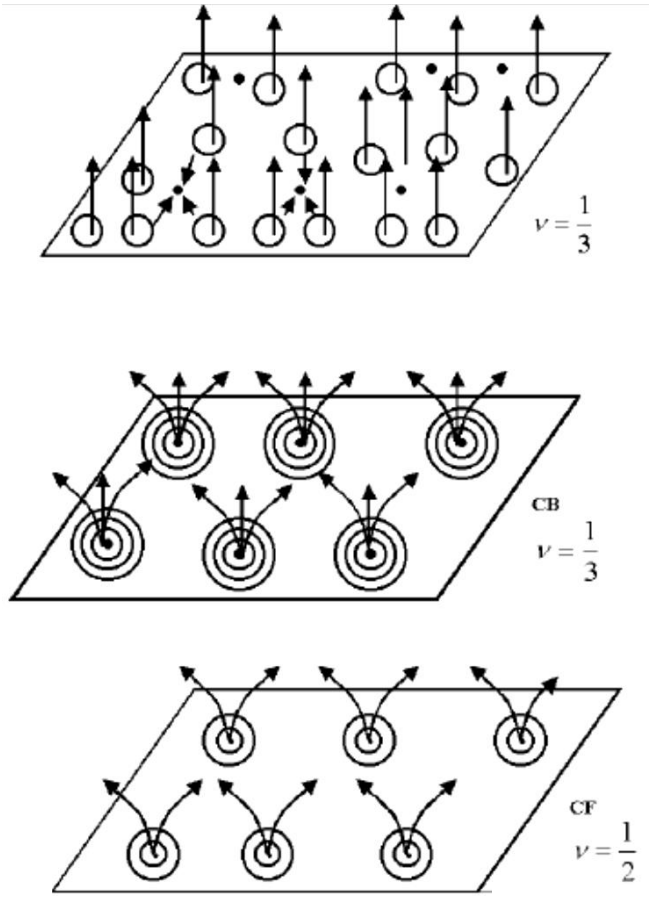

Fig. 13. Vortex content in the composite bosons and composite fermions [6].

Particle statistics are altered from fermionic to bosonic. These properties were revealed studying the 2D electron gas under conditions of the fractional filling factor of the lowest Landau level. When the filling factors of the lowest Landau levels for the electrons and the holes are approaching fractional values, such as $1/2$ and $1/3$, we can expect a similar behavior. The first result in this direction will be communicated. It is well known that new stunning states of the matter were discovered [6–9]. They can be explained using the concept of composite particles arising in the form of electrons with attached flux quanta ϕ_0, as was proposed by Wilczek [7] or, in another version, with attached vortices, as was proposed by Read [8].

The new gauge field created by the quantum point vortices can be introduced into the Hamiltonian by the Chern and Simons unitary transformation $\hat{U}(\vec{r})$, as was proposed by Halperin, Lee, and Read [9].

The flux quanta and the attached vortices to the electrons for filling factor $\nu = 1/2$ and $1/3$ are shown in Fig. 13. It is supposed that each flux quantum generates one quantum point vortex.

Each vortex generates its magnetic field. The flux Φ of the external magnetic field with strength B through the layer surface area S equals to N flux quanta ϕ_0 as follows:

$$\Phi = BS = N\phi_0, \tag{11}$$

where

$$\phi_0 = \frac{2\pi\hbar c}{e} = B\cdot 2\pi l_0, \;\; N = \frac{S}{2\pi l_0^2}, \;\; l_0^2 = \frac{\hbar c}{eB}. \tag{12}$$

The generated magnetic field compensates the external magnetic field B. It is apparently eliminated and the new composite particles undergo their Fermi degeneracy or their BEC.

Our version with two-component e–h system is shown below. The unitary transformation introducing the Chern–Simons gauge field has the form

$$\hat{U}\left(\vec{r}\right) = e^{\frac{ie}{\hbar c}\hat{\omega}(\vec{r})} \tag{13}$$

with vector potential $\vec{a}(\vec{r})$

$$\vec{a}(\vec{r}) = \vec{\nabla}\hat{\omega}\left(\vec{r}\right) = -\frac{\phi e}{\alpha}\int d^2\vec{r}\,'\vec{\nabla}\theta\left(\vec{r}-\vec{r}\,'\right)(\hat{\rho}_e\left(\vec{r}\,'\right)-\hat{\rho}_h\left(\vec{r}\,'\right)), \tag{14}$$
$$\phi = 1, 2, 3..., \quad \alpha = e^2/(\hbar c) = 1/137.$$

depending on value $\vec{V}\left(\vec{r}-\vec{r}\,'\right)$ proportional to the unit azimuthal vector $\vec{\epsilon}_{(\vec{r}-\vec{r}\,')}$ as follows:

$$\vec{V}\left(\vec{r}-\vec{r}\,'\right) = \frac{\vec{e}_x(\vec{y}-\vec{y}\,')-\vec{e}_y(\vec{x}-\vec{x}\,')}{|\vec{r}-\vec{r}\,'|^2} = \frac{\vec{\epsilon}_{(\vec{r}-\vec{r}\,')}}{|\vec{r}-\vec{r}\,'|}; \qquad \vec{\epsilon}_{(\vec{r}-\vec{r}\,')} = \frac{\vec{e}_x(\vec{y}-\vec{y}\,')-\vec{e}_y(\vec{x}-\vec{x}\,')}{|\vec{r}-\vec{r}\,'|}. \tag{15}$$

The 2D quantum vortex has the center at point $\vec{r}$ and the velocity at point $\vec{r}\,'$, as shown in Fig. 14 with the property

$$\mathrm{curl}\,\vec{V}\left(\vec{r}-\vec{r}\,'\right) = \Delta\ln\left|\vec{r}-\vec{r}\,'\right| = 2\pi\delta^2\left(\vec{r}-\vec{r}\,'\right). \tag{16}$$

The bare and the dressed field operators are

$$\hat{\psi}_e\left(\vec{r}\right) = \hat{U}^+\left(\vec{r}\right)\hat{\psi}_e^0\left(\vec{r}\right); \quad \hat{\psi}_h\left(\vec{r}\right) = \hat{U}\left(\vec{r}\right)\hat{\psi}_h^0\left(\vec{r}\right). \tag{17}$$

The bare electron and hole operators obey the Fermi statistics:

$$\hat{\psi}_i^0\left(\vec{r}\right)\hat{\psi}_j^{0\dagger}\left(\vec{r}\,'\right)+\hat{\psi}_j^{0\dagger}\left(\vec{r}\,'\right)\hat{\psi}_i^0\left(\vec{r}\right) = \delta_{ij}\delta^2\left(\vec{r}-\vec{r}\,'\right), \tag{18}$$

whereas the composite particles are described by new operators (17). They obey Fermi or Bose statics depending on the even or odd numbers, respectively, of parameter ϕ in definition (14).

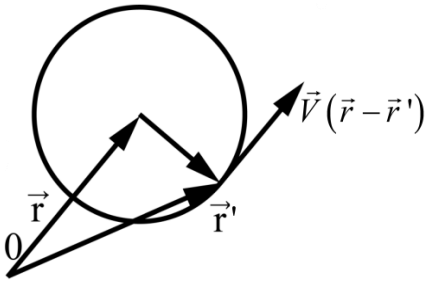

Fig. 14. 2D quantum point vortex with the velocity at point $\vec{r}'$ and singular vorticity at point $\vec{r}$.

In our case, vector potential $\vec{a}(\vec{r})$ of the Chern–Simons field depend on the difference between the densities of the electrons and the holes, $\hat{\rho}_e(\vec{r}')$ and $\hat{\rho}_h(\vec{r}')$. In the zeroth approximation, when the density operators can be substituted by their average values, the new vector potential vanishes. The external magnetic field does not disappear. It continues to effectuate the Landau quantization of the composite particles.

The statistics of the composite particles is changed simultaneously for the electrons and the holes because they attach an equal number of vortices. Kinetic energies of the composite particles look as follows:

$$\frac{\hbar^2}{2m_e}\left(-i\vec{\nabla}_e+\frac{e}{\hbar c}\vec{A}(\vec{r}_e)+\frac{e}{\hbar c}\hat{\vec{a}}(\vec{r}_e)\right)^2+\frac{\hbar^2}{2m_h}\left(-i\vec{\nabla}_h-\frac{e}{\hbar c}\vec{A}(\vec{r}_h)-\frac{e}{\hbar c}\hat{\vec{a}}(\vec{r}_h)\right)^2. \qquad (19)$$

The Coulomb interaction gives rise to the binding energy, the ionization potential, and the dispersion law (Fig. 15) due to the strong interdependence between the center-of-mass and the relative e–h motions.

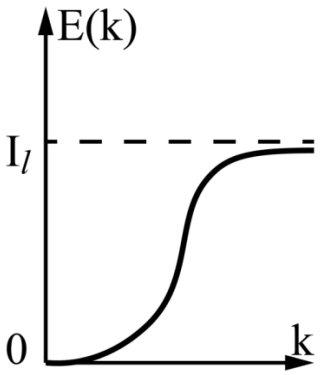

Fig. 15. Dispersion law of the magnetoexciton.

In the first order of the perturbation theory, one can observe how the new gauge field affects the magnetoexcitons currently consisting of composite electrons and holes. It was shown that, in addition to the previous isotropic term of the dispersion law shown above in Fig. 15, new anisotropic components of the magnetic mass appear. The isotropic magnetic mass $M(B)$ due to the Coulomb interaction and anisotropic components M_x and M_y due to new gauge vector potential are as follows:

$$M(B) = \frac{\hbar^2}{2I_l l_0^2} = \frac{\hbar^2 \varepsilon_0}{\sqrt{2\pi} e^2 l_0},$$

$$\left(\frac{1}{m_e} - \frac{1}{m_h}\right) M_x = \frac{2\alpha\hbar^2 c^2}{3\phi e^3 l_0^2 B} \approx 0.4; \quad M_y = 3M_x, \tag{20}$$

where $l_0 = 10^{-6}$ cm^2 at a magnetic field strength of B = 6 T. It takes place when effective masses m_e and m_h do not coincide. The isotropic mass increases with increasing magnetic field strength B, whereas the anisotropic component does not depend on it.

4. Conclusions

In the lowest Landau levels approximation, stable bound states of the magnetic biexcitons do not exist due to the hidden symmetry in the e–h system.

The metastable bound state with a lifetime of about few picoseconds has been revealed.

The conversion of the metastable bound state into the para-magnetoexciton state gives rise to a new luminescence band situated at higher frequencies than those of the para-magnetoexciton luminescence line.

The allowance for the exchange e–h Coulomb interaction in the case of the dipole-active para-magnetoexcitons leads to the dispersion law of the anisotropic Dirac cone-type.

The isotropic Dirac cone-type dispersion law gives rise to the finite temperature of the BEC of the 2D magnetoexciton gas.

The Chern–Simons gauge field leads to the formation of composite electrons and holes with equal numbers of attached quantum point vortices.

The effective magnetic field created by quantum point vortices in the case of the coplanar 2D e–h system vanishes in the mean-field approximation, and the composite particles undergo the Landau quantization as a whole in an external magnetic field.

The vector potentials of the external magnetic field and of the gauge Chern–Simons field lead to the anisotropy of the 2D magnetoexciton magnetic mass.

References

[1] D. Paquet, T. M. Rice, and K. Ueda, Phys. Rev. B 32, 5208 (1985).
[2] I. V. Lerner and Yu. E. Lozovik, Zh. Eksp. Teor. Fiz. 80, 1488 (1981) [Sov. Phys. – JETP 53, 763 (1981)].
[3] D. I. Blokhintsev, Quantum Mechanics, D. Reidel Publishing Company, Dordrecht, Holland, Springer Netherlands, 1964.
[4] P. C. Hohenberg, Phys. Rev. 158, 3837 (1967).
[5] S. A. Moskalenko, M. A. Liberman, D. W. Snoke, and V. Botan, Phys. Rev. B 66, 245316 (2002).
[6] H. L. Stormer, Rev. Mod. Phys. 71, 4, 875 (1999).
[7] F. Wilczek, Phys. Rev. Lett. 48, 1144 (1982); 49, 957 (1982).
[8] N. Read, Phys. Rev. B 58, 16262 (1998).
[9] B. I. Halperin, P. A. Lee, and N. Read, Phys. Rev. B 47, 7312 (1993).

RELAXATION OF THE BINDING ENERGY OF ELECTRONS WITH PHONONS IN METALS

Nicolas I. Grigorchuk

Bogolyubov Institute for Theoretical Physics, National Academy of Sciences of Ukraine,
14-b Metrologichna Str., Kyiv-143, Ukraine 03143
E-mail: ngrigor@bitp.kiev.ua

(Received June 11, 2018)

Abstract

The relaxation of the electron energy on the lattice fluctuations in metals is studied. The energy distribution of the electrons and phonons over states is considered to be equilibrium, so that it can be described by the Fermi and Bose functions correspondingly. An analytical formula for loss of electronic energy per unit time required to start acoustic oscillations of a lattice is obtained. It is shown that the magnitude of the power absorbed by the lattice is determined by the Debye and lattice ratios as well as by the ratio of the lattice and electron temperatures.

1. Introduction

Interaction between electrons and phonons is one of the main characteristics in the study of the fundamental properties of the physics of condensed media. A general theory of electron scattering on phonons has been developed by many authors; the main results can be found, for example, in the Ziman's monograph [1]. Different aspects of this problem in the case of bulk metals were studied in [2–12]. Fundamentals of the theory of electron–phonon interaction were developed in [2–4]. Electron–phonon relaxation plays an important role in high-frequency electronic devices [5, 6] and ultrashort laser processes [7], when electrons and phonons are in a nonequilibrium state due to a significant difference in their heat capacities. The unbalanced energy exchange between the electrons and the grating has been first theoretically estimated in [8]. In terms of practice, it is necessary to know both the electron temperature and the lattice temperature during the heating of the metals with a short laser pulse. To a certain extent, this problem can be solved by a well-known two-temperature model [9–12], which is based on two differential equations of balance of heat fluxes in bulk metals.

There is considerable interest in determining the change in the energy of the electron–phonon coupling when the volumetric metals are reduced to metal nanoparticles, metal islands, films, or clusters, where the particle surface has a significant effect on all processes [13–16]. It is caused by a more general physical problem: how are the well-known physical parameters transformed when the spatial dimensions of the metal are reduced and the surface begins to act as an additional diffuser? To solve this problem, it is primarily necessary to clarify the features of the electron-phonon coupling in the bulk metals.

In this paper, we propose a new approach to calculating the energy of electron–phonon interaction in metals. This approach makes it possible analytically to estimate the energy of the damping of electrons on the fluctuations of the lattice in a bulk metal depending on the temperatures of both the electrons and the lattice.

The paper is constructed as follows: general theoretical statements are given in the second section; Section 3 is devoted to the calculation of the change in the energy of electrons in collisions with phonons; and the last section contains brief conclusions.

2. General Statements

The interaction of an electromagnetic (EM) wave with metals will be studied in terms of classical optics. It is believed that every electron receives an impulse from an external field that accelerates of it movement, and for some time, which is referred as the lifetime τ, it moves freely. However, in the collision with the lattice, the electron velocity is lost, and excess energy is transmitted by the vibration of the ions. In this case, the creation and annihilation of phonons take place.

The efficiency of the energy transfer from the laser beam to the metal essentially depends on the mean free path (MFP) of the conduction electron in infinite volume l_∞ and on Debye length $l_D = \pi\upsilon_F\omega_D$, where υ_F is the electron velocity at the Fermi surface and ω_D is the Debye frequency. The parameter l_D plays an important role in the energy exchange between hot electrons and the lattice. The values of this parameter for noble metals are given in Table 1 together with the electron concentration n and the Debye temperature T_D.

In the classical case of free electrons in the metal volume, the damping ($\gamma_b = \nu$, where ν is the frequency of electron collisions) is due to the scattering of electrons by phonons, lattice defects, or impurities, which, in general, reduce the electron MFP. In this case, the volumetric damping is commonly given as $\gamma_b = \upsilon_F/l_\infty$.

Table 1. Values of some parameters for noble metals

Metals	l_D (Å)	l_∞ (Å) [17]	υ_F (cm/s) [18]	n_e (cm^{-3}) [18]	ω_D (s^{-1}) [19]	T_D (K) [19]
Cu	1197	399	$1.57 \cdot 10^8$	$8.45 \cdot 10^{22}$	$4.49 \cdot 10^{13}$	315
Ag	1552	533	$1.39 \cdot 10^8$	$5.85 \cdot 10^{22}$	$2.95 \cdot 10^{13}$	215
Au	1968	377	$1.394 \cdot 10^8$	$5.90 \cdot 10^{22}$	$2.16 \cdot 10^{13}$	170

Volumetric scattering does not cause significant damping at high frequencies when $\omega\tau >> 1$. Here, ω is the angular frequency of light and τ is the lifetime of the electron (or relaxation time), which can be estimated as $1/\tau = \gamma_b$. On the other hand, the contribution of surface scattering to damping is negligible only when

$$l_\infty / d << \sqrt{1+\omega^2\tau^2}, \tag{1}$$

where d is the particle size, and becomes important if

$$\omega\tau >> \max(1, l_\infty / d). \tag{2}$$

To estimate the effect of electron scattering on the surface, the following empirical ratio is generally used [20–22]:

$$\gamma_s = A\upsilon_F/l_{ef}, \tag{3}$$

where l_{ef} is the effective MFP of electron and A is a phenomenological factor. However, this

formula can only be applied to the spherical metal clusters if the electron MFP l is smaller than their size.

3. Variation in the Electron Energy Interaction with Phonons by Collisions

Let us consider the scattering of EM waves in a metal with much larger dimensions as l. In this case, the collisions of conduction electrons with the lattice oscillations become the most important relaxation process and no other electron energy exchanges will be considered.

The irradiation of a massive metal at an initial stage leads to the heating of the electron gas inside of it. Since the time of establishment of equilibrium between the electrons after excitation is much shorter than the time of establishment of equilibrium between the electrons and the lattice, we can assume that the electron gas is in equilibrium, with the Fermi–Dirac distribution over the energy of an individual electrons; that is,

$$n_k = \frac{1}{e^{\frac{\varepsilon_k - \mu}{k_B \Theta}} + 1}, \tag{4}$$

where Θ is the electron temperature and μ is the chemical potential, which is determined by the concentration of electrons n_e using the expression [23]

$$\mu = \left(\frac{3n_e}{8\pi}\right)^{2/3} \frac{(2\pi\hbar)^2}{2m}, \tag{5}$$

where m is the electron mass.

It is believed that electron temperature Θ is much higher than the lattice temperature, which will be denoted by the letter *T*; namely, $\Theta \gg T$. The maximum of the temperature difference between the electrons and the lattice, which defines the relaxation time of the electrons, is determined by the rate of heat transfer from the electrons to the lattice.

Let us calculate the amount of energy transmitted by the lattice to electrons per unit volume per unit time at arbitrary temperatures. In accordance with the standard method [24],

$$\frac{dU}{dt} = W = \frac{V}{(2\pi)^3} \int \frac{dN_{\mathbf{q}}(t)}{dt} E(\mathbf{q})\, d\mathbf{q}, \tag{6}$$

where V is the volume of the crystal, the time derivative under the integral describes the change in the number of phonons per unit time in unit volume, $E(\mathbf{q}) = \hbar \mathbf{q} \overleftarrow{\upsilon}_s$ is the energy of the phonon with momentum $\mathbf{q}$, and $\overleftarrow{\upsilon}_s$ denotes the speed of sound in the crystal.

Let $P_{\mathbf{k}_i, \mathbf{k}_i + \mathbf{q}}$ be the probability of transition of an electron from a state with wave vector $\mathbf{k}_i$ to a state with wave vector $\mathbf{k}_i + \mathbf{q}$. In the case of interaction of an electron with a lattice, a phonon is generated or absorbed, while the laws of the momentum $\mathbf{q} = \mathbf{k}_f - \mathbf{k}_i$ and the energy conservation are fulfilled:

$$\delta\varepsilon = \frac{m\upsilon_f^2}{2} - \frac{m\upsilon_i^2}{2} = \frac{\hbar^2}{2m}(k_f^2 - k_i^2) = \pm E(q),$$
$$2m\upsilon_F \sin\frac{\varphi}{2} \approx \frac{E(q)}{\upsilon_s}, \tag{7}$$

where υ_i is the initial electron velocity, υ_f is the final electron velocity, υ_F is the electron velocity on the Fermi sphere, and φ is the angle between the initial and the final direction of the electron velocity. The signs (–) and (+) correspond to the absorption and creation of the phonon, respectively. For about half a lifetime, the electron undergoes collisions with the radiation of the phonon, while the other half of this time is characterized by collisions with the absorption of the phonon. Considering the interaction of electrons with a lattice being linear in relation to the coordinates of the sound field oscillators, i.e., proportional to the displacement of the ions, then the probability of the phonon radiation is proportional to the number $N_{\mathbf{q}} + 1$, and the probability of phonon absorption is proportional to the number $N_{\mathbf{q}}$. In accordance with the energy conservation law, this probability will be as follows: $P_{\mathbf{k},\mathbf{k}\pm\mathbf{q}}\delta(\varepsilon_{\mathbf{k_i}} + E(\mathbf{q}) - \varepsilon_{\mathbf{k}_f})$. Thus, proceeding from the above,

$$P_{\mathbf{k},\mathbf{k}'} = \frac{\pi D^2}{\rho V \hbar \upsilon_s^2} E(\mathbf{q}), \tag{8}$$

where D is the interaction constant of an electron with a lattice, ρ is the mass density of the crystal, and $\mathbf{k}' = \mathbf{k} \pm \mathbf{q}$.

Let us find a change in the number of phonons per unit time, which appear in Eq. (6). According to the Harrison [24],

$$\frac{N_{\mathbf{q}}(t)}{dt} = \int P_{\mathbf{k_i},\mathbf{k_i}\pm\mathbf{q}} \Big[(N_{\mathbf{q}} + 1) n_{\mathbf{k}_f} (1 - n_{\mathbf{k_i}}) - N_{\mathbf{q}}$$
$$\times n_{\mathbf{k_i}} (1 - n_{\mathbf{k}_f}) \, \delta(\varepsilon_{\mathbf{k}_i} + E(\mathbf{q}) - \varepsilon_{\mathbf{k}_f}) \Big] dV_{\mathbf{k}_f}. \tag{9}$$

Here,

$$N_q = \frac{1}{e^{\frac{E(q)}{k_B T}} - 1}. \tag{10}$$

The change in the number of phonons in time in Eq. (9) is due to their creation and annihilation. These processes can occur provided that the electron velocity is greater than the speed of sound in the crystal. In this case, the "creation" of a phonon corresponds to the classical Cherenkov radiation. When the temperatures of the electrons and the phonons are equal, expression (9) becomes zero. Let us calculate expression (9) when these temperatures are different. Let us first explicitly express the expression in the square brackets of Eq. (9) in terms of the respective energy and temperature using the distribution functions for $n_{\mathbf{k}}$ and $N_{\mathbf{q}}$ and the law

of energy conservation $\varepsilon_{\mathbf{k}_i} = \varepsilon_{\mathbf{k}_f} - E(\mathbf{q})$. After simple algebraic transformations, we obtain

$$(N_{\mathbf{q}}+1)n_{\mathbf{k}_f}(1-n_{\mathbf{k}_i}) - N_{\mathbf{q}}n_{\mathbf{k}_i}(1-n_{\mathbf{k}_f})$$
$$= \frac{1}{e^{(\varepsilon_{\mathbf{k}_f}-\mu)/k_B\Theta}+1}\frac{e^{E(\mathbf{q})/k_BT}-e^{E(\mathbf{q})/k_B\Theta}}{e^{E(\mathbf{q})/k_BT}-1}$$
$$\times\frac{e^{(\varepsilon_{\mathbf{k}_f}-\mu-E(\mathbf{q}))/k_B\Theta}}{e^{(\varepsilon_{\mathbf{k}_f}-\mu-E(\mathbf{q}))/k_B\Theta}+1}. \tag{11}$$

Substituting this expression into Eq. (9), we pass in it to the integration over finite states in the space of quasi-impulses by the rule

$$\int dV_{\mathbf{k}_f} = \int_0^{2\pi}\int_0^{\pi}\sin\vartheta\, d\vartheta\int_0^{k_{max}}k_f^2\, dk_f, \tag{12}$$

where $k_{max} = k_F$ is the maximum momentum of an electron (Fermi pulse), and we take into account the property of the δ-function:

$$\delta(x^2-a^2) = \frac{1}{2a}[\delta(x-a)+\delta(x+a)]. \tag{13}$$

As a result, we find

$$\frac{N_{\mathbf{q}}(t)}{dt} = \frac{(2m)^{3/2}D^2E(\mathbf{q})}{4\pi\hbar^4\rho V\upsilon_s^2}\sqrt{\varepsilon_F+E(\mathbf{q})}$$
$$\times\frac{e^{E(\mathbf{q})/k_BT}-e^{E(\mathbf{q})/k_B\Theta}}{(e^{E(\mathbf{q})/k_B\Theta}+1)(e^{E(\mathbf{q})/k_BT}-1)}. \tag{14}$$

If we take into account under the root the equality

$$\frac{m\upsilon_s^2}{2} = \varepsilon_F + E(\mathbf{q}), \tag{15}$$

then the formula (14) is rewritten as follows:

$$\frac{N_{\mathbf{q}}(t)}{dt} = \frac{m^2D^2E(\mathbf{q})}{2\pi\hbar^4\rho V\upsilon_s}\frac{e^{E(\mathbf{q})/k_BT}-e^{E(\mathbf{q})/k_B\Theta}}{(e^{E(\mathbf{q})/k_B\Theta}+1)(e^{E(\mathbf{q})/k_BT}-1)}, \tag{16}$$

which, with the precision to the sign in the denominator distinguishes it from the previously known expression from [8]. The difference arose from a number of assumptions made in [8], which greatly facilitated further calculations for the authors.

Knowing the dynamics of $N_{\mathbf{q}}(t)$, let us pass on to the calculation of the magnitude of absorbed power W and turn to a spherical coordinate system in Eq. (6). Using Eq. (16), we obtain

$$W = \frac{2}{(2\pi)^3}\frac{m^2D^2\upsilon_s}{\hbar^2\rho}$$
$$\times\int_0^{q_D}q^4\frac{e^{E(q)/k_BT}-e^{E(q)/k_B\Theta}}{(e^{E(q)/k_B\Theta}+1)(e^{E(q)/k_BT}-1)}dq. \tag{17}$$

Here, the following replacement of variables is performed:

$$\frac{\hbar \upsilon_s}{k_B T} q = x, \tag{18}$$

and the equality of energy is used:

$$\hbar \upsilon_s q_D = k_B T_D. \tag{19}$$

In this case,

$$x = \frac{q}{q_D}\frac{T}{T_D}, \tag{20}$$

and expression (17) will be rewritten as follows:

$$W = \frac{2}{(2\pi)^3}\frac{\upsilon_s}{\rho}\left(\frac{mD}{\hbar}\right)^2 I, \tag{21}$$

where I denotes the integral:

$$I = q_D^5\left(\frac{T}{T_D}\right)^5 \int_0^{T_D/T} x^4 \frac{e^x - e^{xT/\Theta}}{(e^x - 1)(e^{xT/\Theta} + 1)} dx. \tag{22}$$

Since the Debye temperature averaged for 39 metals is $T_D = 250K$, and the average electronic temperature Θ is 7500 K, then, on the upper limit of the integral in Eq. (22), the exponent (with the temperature ratio) reaches a value of $T_D/\Theta \approx 1/30$, and the exponent will be $e^{1/30} \approx 1.034$. Consequently, within the limits of integration, the multiplier $(e^{xT/\Theta} + 1)$ in the denominator of the integral (22) can be assumed to be equal to 2. Thus, with high accuracy, the computation of integral I reduces to the calculation of the integral:

$$I_0 = \frac{q_D^5}{2}\left(\frac{T}{T_D}\right)^5 \int_0^{T_D/T} x^4 \frac{e^x - e^{xT/\Theta}}{e^x - 1} dx. \tag{23}$$

It is obvious that, at equal temperatures ($T = \Theta$), $I_0 = 0$.

If we use the equality,

$$ze^{xz}(e^z - 1)^{-1} = \sum_{n=0}^{\infty} B_n(x)\frac{z^n}{n!}, \qquad |z| < 2\pi, \tag{24}$$

where $B_n(x)$ is the Bernoulli *n*th order function [25], then the result of integration can be presented as follows:

$$I_0 = \frac{q_D^5}{2}\left(\frac{T}{T_D}\right)^5 \sum_{n=0}^{\infty}\left(\frac{T_D}{T}\right)^{n+4} \frac{1}{n!(n+4)}$$
$$\times\left[(-1)^n B_n - B_n\left(\frac{T}{\Theta}\right)\right], \quad \frac{T_D}{T} < 2\pi. \tag{25}$$

In the case of $T = \Theta$, $B_n(1) = (-1)^{-n} B_n(0) = (-1)^{-n} B_n$, where B_n are the Bernoulli numbers and $I_0 = 0$.

The calculation of an infinite sum with Bernoulli functions in Eq. (25) can be

complicated. Therefore, let us go another way. Using the value

$$I_s = \int_0^{T_D/T} x^s e^{-k\,x}\,dx = \frac{\Gamma(s+1)}{k^{s+1}} - e^{-k_D T_D/T} \times \sum_{n=1}^{s+1} \frac{1}{k^n} \left(\frac{T_D}{T}\right)^{s+1-n} \frac{\Gamma(s+1)}{(s+1-n)!}, \tag{26}$$

and identities [25]

$$\frac{1}{1-e^{-x}} = 1 + \sum_{k=1}^{\infty} e^{-k\,x}, \qquad \sum_{k=1}^{\infty} \frac{1}{k^n} = \varsigma(n), \tag{27}$$

$$\sum_{k=1}^{\infty} \frac{1}{k^n} e^{-k\frac{T_D}{T}} = e^{-\frac{T_D}{T}} \Phi\left(e^{-\frac{T_D}{T}}, n, 1\right), \tag{28}$$

$$\sum_{k=1}^{\infty} \frac{1}{\left(k+1-\frac{T}{\Theta}\right)^n} = -\frac{1}{\left(1-\frac{T}{\Theta}\right)^n} + \frac{(-1)^n}{(n-1)!} \Psi^{(n-1)}\left(1-\frac{T}{\Theta}\right), \tag{29}$$

$$\sum_{k=1}^{\infty} \frac{e^{-k\frac{T_D}{T}}}{\left(k+1-\frac{T}{\Theta}\right)^n} = -\frac{1}{\left(1-\frac{T}{\Theta}\right)^n} + \Phi\left(e^{-\frac{T_D}{T}}, n.1-\frac{T}{\Theta}\right), \tag{30}$$

we find

$$W = \frac{q_D^5}{(2\pi)^3} \frac{\upsilon_s}{\rho} \left(\frac{mD}{\hbar}\right)^2 \left(\frac{T}{T_D}\right)^5 \left\{\frac{1}{5}\left(\frac{T_D}{T}\right)^5 + \Gamma(5)\varsigma(5) - \left|\Psi^{(4)}\left(1-\frac{T}{\Theta}\right)\right| + e^{-\frac{T_D}{T}} \sum_{n=1}^{5} \left(\frac{T_D}{T}\right)^{5-n} \frac{\Gamma(5)}{(5-n)!} \times \left[e^{\frac{T_D}{\Theta}} \Phi\left(e^{-\frac{T_D}{T}}, n, 1-\frac{T}{\Theta}\right) - \Phi\left(e^{-\frac{T_D}{T}}, n, 1\right)\right]\right\}. \tag{31}$$

Here, $\Phi(a,b,z)$ is the confluent or degenerate Cummer hypergeometric function, $\Gamma(z)$ is the Euler gamma function, $\varsigma(z)$ denotes the Riemann zeta function, and $\Psi^{(n)}(z)$ is the polygamma function [25].

The analytical result (31) was numerically compared with the numerical integration of formulas (22) and (23). In the wide range of T/Θ ratios, we obtained a coincidence of results. The smaller the T/Θ ratio is, the better is the coincidence. In the case of $T << \Theta$, the polygamma function $\Psi^{(4)} = -\Gamma(5)\varsigma(5)$, and we finally obtain

$$W \approx \frac{q_D^5}{5(2\pi)^3}\frac{\upsilon_s}{\rho}\left(\frac{mD}{\hbar}\right)^2\left\{1+e^{-\frac{T_D}{T}}\frac{T_D}{\Theta}\sum_{n=1}^{5}\left(\frac{T}{T_D}\right)^n \times\frac{5\Gamma(5)}{(5-n)!}\Phi\left(e^{-\frac{T_D}{T}},n,1\right)\right\}. \quad (32)$$

4. Conclusions

The general formula for an energy transmitted from electrons to the lattice per unit volume per unit time for arbitrary electron and lattice temperatures is obtained. The formula makes it possible analytically to estimate the decay rate (or decay time) due to the scattering of electrons in a bulk metal. This result may be important for analysis of the transport and optical properties for an arbitrary metals and for a more accurate estimation of the electron–phonon coupling in the metallic nanoparticles.

Acknowledgment . This work was supported in part by the Program of the Fundamental Research of the Department of Physics and Astronomy of the National Academy of Science of Ukraine (project No 0117U000240).

References

[1] J.M. Ziman, Electrons and Phonons, Clarendon Press, Oxford, 1960.
[2] V.L. Ginzburg and V.P. Shabanski, Sov. Dokl. Akad. Nauk SSSR 100, 445 (1955).
[3] J. Bardin, L.N. Cooper, and J.R. Schriffer, Phys. Rev. 106, 162 (1957); ibid., 108, 1175 (1957).
[4] T. Holstein, Ann. Phys. 29, 410 (1964).
[5] P.E. Hopkins, J.L. Kassebaum, and P.M. Norris, J. Appl. Phys. 105, 023710 (2009).
[6] A.N. Smith and J.P. Calame, Int. J. Thermophys. 25, 409 (2004).
[7] J.K. Chen, W.P. Latham, and J.E. Beraun, J. Laser. Appl. 17, 63 (2005).
[8] M.I. Kaganov, I.M. Lifshitz, and L.V. Tanatarov, Sov. Phys. JETP 4, 173 (1957).
[9] S.I. Anisimov, B.L. Kapeliovich, and T.L. Perelman, Sov. Phys. JETP 39, 375 (1974).
[10] T.Q. Qui and C.L. Tien, Trans. ASME J. Heat Transfer 115, 835 (1993).
[11] R.D. Fedorovich, A.G. Naumovets, and P.V. Tomchuk, Phys. Rep. 328, 73 (2000).
[12] P.M. Tomchuk and N.I. Grigorchuk, Phys. Rev. B 73, 155423 (2006).
[13] N.I. Grigorchuk, J. Opt. Soc. Am. B, 35, 2851-2858 (2018).
[14] A. Crut, P. Maioli, N. Del Fatti, F. Vallee, Chem. Soc. Rev. 43, 3921 (2014).
[15] N.I. Grigorchuk, Metallofiz. Noveishie Tekhnol. 39, 1445 (2017).
[16] N.I. Grigorchuk, Eur. Phys. Lett. 121, 67003 (2018).
[17] D. Gall, J. Appl. Phys. 119, 085101 (2016).
[18] C. Kittel, Introduction to Solid State Physics, Wiley, New York, 1995, 6th ed.
[19] F. Zeitz, The Modern Theory of Solids, McGraw-Hill Book, New York, 1940.
[20] E.A. Coronado and G.C. Schatz, J. Chem. Phys. 119, 3926 (2003).
[21] N.I. Grigorchuk and P.M. Tomchuk, Low Temp. Phys. 31, 411 (2005).
[22] N.I. Grigorchuk, J. Phys. Chem. C 116, 23704 (2012).

[23] S.L. Koroljuk, Osnovy statystychnoi fizyky ta termodynamiky, Knygy-XXI, Chernivtsi, 2004.
[24] W.A. Harrison, Solid State Theory, McGraw-Hill, New York–London–Toronto, 1970.
[25] Handbook of Mathematical Functions, Dover Publ., New York, 1972.

COMMENTS ON ACOUSTIC WAVE PROPAGATION IN STRATIFIED MEDIA

S. Cojocaru

Department of Theoretical Physics,
Horia Hulubei National Institute for Physics and Nuclear Engineering,
077125 Magurele, Romania
E-mail: scojocaru@theory.nipne.ro

(Received July 26, 2018)

Abstract

In a layered system, the interface between two media presents an intrinsic inhomogeneity even when the materials are isotropic and homogeneous in the sense of continuum medium description of wave propagation. In terms of the rigid bonding (RB) model, the material parameters behave as piecewise continuous functions with an abrupt change across the interface. Therefore, it is reasonable to expect that the wave experiences a singular potential at the border formed by the space derivatives of the material parameters. However, we prove that this potential is strictly cancelled due to continuity of the stress field. The equations governing acoustic wave propagation are derived by the partial wave decomposition method.

1. Introduction

Wave propagation in composite elastic media is a topic of major interest with a large spectrum of applications in various areas of physics spanning a large scale from geophysics [1] to nanophysics [2–4]. In relation to this topic, a large number of theoretical models, methods and approaches have been developed to describe the situation in terms of continuum medium (see, e.g., [5–11]).

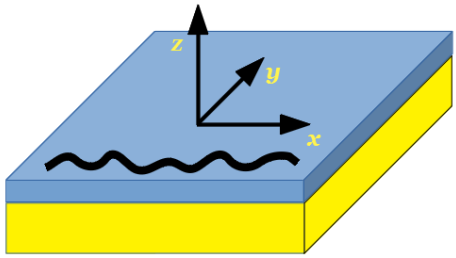

One of the most general methods uses the decomposition of displacement field vector $\boldsymbol{U}(\boldsymbol{r},t)$ into partial waves (point $\boldsymbol{r}=(x,y,z)$ at time t). For the case of a composite slab or plate geometry (Fig. 1), translation symmetry is broken in one of the space directions (z in the figure) so that natural modes of vibration are formed due to multiple wave reflections and refractions. Translation symmetry is assumed to hold in the other two directions; therefore, the decomposition can be represented as follows:

$$\mathbf{U}(\mathbf{r},t) = \sum_n \int \mathbf{u}_n(z,q,\omega_n)\exp(iqx - i\omega_n t)\frac{dq}{(2\pi)}. \quad (1)$$

The x axis is chosen along the direction of wave propagation; index n of the branches in the frequency dispersion spectrum $\omega(q)$ is further dropped. The interface is at $z = 0$; the outer surfaces correspond to $z = d_a$ and $z = -d_b$, so that the total thickness is $d = d_a + d_b$. Considering the wave reflection from the surfaces [12], it can be shown that the spectrum decouples into shear horizontal waves $u(z) = (0,u_y(z),0)$ and Rayleigh–Lamb modes with a mixed shear vertical (s) and longitudinal (l) polarization $u(z) = (u_x(z),0,u_z(z))$. Below, we consider these last ones for definiteness.

2. Equation for the Rayleigh–Lamb Waves

According to the linear elasticity theory, displacement field vector $\boldsymbol{U}(\boldsymbol{r},t)$ is linearly related to the strain tensor

$$\varepsilon_{ij} = \left(\frac{\partial U_i}{\partial r_j} + \frac{\partial U_j}{\partial r_i}\right)/2. \quad (2)$$

For an isotropic medium, stiffness tensor λ_{ijkm} linking the strain to stress tensor $\Sigma_{ij}(\mathbf{r},t)$ simplifies to $\lambda_{ijkm} = \lambda\delta_{ij}\delta_{km} + \mu(\delta_{ik}\delta_{jm}+\delta_{im}\delta_{jk})$, where λ and μ are the two Lamé parameters and δ_{ij} is the Kronecker δ-symbol with $\{i,j,k,m\} = x,y,z$. Then the constitutive equation takes the form

$$\Sigma_{ij} = \lambda\delta_{ij}\varepsilon_{kk}+2\mu\varepsilon_{ij}. \quad (3)$$

The equation of e lastodynamics essentially derives from the Newton's second law

$$\rho\frac{\partial^2 U_i(\mathbf{r},t)}{\partial t^2} = \frac{\partial\Sigma_{ij}(\mathbf{r},t)}{\partial r_j}. \quad (4)$$

Here, ρ is the mass density. The partial wave decomposition of the stress tensor corresponding to (1) is as follows:

$$\Sigma_{ij}(\mathbf{r},t) = \sum_n \int \sigma_{ij}(z)\exp(iqx - i\omega_n t)\frac{dq}{(2\pi)}. \quad (5)$$

The traction free boundary conditions and the continuity on the interface provide eight equations for the unknown amplitudes and frequency ω:

$$\begin{aligned} u_{x,a}(z=0) &= u_{x,b}(z=0), \quad u_{z,a}(z=0) = u_{z,b}(z=0), \\ \sigma_{zx,a}(z=0) &= \sigma_{zx,b}(z=0), \quad \sigma_{zz,a}(z=0) = \sigma_{zz,b}(z=0), \end{aligned}$$

$$\begin{aligned} \sigma_{xz,a}(z=d_a) &= 0, \ \sigma_{xz,b}(z=-d_b) = 0, \\ \sigma_{zz,a}(z=d_a) &= 0, \ \sigma_{zz,b}(z=-d_b) = 0. \end{aligned} \quad (6)$$

The "trouble" with this model is that the elastic constants in (3) are actually not constant at the interface where they change abruptly from one material to the other, while in the published literature this variation is usually ignored [7–11]. On general grounds, one expects that near the interface, the material parameters would have a smooth variation, which can be modeled either dynamically via springs or by specifying the space variation of all the material parameters [4–6, 13]. This leads to more complicated equations than the ones usually considered in the model with rigidly bonded layers. It is clear that the steeper the variation in, e.g., $\lambda(z)$ and $\mu(z)$, the more significant the effect of the respective derivative terms $d\lambda(z)/dz$, $d\mu(z)/dz$ in (4). This argument appears to be in contrast to the treatment of the rigid bonding (RB) limit mentioned before.

The continuity conditions in (6) allow representing the z-functions in (1) and (5) as follows:

$$\begin{aligned}
\sigma_{xz}(z) &= \theta(z)\,\sigma_{xz,a}(z) + (1-\theta(z))\,\sigma_{xz,b}(z),\\
\sigma_{zz}(z) &= \theta(z)\,\sigma_{zz,a}(z) + (1-\theta(z))\,\sigma_{zz,b}(z),\\
u_i(z) &= \theta(z)\,u_{i,a}(z) + (1-\theta(z))\,u_{i,b}(z).
\end{aligned} \tag{7}$$

The Heaviside θ-function has the known property $d\theta(z)/dz = \delta(z)$. After substitution of the above expressions into (4), we obtrain

$$\begin{aligned}
\rho\frac{\partial^2 U_x}{\partial t^2} &= \sum_n \int \left(iq\sigma_{xx}(z) + \frac{\partial \sigma_{xz}}{\partial z} \right) \exp(iqx - i\omega t)\,\frac{dq}{2\pi},\\
\rho\frac{\partial^2 U_z}{\partial t^2} &= \sum_n \int \left(iq\sigma_{xz}(z) + \frac{\partial \sigma_{zz}}{\partial z} \right) \exp(iqx - i\omega t)\,\frac{dq}{2\pi}.
\end{aligned} \tag{8}$$

The contribution of the derivatives in the right-hand-side of the above expressions contains terms with Dirac delta-function

$$\delta(z)(\sigma_{ij,a}(z) - \sigma_{ij,b}(z), \tag{9}$$

which vanish under the continuity condition. It should be noted that when equations (6) are solved numerically, e.g., by finite difference methods, this cancellation can be easily "miscalculated". All the remaining terms have either $\theta(z)$ or $(1 - \theta(z))$ as a prefactor and, by definition, refer to one of the two layers where the material parameters are constants. In addition, note that generally $\sigma_{xx}(z)$, as well as $\sigma_{yy}(z)$, are not continuous functions of z: by definition, the respective tensor components represent forces acting normally to the surfaces, respectively, x = const and y = const in the figure; that is, they are parallel to the interface and, therefore, counterbalanced by an equal and opposite internal force within each layer by the Newton's third law. Therefore, the values of these forces on the two sides of the interface can differ; they can be written in the form with the θ-function similar to (7).

From (2), (3), and (5) we obtain the explicit expressions

$$\begin{aligned}\sigma_{xx} &= \left(\lambda\frac{\partial u_z}{\partial z} + (\lambda+2\mu)\,(iq)\,u_x\right),\\ \sigma_{xz} &= \mu\left(\frac{\partial u_x}{\partial z} + iqu_z\right),\\ \sigma_{zz} &= \lambda iqu_x + (\lambda+2\mu)\,\frac{\partial u_z}{\partial z}.\end{aligned} \tag{10}$$

It is evident that these equations are consistent with representation (7) by virtue of property (8), where stresses are replaced by displacement amplitudes. By taking the remaining derivatives in (4), we recover the commonly used form of the elastodynamic equations describing Rayleigh–Lamb waves in stratified isotropic media in terms of the RB model, e.g., [7–10]:

$$\begin{aligned}\mu_\gamma\frac{\partial^2 u_{x,\gamma}}{\partial z^2} - (\lambda_\gamma+2\mu_\gamma)q^2w_\gamma^2u_{x,\gamma} + (\lambda_\gamma+\mu_\gamma)q\frac{\partial iu_{z,\gamma}}{\partial z} = 0,\\ (\lambda_\gamma+2\mu_\gamma)\frac{\partial^2 iu_{z,\gamma}}{\partial z^2} - \mu_\gamma q^2v_\gamma^2iu_{z,\gamma} - (\lambda_\gamma+\mu_\gamma)q\frac{\partial u_{x,\gamma}}{\partial z} = 0,\end{aligned} \tag{11}$$

where γ = a,b and the quantities

$$w_\gamma = \sqrt{1-\left(\frac{\omega}{q\ell_\gamma}\right)^2},\quad v_\gamma = \sqrt{1-\left(\frac{\omega}{qs_\gamma}\right)^2}, \tag{12}$$

contain the normal mode frequencies scaled with the phase velocities of the bulk longitudinal and transverse sound waves for each of the materials:

$$\ell = \sqrt{(\lambda+2\mu)/\rho},\quad s = \sqrt{\mu/\rho}. \tag{13}$$

Boundary conditions (6), together with the normalization condition

$$\int_{-d_b}^{d_a}|u_n(z)|^2dz = 1, \tag{14}$$

completely determine the wave propagation spectrum in the layered system.

3. Conclusions

One of the basic assumptions of the continuum description of the elastic wave propagation is that the wavelength is significantly larger than the atomic scale variation of the material properties. It is therefore justifiable to use the RB model with an abrupt change in material parameters, provided the interface of a layered system occupies a few atomic layers. In this case, the singular terms originating from the derivatives of the elastic parameters at the boundary do not produce any effect on the wave propagation and can be safely ignored. The physical reason for this "annihilation of singularity" effect is the continuity of stresses or forces acting on the interface.

Acknowledgments. This work was financially supported by ANCS Romania (project no. PN 18090101/2018).

References

[1] A.A. Kaufman and A.L. Levshin, Acoustic and Elastic Wave Fields in Geophysics (Elsevier, Amsterdam, 2005).
[2] M.A. Stroscio and M. Dutta, Phonons in Nanostructures (Cambridge University Press, Cambridge, 2004).
[3] A.N. Cleland, Foundations of Nanomechanics (Springer-Verlag, Berlin, Heidelberg, 2003).
[4] D.L. Nika, Phonon Engineering in Graphene and Semiconductor Nanostructures, (USM, Chisinau, 2015).
[5] B.A. Auld, Acoustic Fields and Waves in Solids, 2nd ed. (Krieger, Malabar, FL, 1990).
[6] L.M. Brekhovskikh and O.A. Godin, Acoustics of Layered Media I (Springer, New York, 1990).
[7] J.L. Rose, Ultrasonic Waves in Solid Media (Cambridge University Press, Cambridge, 2004).
[8] J.L. Rose, Ultrasonic Guided Waves in Solid Media (Cambridge University Press, New York, 2014).
[9] J.D.N. Cheeke, Fundamentals and Applications of Ultrasonic Waves (CRC Press, Boca Raton, 2002).
[10] M.J.S. Lowe, IEEE Trans. UFFC, 42, 525 (1995).
[11] S.K. Datta and A.H. Shah, Elastic Waves in Composite Media and Structures (CRC Press, Boca Raton, 2009).
[12] H. Ezawa, Ann. Phys. (N.Y.) 67, 438 (1971).
[13] E.P. Pokatilov, D.L. Nika, and A.A. Balandin, Phys. Rev. B 72, 113311 (2005).

PECULIARITIES OF DISPERSION LAWS OF A HIGHLY EXCITED THREE-LEVEL ATOM WITH AN EQUIDISTANT ENERGY SPECTRUM

P. I. Khadzhi[a], O. V. Korovai[b]*, and L. Yu.Nad'kin[b]

[a]*Institute of Applied Physics, Academy of Sciences of Moldova, Chisinau, MD-2028 Republic of Moldova*

[b]*Taras Shevchenko Transnistria State University, Tiraspol, MD-3300 Republic of Moldova*

*****E-mail: olesya-korovai@mail.ru*

(Received July 17, 2018)

Abstract

A dispersion law for the system of three-level atoms with an equidistant energy spectrum interacting with resonant laser radiation has been obtained taking into account two successive optically allowed one-photon transitions and an optically allowed two-photon transition between the lower and upper levels. It has been shown that the dispersion law consists of three polariton branches. The effects of repulsion and attraction of branches of the dispersion law and their intersection, as well as the self-consistent variation of the photon– atom coupling constant, have been predicted.

1. Introduction

Increased attention is currently focused on the study of processes of the interaction of laser radiation with matter in low-dimensional media. Bose–Einstein condensation and superfluidity in exciton–polariton systems in microcavities were studied in [1–5]. Studies of phenomena caused by the strong coupling of photons to atomic systems are of particular interest. Nonlinear optical phenomena in three- and multilevel atomic systems were studied taking into account optically induced one-photon transitions between successive pairs of neighboring levels [6–10]. At the same time, direct two-photon transitions between the first and third levels are optically allowed in three-level atomic systems. In terms of this model, a number of active levels, e.g., three levels, which are in resonance with the incident laser radiation, are "cut" from the system. Optically induced one-photon transitions from the ground state of a crystal to an exciton state and from the exciton state to a biexciton state, as well as a direct two-photon transition from the ground state of the crystal to the biexciton level, occur in the exciton region of the spectrum. In CdS and CdSe semiconductors, where the binding energy of a biexciton is vanishingly low, this model of matter is in essence an equidistant three-level model. Equidistant multilevel systems are commonly used in the theory of cascade lasers [11, 12]. It is noteworthy that the model of quantum oscillator is also equidistant. To the best of our knowledge, one-photon and two-photon transitions in the dynamics of three-level atoms have not been taken into account simultaneously.

2. Formulation of the Problem: Dispersion Relation

Below, studies of the dispersion law of three-level atoms with an equidistant energy spectrum interacting with photons of an ultrashort pulse of resonant laser radiation are reported. States 1 and 3 (Fig. 1) have the same parity; therefore, a one-photon transition between them is optically forbidden. However, a direct two-photon transition between these levels is optically allowed. For this reason, we take into account one photon transitions between levels $1 \leftrightarrows 2$ and $2 \leftrightarrows 3$ and two-photon transitions induced by photons of a single pulse between levels 1 and 3 (Fig. 1). Although the used scheme of an equidistant energy spectrum seems specific, the Λ, V, and Σ models of three-level atoms are widely used in atomic optics [10]. The Hamiltonian of the interaction of an atom with photons can be written in the form

$$\frac{1}{\hbar}\widehat{H}_{int} = -g_{12}\hat{a}_1\hat{c}\hat{a}_2^+ - g_{12}^*\hat{a}_2\hat{c}^+\hat{a}_1^+ - g_{23}\hat{a}_2\hat{c}\hat{a}_3^+ - g_{23}^*\hat{a}_3\hat{c}^+\hat{a}_2^+ - \\ -g_{13}\hat{a}_1\hat{c}\hat{c}\hat{a}_3^+ - g_{13}^*\hat{a}_3\hat{c}^+\hat{c}^+\hat{a}_1^+, \quad (1)$$

where $\hat{a}_j(j = 1,2,3)$ is the annihilation operator of the atom at the *j*th level, $\hat{c}$is the photon operator with frequency ω_c, and g_{ij} are the constants of single photon conversion of the atom from the *i*th level to the *j*th level. The eigenfrequencies of atoms at levels 2 and 3 are ω_0 and $2\omega_0$, respectively (Fig. 1). Successive one-photon transitions between levels $1 \leftrightarrows 2$ and $2 \leftrightarrows 3$ are considered as optically allowed. At the same time, a two-photon transition between levels $2 \leftrightarrows 3$ is also optically allowed under the action of photons of the same pulse, which is described by the last two terms in Eq. (1).

In addition, we assumed that the half-width of the incident pulse is smaller than the relaxation time of atoms. In this case, relaxation processes can be neglected because the time of action of the pulse is insufficient for their development.

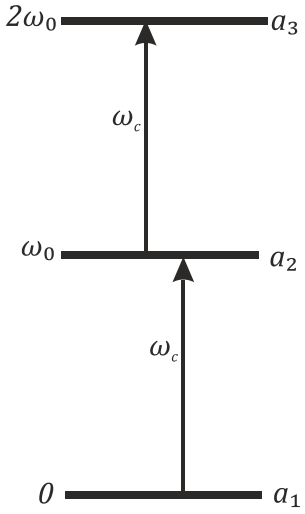

Fig. 1. Scheme of the equidistant energy spectrum of the three-level atom interacting with photons with frequency ω_c.

Using Eq. (1), one can obtain equations of motion for operators $\hat{a}_j$ and $\hat{c}$; the averaging of these equations in the mean field approximation gives the system of nonlinear evolution equations for amplitudes $a_j = \langle \hat{a}_j \rangle (j = 1,2,3)$ and $c = \langle \hat{c} \rangle$:

$$\begin{cases} i\dot{a}_1 = -g_{12}^* c^* a_2 - g_{13}^* c^* c^* a_3, \\ i\dot{a}_2 = \omega_0 a_2 - g_{12} a_1 c - g_{23}^* c^* a_3, \\ i\dot{a}_3 = 2\omega_0 a_3 - g_{23} a_2 c - g_{13} a_1 cc, \\ i\dot{c} = \omega_c c - g_{12}^* a_1^* a_2 - g_{23}^* a_2^* a_3 - 2g_{13}^* a_1^* c^* a_3. \end{cases} \quad (2)$$

We now derive a dispersion relation for the system near frequency ω_0 of the second atomic level. According to the equation for $\dot{a}_2$, the rate of variation in amplitude a_2 is determined by $a_1 c$ and $c^* a_3$. The term with $(a_1 c)$ describes the contribution to the rate of variation in amplitude a_2 owing to the disappearance of the atom at the first level and the disappearance of a photon with frequency ω_c with the transition of the atom to level 2. The term with $(c^* a_3)$ describes the process of disappearance of the atom at level 3 with the creation of a photon at frequency ω_2 with the transition of the atom to level 2. The respective operators $\hat{c}\hat{a}_1$ and $\hat{c}^* \hat{a}_3$ describe states with energies $\hbar\omega_c$ and $\hbar(2\omega_0 - \omega_c)$, which are equal to energy ω_0 of the second atomic level. Consequently, the state of the atom at level 2 and the replica of excited state 3 shifted below by photon energy ω_c are degenerate in energy.

Below, we assume that amplitude c is much larger than the amplitudes of atoms at the respective levels $(c \gg a_1, a_2, a_3)$. We refer to this approximation as the given photon density approximation. In this approximation, the second, third, and fourth terms in the last equation in Eqs. (2) are vanishingly small and can be neglected. In this case, the solution of this equation has a simple form: $c = \mathrm{c}_0 e^{-i\omega_c t}$, where c_0 is the initial amplitude of photons. Accordingly, it is evident that the envelope of function $c(t)$ in the given photon density approximation does not vary with time: $|c|^2 = c_0^2 \equiv f_0 = const$. Then, the equation for a_2 in Eqs. (2) and the equations for $a_1 c$ and $c^* a_3$ in the given photon density approximation form a closed system of three equations for the amplitudes of quasiparticles with the same quasi-energy $\hbar\omega_0 \approx \hbar\omega_c \approx \hbar(\Omega_0 - \omega_c)$:

$$\begin{aligned} i\dot{a}_2 &= \omega_0 a_2 - g_{12}(a_1 c) - g_{23}^*(c^* a_3), \\ i(a_1 c)^{\bullet} &= \omega_c (a_1 c) - g_{12}^* f_0 a_2 - g_{13}^* f_0 (c^* a_3), \\ i(c^* a_3)^{\bullet} &= (\Omega_0 - \omega_c)(c^* a_3) - g_{23} f_0 a_2 - g_{13} f_0 (a_1 c), \end{aligned} \quad (3)$$

where f_0 is the (given) photon density. Thus, in the given photon density approximation, the derived system of Eqs. (3) for functions a_2, $a_1 c$and $c^* a_3$is linear. We seek a solution in the form $a_2, a_1 c, c^* a_3 \sim e^{-i\omega t}$, where ω is the desired eigenfrequency of atomic polaritons. Then, we obtain a system of three linear algebraic equations for the steady-state amplitudes; the determinant of this system specifies the dispersion law of atomic polaritons in the form

$$\begin{aligned} &(\omega - \omega_0)(\omega - \omega_c)(\omega - 2\omega_0 + \omega_c) - \Omega_{12}^2(\omega - 2\omega_0 + \omega_c) - \Omega_{23}^2(\omega - \omega_c) - \\ &-\Omega_{13}^2(\omega - \omega_0) + 2\Omega_{12}\Omega_{23}\Omega_{13}\cos\vartheta = 0, \end{aligned} \quad (4)$$

where $\Omega_{12}^2 = g_{12}^2 f_0$, $\Omega_{23}^2 = g_{23}^2 f_0$ and $\Omega_{13}^2 = g_{13}^2 f_0^2$ are the respective Rabi frequencies and $\vartheta$is the phase difference between the coupling constants. It is evident that the squared Rabi frequency Ω_{12}^2 of the optically allowed one-photon transition between the first and second levels is proportional both to squared transition matrix element g_{12}^2 and to photon density f_0. The squared Rabi frequency Ω_{23}^2 of the optically allowed one-photon transition between levels 2 and 3 is proportional to the square of the matrix element of transition dipole moment g_{23}^2 and the photon density. Finally, the squared Rabi frequencyΩ_{13}^2 is proportional to the matrix element squared g_{13}^2 of the optically allowed two-photon transition between levels 1 and 3 and the squared photon density. The dispersion relation given by Eq. (4) includes six frequency parameters $(\omega, \omega_0, \omega_c, \Omega_{12}, \Omega_{23}, и\Omega_{13})$ and phase difference ϑ. Below, frequencies $\omega, \omega_0, \omega_c, \Omega_{23}$ and Ω_{13} are normalized to the lowest Rabi frequency Ω_{12}. In most semiconductors, frequencies ω, ω_0, and ω_c are about 10^{15} s^{-1}, whereas Rabi frequencies Ω_{12}, $\Omega_{23}$and Ω_{13} are two or three orders of magnitude lower. In addition, it is generally clear that the Rabi frequencies are approximately identical at moderate excitation levels and frequency Ω_{13} at low (high) levels is lower (higher) than frequencies Ω_{12} and Ω_{23}. With an increase in the photon density, Rabi frequency Ω_{13} increases more rapidly than frequencies Ω_{12} and Ω_{23}.

According to Eq. (4), the dispersion law for frequency ω of atomic polariton waves has three real roots, which form three dispersion branches depending on frequency $\omega_c = ck_c$ of incident photons, where k_c is the wavenumber. The shape and location of branches significantly depend on photon density f_0. Equations (4) include three terms, each proportional to the respective squared Rabi frequency or to the square of the absolute value of the respective transition matrix element. These three terms describe independent contributions from the respective processes to the dispersion law. The sign of the corresponding coupling constant with respect to two other signs in the Hamiltonian given by Eq. (1) is of no significance. The last term in Eq. (4) is proportional to the product of three different Rabi frequencies (or three coupling constants $g_{12}, g_{23}$and g_{13}). This term is due to the joint action (quantum interference) of all three processes. If at least one coupling constant is zero, then this term is absent. In this case, it is very important to take into account the signs of the coupling constants or, more precisely, phase relations between them because the dispersion law depends also on phase difference ϑ between these constants. The last term in Eq. (4) is due to the coherence of the interaction of photons with atoms. Hence, the experimental establishment of the features of the dispersion law with the simultaneous inclusion of all three optical transitions can promote determining the phase relations between the coupling constants.

3. Dispersion Law of the Three-Level Atom with the Equidistant Energy Spectrum

We now consider the features of the dispersion law for the three-level atom with the equidistant energy spectrum in more detail. The eigenfrequencies of the second and third (excited) levels are $\omega_0$and $2\omega_0$, respectively. Photons of a single pulse with frequencyω_c are incident on the atom. It is evident that, at $\Omega_{13} = 0$and $\Omega_{23} = 0$ (limit of two-level atom), Eq. (4) is split into two equations, namely, $(\omega - \omega_0)(\omega - \omega_c) - \Omega_{12}^2 = 0$and $\omega - 2\omega_0 + \omega_c = 0$. The former equation is the well-known polariton equation, while the latter equation is the dispersion ratio for "bare" photons that do not interact with the medium. Both polariton-like branches of the dispersion law intersect the straight line $\omega - 2\omega_0 + \omega_c = 0$at two points $C\left(\omega - \Omega_{12}/\sqrt{2}, \omega + \Omega_{12}/\sqrt{2}\right)$and $D\left(\omega + \Omega_{12}/\sqrt{2}, \omega - \Omega_{12}/\sqrt{2}\right)$ (Fig. 2a).

If, e.g., $\Omega_{23} \neq 0$but $\Omega_{13} = 0$, i.e., if the photon interacts with the atom through the $2 \leftrightarrow 3$ transition, Eq. (4) is not split into two independent equations. In view of the interaction, the branches of the dispersion law intersect at the points of energy degeneracy *C* and *D*. As a result, the dispersion law is split into three separate branches, namely, upper, middle, and lower. The upper and middle branches have extrema near point *C*, whereas the middle and lower branches have extrema near point *D*. With an increase in Ω_{23}, splitting increase and the positions of the extrema are shifted. In terms of the dimensionless frequencies

$$\Delta = \frac{\omega-\omega_0}{\Omega_{12}}, \quad \delta = \frac{\omega_c-\omega_0}{\Omega_{12}}, \quad \omega_{23} = \frac{\Omega_{23}}{\Omega_{12}}, \quad \omega_{13} = \frac{\Omega_{13}}{\Omega_{12}}. \tag{5}$$

dispersion relation (4) is represented in the form

$$\Delta^3 - \Delta(1 + \delta^2 + \omega_{23}^2 + \omega_{13}^2) + \delta(\omega_{23}^2 - 1) + 2\omega_{23}\omega_{13}\cos\vartheta = 0. \tag{6}$$

According to Eq. (6), the dispersion law $\Delta(\delta)$ consists of three branches having both ascending and descending sections of the $\Delta(\delta)$ dependence. In the general case, the solutions of Eq. (6) are given by the formulas

$$\Delta_1 = \left(2/\sqrt{3}\right)\sqrt{1 + \delta^2 + \omega_{23}^2 + \omega_{13}^2}\cos\frac{\alpha}{3},$$
$$\Delta_{2,3} = -\left(2/\sqrt{3}\right)\sqrt{1 + \delta^2 + \omega_{23}^2 + \omega_{13}^2}\cos\frac{\alpha\pm\pi}{3}, \tag{7}$$

where

$$\cos\alpha = \frac{\left(\omega_{23}^2-1\right)\delta+2\omega_{23}\omega_{13}\cos\vartheta}{\left(2/3\sqrt{3}\right)\left(1+\delta^2+\omega_{23}^2+\omega_{13}^2\right)^{3/2}}. \tag{8}$$

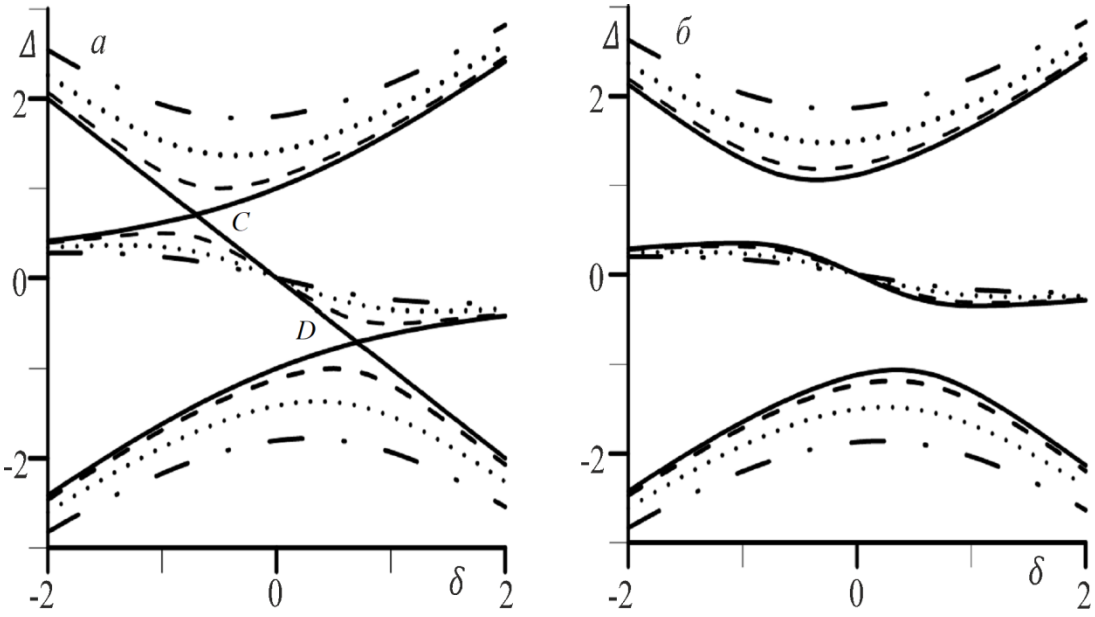

Fig. 2. Dispersion laws of $\Delta = \frac{\omega-\omega_0}{\Omega_{12}}$versus $\delta = \frac{\omega_c-\omega_0}{\Omega_{12}}$ at Ω_{23}= (a) 0 and (b) 0.5; Ω_{13}= (solid lines) 0, (dashed lines) 0.5, (dotted lines) 1, and (dash-dotted lines) 1.5; and phase difference $\vartheta = \pi/2$.

We consider $\vartheta = \frac{\pi}{2}$ (Fig. 2). It is evident from Fig. 2a that, at $\omega_{13} \neq 0$ and $\omega_{23} \neq 0$, points *C* and *D* are split and three separate branches of the dispersion law, which are characterized by the presence of ascending and descending sections of the $\Delta(\delta)$ dependence, appear. The distances between the branches of the dispersion law increase with ω_{13} (Figs. 2a, 2b). The minima on the upper branch are gradually shifted toward shorter wavelengths, whereas the maxima on the lower branch are shifted toward longer wavelengths, and the middle branch slowly changes its profile with an increase in δ remaining near the straight line $\Delta = 0$. At $\omega_{23} = \omega_{13}$, the upper and lower branches become symmetric with respect to both $\Delta = 0$ and $\delta = 0$, and the middle branch is on the straight line $\Delta = 0$ at any ω_{13} values. Accordingly, the coordinates of the upper and lower polariton branches are given by the formulas $\Delta = \pm\sqrt{1 + \delta^2 + \omega_{23}^2 + \omega_{13}^2}$. Thus, the eigenfrequencies of the lower and upper polariton branches increase with $|\delta|$. The shift of the lower and upper polariton branches continues at high ω_{23} values. Furthermore, the behavior of the middle branch becomes more distinct and its variation along the Δ axis increases significantly. It is remarkable that the middle branch of the dispersion law lies on the straight line $\Delta = 0$ (i.e., it does not change under a variation in δ) at the parameter $\omega_{23} = 1$and anyω_{13} values. Thus, according to Fig. 2, the shapes and positions of the branches of the dispersion law of atomic polaritons significantly depend on Rabi frequencies Ω_{12}, Ω_{23}, and Ω_{13}.

We now discuss the behavior of the branches of the dispersion law for the case $\vartheta = 0$ (Fig. 3). Plots $\Delta(\delta)$ at $\vartheta = \frac{\pi}{2}$and $\vartheta = 0$in Fig. 3a coincide with Fig. 2a at $\omega_{23} = 0$, because the term with $\cos\vartheta$ vanishes at $\omega_{23} = 1$. Differences in the behavior of the branches of the dispersion law appear only when all Rabi frequencies are nonzero, i.e., when the term with cosϑ is nonzero. It is evident from Eq. (6) that the middle branch of the dispersion law coincides with the straight line $\Delta = 0$ at $\omega_{23} = 1$and $\omega_{13} = 1$. Significant differences are seen in Figs. 2b and 3. Figure 2b shows the increasing repulsion between the middle and upper branches of the dispersion law with an increase in ω_{13} at the fixed value of $\omega_{23} = 0.5$. At the same time, in Fig. 3, this process is slower; with an increase in ω_{13}, the branches of the dispersion law are located in a certain region bounded by the middle and lower branches (solid lines). With an increase in ω_{13}, the middle and upper branches first attract each other and then repulsion between them appears, whereas the lower and middle branches only repel each other. At $\omega_{13} = 0$, the upper and lower polariton branches are symmetric with respect to the middle branch.

Asymmetry appears with an increase in ω_{13}, when the middle and upper branches first approach each other with increasing ω_{13} and then begin to deviate from each other. Moreover, the upper and middle branches of the dispersion law intersect each other at $\omega_{13} = \omega_{23} = 1$ and, then, again deviate from each other. Thus, the upper and middle branches spectrally approach each other with increasing ω_{13}, intersect each other at $\omega_{13} = \omega_{23} = 1$ (dotted lines), and then deviate from each other (Fig. 3).

It is evident from Fig. 3 that the lower and middle branches of the dispersion law strongly deviate from each other. This feature of the branches of the dispersion law can be interpreted as a change in the photon–atom coupling constant. Thus, the renormalization of the energy spectrum of polaritons is clearly manifested in strong coupling in the long-wavelength region from frequency ω_0 and in weakening of the coupling in the short-wavelength region. This fact also indicates the displacement of the actual points of the *k*-space. It can be stated that an increase in

the pump intensity in experiments will lead to a change in the coupling strength and to the spectral displacement of the actual points in the *k*-space.

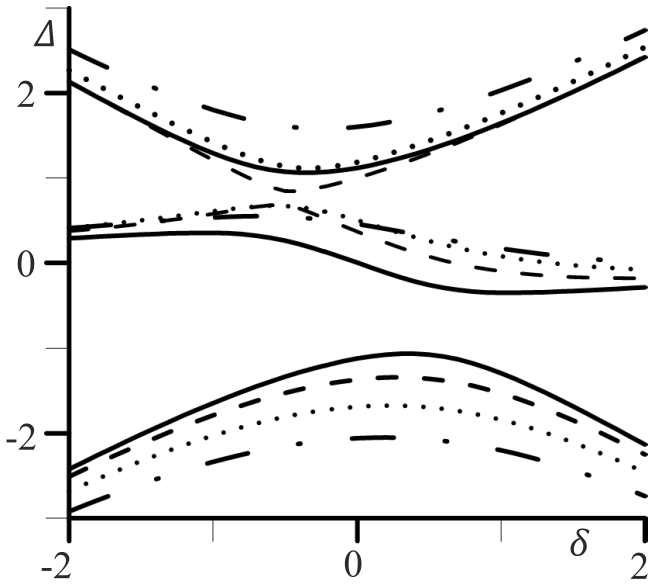

Fig. 3. Dispersion laws of $\Delta = \frac{\omega-\omega_0}{\Omega_{12}}$versus $\delta = \frac{\omega_c-\omega_0}{\Omega_{12}}$ at Ω_{23}=0.5, Ω_{13} = (solid lines) 0, (dashed lines) 0.5, (dotted lines) 1, and (dash-dotted lines) 1.5; and phase difference ϑ = 0.

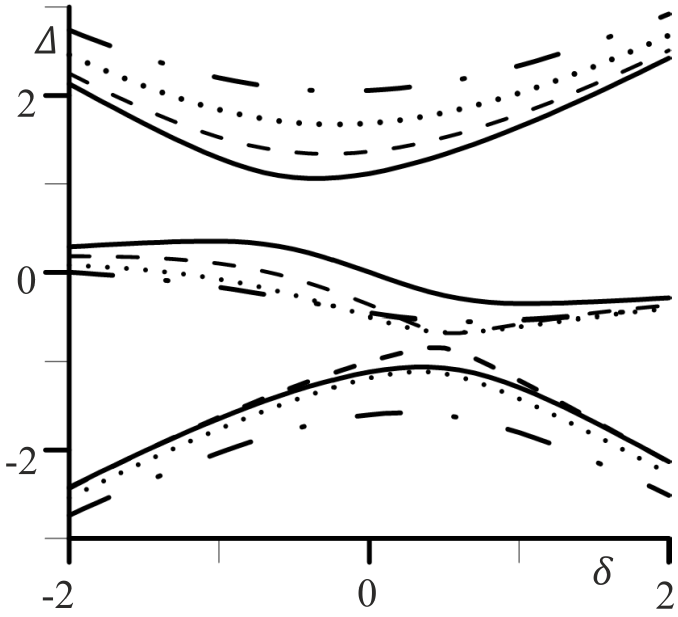

Fig. 4. Dispersion laws of $\Delta = \frac{\omega-\omega_0}{\Omega_{12}}$ versus $\delta = \frac{\omega_c-\omega_0}{\Omega_{12}}$ at Ω_{23}= 0.5, Ω_{13} (solid lines) 0, (dashed lines) 0.5, (dotted lines) 1, and (dash-dotted lines) 1.5; and phase difference $\vartheta = \pi$.

The results shown in Fig. 4 for $\vartheta = \pi$ are similar to those shown in Fig. 3 for $\vartheta = 0$ (after the substitution of $-\Delta$ and $-\delta$ for Δ and δ, respectively). It is evident that the main features, namely, spectral approach, intersection, and subsequent deviation, appear now between the lower and middle branches of the dispersion law.

The eigenfrequencies of the three branches of polaritons significantly depend on the level of excitation of the atomic system. They determine nutation frequencies $\tilde{\Omega}_{12}$, $\tilde{\Omega}_{23}$, and $\tilde{\Omega}_{13}$ (new Rabi frequencies) of polaritons, which are the differences of the eigenfrequencies of polaritons. If the frequencies of two polaritons, e.g., the upper and middle polaritons, coincide with each other, the respective nutation frequency is zero. In this case, the process of nutation is not due to beating of the three polariton branches; it includes nutation oscillations at a single frequency.

4. Conclusions

To summarize, the dispersion law of atomic polaritons has been studied for three-level atoms with the equidistant energy spectrum that interact with intense resonant laser radiation. It has been shown that the dispersion law of atomic polaritons consists of three branches whose position and shape are determined by the Rabi frequencies of optically allowed one-photon transitions between levels $1 \leftrightarrows 2$and $2 \leftrightarrows 3$ and an optically allowed two-photon transition between levels $1 \leftrightarrows 3$. The repulsion and attraction of the branches of the dispersion law, their intersection, self-consistent variation of the coupling strength of photons with atoms, and a significant dependence on the phase difference between the coupling constants are predicted.

References

[1] H. Deng, H. Haug, and Y. Yamamoto, Rev. Mod. Phys. 82, 1489 (2010).
[2] I. Carusotto and C. Ciuti, Rev. Mod. Phys. 85, 299 (2013).
[3] Y. Kasprzak, M. Richard, S. Kindermann, A. Baas,P. Jeambrum, J. M. J. Keeling, F. M. Marchetti, M. H. Szymanska, R. Andre, J. L. Staehli, V. Savona, P. B. Littlewod, B. Deveaud, and L. S. Dang, Nature (London, U.K.) 443, 409 (2006).
[4] R. Balili, V. Hartwell, D. Snoke, L. Pfeiffer, and K. West, Science (Washington, DC, U. S.) 316, 1007 (2007).
[5] A. Kogar, M. S. Rak, S. Vig, A. A. Husain, F. Flicker, Y. I. Joe, L. Venema, G. J. MacDougall, T. C. Chiang, E. Fradkin, Y. van Vezel, and P. Abbamonte, Science (Washington, DC, U. S.) 358, 1314 (2017).
[6] D.I.Gruev, Sov. J. Quantum Electron. 5, 1355 (1975).
[7] M. L. Ter-Mikaelyan, Phys. Usp. 40, 1195 (1997).
[8] N. B. Delone and V. P. Krainov, Atoms in Strong Laser Fields (Atomizdat, Moscow, 1978; Springer, Berlin, Heidelberg, 1985).
[9] R. M. Whitly and C. R. Stroud, Jr., Phys. Rev. A 14, 1498 (1976).
[10] M. O. Scully and M. S. Zubairy, *Quantum Optics* (Cambridge Univ., Cambridge, 1997; Fizmatlit, Moscow, 2003), Chap. 14.
[11] T. C. H. Liew and A. V. Kavokin, arXiv:1706.08635 (2017).
[12] T. C. H. Liew, M. M. Glazov, K. V. Kavokin, I. A. Shelykh, M. A. Kaliteevski, and A. V. Kavokin, Phys. Rev. Lett. 110, 047402 (2013).

THEORY OF HIGH-TEMPERATURE SUPERCONDUCTIVITY IN A TWO-LAYER SYSTEM: $FeSe/SrTiO_3$

M. E. Palistrant, D. F. Digor, and S. A. Palistrant

Institute of Applied Physics, Academy of Sciences of Moldova, str. Academiei 5, Chisinau, 2028 Republic of Moldova
E-mail: mepalistrant@yandex.ru

(Received December 2, 2017)

Abstract

The proposed model can qualitatively describe the occurrence of high-temperature superconductivity in $FeSe/SrTiO_3$. The Hamiltonian of a two-layer system is reduced to a two-band Hamiltonian, taking into account all possible pairing of electrons inside one energy band and electrons in the different energy bands. The superconductivity mechanism can be both phononic and electronic. The main factor is the presence of a large number of constants of the electron–electron interactions that contribute to the formation of Cooper pairs and also the possibility of increasing the ratio of densities of electronic energy bands N_2/N_1 by doping the systems or in some other way. A method for experimental verification of the dominance of interband interactions over intraband interactions is proposed.

1. Introduction

The discovery of high-temperature superconductivity in oxide ceramics at the end of the last century was a significant event in condensed matter physics. This discovery caused a fruitful scientific activity of experimentalists and theoreticians from different countries of the world. Activity is increased mainly in two directions: identification of the superconductivity mechanisms and the conditions leading to the occurrence of high-temperature superconductivity and the desire to design novel materials sustainable in a superconducting phase corresponding to high-temperature superconductivity. In the last decade, a large number of scientific works have been focused on the study of the properties of a class of materials represented by iron pniktides and chalcogenides. According to the studies**,** these materials are layered anisotropic multiband systems. A review of the recent studies of the properties of these compounds is given, for example, in [1]. In numerous compounds of this class of materials, superconductivity occurs both at low and high values of superconducting transition temperature T_c (up to 55 K). An important role in determining the superconducting properties of this class of compounds is played by the features of the electronic energy spectrum of charge carriers. These features primarily include the presence of several energy bands (electron and hole) on the Fermi surface and "nesting" conditions leading to the transition of the system in the antiferromagnetic state of the spin density wave. A violation of nesting, for example, during the doping of the system with charge carriers, contributes to the possibility of the occurrence of superconductivity.

Superconductivity can be accompanied by magnetism in a number of compounds. This fact has led to the idea of the possibility of superconductivity due to the formation of Cooper pairs and the magnetic exchange interaction of charge carriers owing to the presence of spin fluctuations.

Long-term studies have led scientists to the conclusion that most of the class of compounds under consideration obey the magnetic mechanism of superconductivity.

In superconductors in which only electron cavities or only hole cavities are observed on the Fermi surface, there are no fluctuation magnetic interactions. This fact leads to the impossibility of magnetic mechanism of superconductivity. In these systems, the main role is played by electron–electron interactions of BCS type (interband and intraband). In the case of the predominance of the interband interactions over intraband interactions, we have an interband mechanism for superconductivity [2].

The effect of overlapping of the energy bands on the Fermi surface and the various anomalies of the superconducting properties of these anisotropic systems, in principle, can be interpreted in terms of the model proposed in [3, 4]. The history of development of this direction associated with high-temperature superconductivity is given in reviews [5, 6], in several monographs and numerous papers written by M.E. Palistrant and coauthors and by other authors. The theory of multiband superconductivity requires taking into account electron–electron interactions both inside each band and between different bands of electrons [7].

Recently, much attention has been paid to studying the superconducting properties of FeSe compounds, both experimentally and theoretically [8]. This interest is mainly due to the discovery of the FeSe/$SrTiO_3$ structure (FeSe monolayer on a $SrTiO_3$ substrate) in which the superconducting transition temperature reaches record values of about 100 K. In [8], the results of a number of theoretical studies are presented, on the basis of which an attempt is made to explain this situation.

In this work, we proposed another approach to solving this problem. Main attention is paid to the mechanisms related to the structure of the FeSe/$SrTiO_3$ system, namely, two layers with significantly different structures (monolayer FeSe and substrate $SrTiO_3$), which can be considered a source of doping of the system with electrons due to oxygen deficiency in the TiO_2 layer.

The paper provides the following information:

(i) The transition from two nonequivalent layers of the system to the band representation.

(ii) The introduction of temperature Green functions by taking into account both the diagonal and off-diagonal approximation in the band indices.

(iii) Derivation of a system of equations for superconducting transition temperature T_c and chemical potential μ. The self-consistency of the solution of this system by numerical methods and the representation of the dependence of T_c on the density of charge carriers $\tilde{x}$ and magnitude μ on temperature at different values of $\tilde{x}$.

(iv) Analysis and comparison of results with experimental data for FeSe/STO.

2. Transformation of the Hamiltonian and Basic Definitions

The Hamiltonian describing the state of the system is represented in the form of two nonequivalent layers. After diagonalization of the Hamiltonian and *u*,*v*-Bogolyubov transformation, the above-mentioned Hamiltonian is transformed to the band representation:

$$H = \sum_{n\,\boldsymbol{k}\,\boldsymbol{\sigma}}(\varepsilon_n(k) - \mu)\, a^{+}_{n\,\boldsymbol{k}\,\boldsymbol{\sigma}}\; a_{n\,\boldsymbol{k}\,\boldsymbol{\sigma}} - \frac{1}{V}\sum_{m_1,\ldots,m_4}\sum_{\boldsymbol{k}\boldsymbol{k}'} V^{m_3\,m_4}_{m_1 m_2}\;(\boldsymbol{k}-\boldsymbol{k}';\,-\boldsymbol{k}\boldsymbol{k}') \\ a^{+}_{m_1\boldsymbol{k}\uparrow}\, a^{+}_{m_2-\boldsymbol{k}\downarrow}\, a^{+}_{m_3-\boldsymbol{k}'\downarrow} a^{+}_{m_4\,\boldsymbol{k}'\uparrow}\;, \qquad (1)$$

where $a^{+}_{n\boldsymbol{k}\boldsymbol{\sigma}}$, $a_{n\boldsymbol{k}\boldsymbol{\sigma}}$are the creation and annihilation operators of an electron in the *n*th band with

spin σ = (↑,↓) and quasi-wave vector **k**, μ is the chemical potential, and $V_{m_1 m_2}^{m_3 m_4}$ are constants of the intraband and interband interactions. This Hamiltonian is written in general terms and contains terms taking into account interactions both within each band and different interactions of electrons of different bands.

Interactions of electrons leading to the formation of Cooper pairs are determined by the following equations:

$$V_{1111} = \frac{1}{4}\,(\mathrm{V}_1 + \mathrm{V}_2 - 4\mathrm{J} + 2\mathrm{Y} + 4\mathrm{W}),$$
$$V_{2222} = \frac{1}{4}\,(\mathrm{V}_1 + \mathrm{V}_2 + 4\mathrm{J} + 2\mathrm{Y} + 4\mathrm{W})\ ,$$
$$V_{1122} = \frac{1}{4}\,(\mathrm{V}_1 + \mathrm{V}_2 + 4\mathrm{J} - 2\mathrm{Y}),$$
$$V_{2211} = \frac{1}{4}\,(\mathrm{V}_1 + \mathrm{V}_2 - 4\mathrm{J} - 2\mathrm{Y}), \qquad (2)$$
$$V_{1112} = V_{1121} = V_{2212} = V_{2221} = V_{1211} = V_{2111} = V_{1222} == V_{2122} = \frac{V_2 - V_1}{4},$$
$$V_{1212} = V_{2121} = \frac{1}{4}\,(V_1 + V_2 - 2Y),$$
$$V_{1221} = V_{2112} = \frac{1}{4}\,(V_1 + V_2 + 2Y - 4W) \qquad (3)$$

Here, V_1, V_2 are intralayer constants and Y, W are interlayer coupling constants of the electrons. On the basis of (1), simpler models can be obtained. For example, if $m_1 = m_2$, $m_3 = m_4$, expression (1) goes into the corresponding expression of [3], in which only intraband pairing and transition of pairs as a whole from one band to another are considered. This model is widely used for the description of superconductivity in systems with a considerable density of charge carriers ($\mu >> T_c$), particularly high temperature. This model allows describing the anomalies of thermodynamic, magnetic, and other properties of anisotropic superconductors.

Let us consider the matrix functions $\hat{G}, \vec{F}$(normal and abnormal):

$$\hat{G} = \begin{pmatrix} G_{11} & G_{12} \\ G_{21} & G_{22} \end{pmatrix}, \qquad \hat{F} = \begin{pmatrix} F_{11} & F_{12} \\ F_{21} & F_{22} \end{pmatrix} \qquad (4)$$

Using the method of Green functions [3] for Hamiltonian (1), we obtain matrix equations in the $n\,\vec{k}\,\omega$-representation for determining the components of the Green functions (see these equations and their solutions in [7]).

In this case, for order parameters Δ_{np}, the resulting system of equations is found

$$\Delta_{np} = \frac{1}{\beta V}\sum_{\boldsymbol{k}\omega}\sum_{l,r} V_{np}^{er}\ F_{lr}\,(i\omega) = \frac{1}{\beta V}\sum_{\boldsymbol{k}\omega}[V_{np}^{11}\ F_{11}\ (i\omega) + V_{np}^{22}\,(i\,\omega) + \\ + V_{np}^{12}\,F\,(i\omega) + V_{np}^{21}\ F_{21}\,(i\omega)] \qquad (5)$$

Let us complete system of equations (5) with the following expression:

$$x = \frac{2}{\beta V}\sum_{\boldsymbol{k}\omega}[\,G_{11}\,(\boldsymbol{k},\omega) + G_{22}\ (\boldsymbol{k}\,\omega)]\,e^{i\omega 0^+}, \qquad (6)$$

that defines chemical potential μ. A self-consistent system of equations (5) and (6) determines order parameters Δ_{np} and chemical potential μ at a given temperature T and arbitrary values of charge carrier concentration x. For small values of the density of charge carriers x, order parameters Δ_{np} become magnitudes of the same order as chemical potentials μ $(\mu \sim \Delta_{np})$. This

feature contributes to a kink in the temperature dependence of quantity μ at the point $T = T_c$. This kink is experimentally observed in a two-band model with a low density of charge carriers and should manifest itself more clearly than in the single-band model [10] due to the presence of several order parameters (Δ_{mn}).

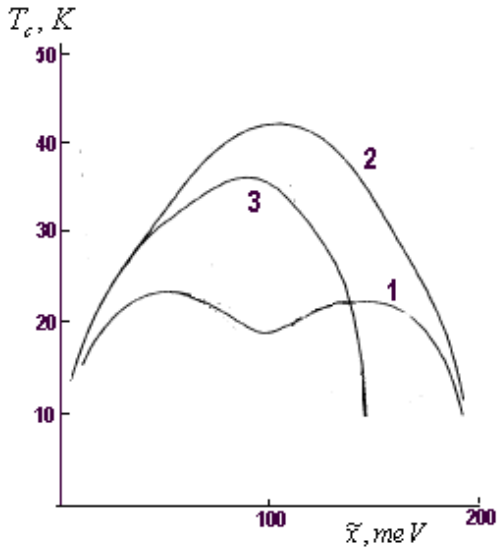

Fig. 1. Dependence of T_c on the density of charge carriers $\tilde{x}$ (see the text for the meaning of the parameters).

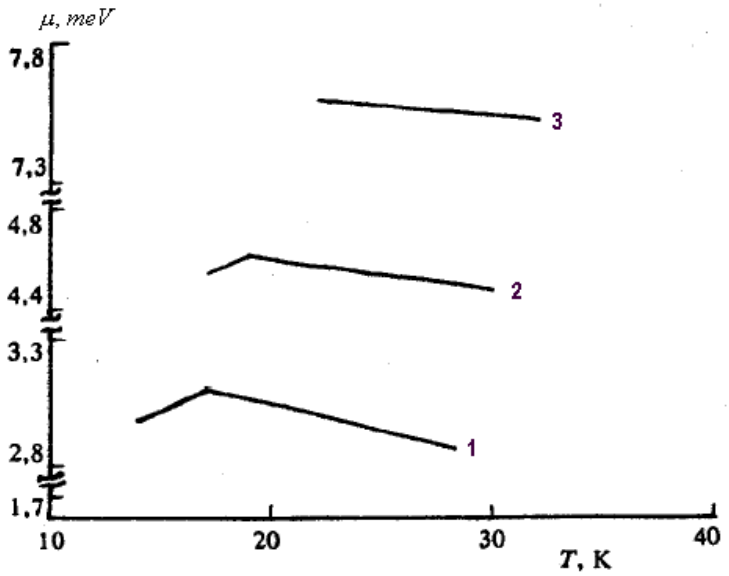

FIg.2. Temperature dependence of chemical potential μ for different concentrations of charge carriers *x*. Curves *1*, *2*, and *3* correspond to $\tilde{x} = x/2N_1$ = 0.015, 0.02, and 0.03, respectively.

3. Superconducting Transition Temperature and Chemical Potential

Let us consider the above-mentioned equations (5) and (6) at a temperature close to the superconducting transition temperature ($T \sim T_c$). With this purpose, we perform the following:

(i) Expand with respect to the product of small parameters $\Delta_{nm}\Delta_{mn}$ in (5), (6) and restrict ourselves to linear terms of the expansion parameters (n; m = 1, 2).
(ii) Present the temperature dependence of order parameter Δ_{nm} as follows:

$$\Delta_{nm} = c_{nm}\,(\beta - \beta_c)^{1/2} + c_{nm}^{(1)}(\beta - \beta_c)^{3/2} + \ldots \quad .$$

(iii) Based on these operations, the resulting self-consistent system of equations is obtained for superconducting transition temperature T_c and chemical potential μ.
(iv) Perform the summation over Matsubara frequency ω by the usual method adopted in statistical physics.
(v) Obtain only electronic energy bands on the Fermi surface, define the dispersion law for each energy band, and switch from summation over momentum $\boldsymbol{k}$ to integration over energy in accordance with the introduced energy law of the dispersion of the electron.
(vi) Input a pseudo-band index by the following rule

$$11 \to 1' \;,\; 22 \to 2' \;,\; 12 \to 3' \;,\; 21 \to 4'$$

and notations

$$V_{nmpl} \to U_{n'm'}, \qquad \text{where } n';\ m' = 1 - 4. \tag{7}$$

We obtain the following system of equations for coefficients c_n:

$$c_{n'} = -\frac{\Sigma}{m'} N_{m'} J_{m'} U_{n'm'} c_{m'}. \tag{8}$$

Equating the determinant of this system to zero, we obtain the equation for determining the superconducting transition temperature. In (8) N_n J_n (n = 1…4) is the expression that depends on T_c and other parameters of the theory (for details, see [7]). The obtained system of equations for Δ_{nm} and for μ did not supply analytical consideration and can be solved by numerical methods.

Figure 1 presents the dependence of the superconducting transition temperature T_c on the concentration of charge carriers $\tilde{x} = \frac{x}{2} N_1$. In this figure, curve *1* corresponds to values of the ratio of the density of electronic states of the two energy bands N_2/N_1 = 1 and the effective constants of electron interaction $\lambda_{11} = \lambda_{22}$ = 0,2, $\lambda_{34} = \lambda_{43}$ = 0.105; $\lambda_{12} = \lambda_{21} = \lambda_{33} = \lambda_{44}$ = 0.01; other λ_{nm} (n,m = 1–4). Curve *2* describes the case in which N_2/N_1= 1 and the following values of parameters λ_{nm}: $\lambda_{11} = \lambda_{22}$ = 0.2; $\lambda_{21} = \lambda_{12} = \lambda_{33} = \lambda_{44}$ = 0.1; $\lambda_{34} = \lambda_{43}$ = 0.15; the rest λ_{nm} = 0.01. For curve *3*, we have N_2/N_1 = 0.5; λ_{nm} values are the same as for curve *2*.

Figure 2 shows the dependence of chemical potential μ on temperature T. In this figure, a kink is observed at the point of $T = T_c$. This result is attributed to the low density of states x in the given system due to the emergence of order parameters Δ_{nm} at $T < T_c$ which are the magnitudes of the order of chemical potential μ. Thus, this anomaly is observed both in single-band discharged systems and in the presence of several energy bands on the Fermi surface. In this paper, numerical studies were performed by self-consistent consideration of equations (5) and (6), after many analytical transformations mentioned above, and ultimately led to an equation for T_c, for example, equation (8).

4. Main Results and Conclusions

In this paper, we have developed a theory of superconductivity of a layered system consisting of two nonequivalent layers with an arbitrary density of charge carriers, including a small one ($\boldsymbol{\mu \sim T_c}$).

The problem has been solved in the case of a discharged system, assuming the occurrence of superconductivity in the BCS scenario, i.e., by the formation of Cooper pairs of electrons.

The method of transition to the band representation and the method of Green's functions in the nondiagonal approximation that contributes to the identification of the role of additional order parameters Δ_{nm} (n; $m = 1 \ldots 4$) has been developed and applied.

The model essentially contains a transition to a pseudo-band representation of four bands. Under these conditions, all interband and intraband pairing of charge carriers are taken into account.

The main results are as follows:

(i) Hamiltonian of a bilayer system with unequal layers has been introduced; the transition to the band representation has been performed. The transformed Hamiltonian takes into account all sorts of both intraband and interband electron–electron interactions leading to the appearance of Cooper pairs within each band and between electrons of different bands. The obtained self-consistent system of equations for determining the superconducting transition temperature T_c (5) and chemical potential μ (6) is presented in the four-band model representation.

(ii) Numerical simulations have been performed; it has been shown that, for discharged systems, it is possible to obtain high T_c values because of the additional interband interactions associated with the formation of superconducting pairs of electrons of the different bands.

(iii) This model has also a great opportunity for various multi-layered or multi-band systems because a substantial role in the theory is played by the N_2/N_1 ratio of the electronic densities of the different bands.

(iv) The solution in Fig. 1 clearly shows the above-mentioned results. The effect of the additional interactions is shown in curves *1* and *3*; the essential role of the N_2/N_1 ratio follows from comparison of curves *3* and *4*.

(v) The temperature dependence of the magnitude of μ, in the region of low densities of charge carriers, exhibits a kink (curves *1–3*), which becomes less sharp with increasing charge carrier concentration and vanishes in the case of the single-band model of a superconductor at $\mu = 2$ meV in [8] and in two-band models for $\mu \sim 8$ meV (Fig. 2). It should be noted that the existence of additional constants of the electron–electron interaction in a double- layered system leads to a stronger manifestation of this anomaly, which can be detected experimentally. Thus, it is possible to confirm the presence of a fairly strong interband electron–electron interaction in nonequivalent double-layered superconducting structures, which are important factors in the emergence of high-temperature superconductivity.

(vi) The structure of the considered double-layered structure is equivalent to the $FeSe/SrTiO_3$ system. The physical properties and anomalies of this structure qualitatively describe the properties of the $FeSe/SrTiO_3$ structure [8]. This statement holds true for both phonon and non phonon mechanisms of superconductivity in a discharged system, such as $FeSe/SrTiO_3$. It is necessary to have high values of the electron–electron interaction constants and the possibility of changing the ratio of electronic densities N_2/N_1.

References

[1] A.Y. Chubukov and P.J. Hirchfield, Phys. Today 68, 46 (1915). arXiv: 14171.
[2] M.E. Palistrant, Zh. Eksp. Teor. Fiz. 150 (1), 97 (2016).
[3] V.A. Moskalenko, Fiz. Met. Metalloved. 8, 503 (1959).
[4] H. Suhl, B.T. Matthias, and L.R. Wolker, Phys Rev. Lett. 3, 552 (1959).
[5] M.E. Palistrant, Cond. Mat. Phys. 12, 677 (2009); Mold. J. Phys. Sci. 3, 133 (2004). arXiv: cond–mat/0305496.
[6] V.A. Moskalenko, M. E. Palistrant, and V. M. Vakalyuk, Usp. Fiz. Nauk 161, 155 (1991).

[7] F.G. Kochorbe and M. E. Palistrant, Zh. Eksp. Teor. Fiz. 104, 3084 (1993).
[8] M.V. Sadovskii, Usp. Fiz. Nauk 186 (10), 1035 (2016).
[9] A.A. Abrikosov, L.P. Gorkov, and I.E. Dzyaloshinski, Metody kvantovoi teorii polya v statisticheskoi fizike, Moscow, Fizmatgiz, 1962.
[10] D. Van Der Marel, Physica C 165, 35 (1965).

NON-CLASSICAL LIGHT SCATTERED BY LASER-PUMPED MOLECULES POSSESSING PERMANENT DIPOLES

A. V. Mirzac*, V. Ciornea, and M. A. Macovei

Institute of Applied Physics, Academiei str. 5, Chisinau, MD-2028 Republic of Moldova
**E-mail: mirzacalexandra71@phys.asm.md*

(Received July 2, 2018)

Abstract

Squeezing in resonance fluorescence processes of a laser-pumped molecule possessing permanent dipoles is shown. A weak low-frequency coherent field pumps the sample near resonance with the dynamically Stark-splitting states induced by a second stronger laser field driving the main two-level transition. The fluorescence spectrum consists of three coherently scattered spectral lines and up to nine incoherently scattered spectral lines. Compared with a similar problem yet in the absence of permanent dipoles, aditional squeezing regions are found.

1. Introduction

The resonance fluorescence phenomenon has attracted great attention in the last decades; the Mollow spectrum is a clear example from this point of view. The potential applications with artificial atomic systems, such as semiconductor quantum dots, have renewed interest in this topic. Furthermore, another important nonclassical feature of the resonance fluorescence spectrum is the squeezing of the field quadratures of a two-level system, which was theoretically adressed by Walls and Zoller [1] and later experimentally verified. Owing to potential appplications in high-precisioon measurements, such as graviational wave detection or quantum computing, the squeezing of the fluorescent field has been widely studied in two- and three-level atoms driven by a laser. In connection with the developement of quantum informatics, squeezed states of the radiation field have been recongized as crucial resources for continous variable quantum information processing. Therefore, the issue of generation of fields with enhanced squeezing is still an important topic [1, 2].

Semiconductor quantum dots are considered attractive candidates for many optoelectronic applications as single-photon sources, lasers, and computational building blocks of a quantum computer. From the fundamental point of view, an outstanding application of the artificial atom model where excitation can be considered as a two-level system is the developement of quantum optics experiments in solid state physics. The emission of photons with a sub-poissonian photon statistics, as well as antibunched photons, has been already shown [3]; these achievements could be used for quantum cryptography [4, 5]. Rabi oscillations are another attractive phenomenon, which can be observed when a single quantum dot is strongly driven by a laser under quasi-resonant excitation [6, 7]. The coupling between the excitonic two-level system and an optical cavity mode leads to the cavity quantum electrodynamics research field in solid state systems, similarly to single atoms in cavity [8]. As a consequence, another approach to coherently control the exciton quantum bit in a single quantum dot and generate non-classical states of light is to benefit from the strong coupling of a quantum dot two-level system with an optical microcavity and from the resulting quantum anharmonicty of the energy structure of the quantum dot–cavity

system [9].

Here, we study a two-level quantum emitter which is pumped by two coherent laser fields and scatters photons coherently or incoherently via the surrounding vacuum modes of the electromagnetic field reservoir. The first low-frequency coherent field pumps the sample near resonance with the dynamically Stark-splitting states induced by a second stronger laser field driving the main two-level transition. Under these conditions, we have found that the fluorescence spectrum consists of three coherently scattered spectral lines and up to nine incoherently scattered spectral lines. In particular, we have shown aditional squeezing regions found in resonance fluorescence processes in comparison with similar problem yet in the absence of permanent dipoles.

This paper is organized as follows. In Section 2, we describe the analytic model and analyze the relevant equations of motion using the system's master equation. In Section 3, we compute the resonance fluorescence spectrum, while in Section 4 we give the squeezed spectrum, respectively. We finalize the paper with a summary given in Section 5.

2. Theoretical Framework

Let us consider a two-level system possessing permanent dipoles and interacting with two external coherent laser fields. The first laser is near resonance with the transition frequency of the two-level sample, while the second laser is close to resonance with the dressed-frequency splitting due to the first laser. In the dipole approximation, the Hamiltonian describing this model, in a frame rotating at the first laser frequency ω_L, is as follows [10, 11]:

$$H = \sum_k \hbar\omega_k a_k^\dagger a_k + \hbar\omega_0 S_z + \hbar\Omega_1\left(S^+ e^{-i\omega_L t} + S^- e^{i\omega_L t}\right) + \hbar\Omega_2(S^+ + S^-)\cos(\omega t) + \\ + \hbar G S_z \cos(\omega t) + \hbar G_1 S_z \cos(\omega_L t) + i\hbar \sum_k \left(\vec{g}_k \cdot \vec{d}\right)\left\{a_k^\dagger S^- - a_k S^+\right\}, \quad (1)$$

In Hamiltonian (1), the first four components are the free energies of the environmental electromagnetic vacuum modes and molecular subsystems together with the laser-molecule interaction Hamiltonian, respectively. Here, $\Omega_1 \equiv \Omega = dE_1/(2\hbar)$ is the corresponding Rabi frequency with $d \equiv d_{21} = d_{12}$ being the transition dipole moment while E_1 is the amplitude of the first laser field. The fifth term accounts for the second laser interacting at frequency ω and amplitude E_2 with the molecular system due to the presence of permanent dipoles incorporated in G, i.e., $G = (d_{22} - d_{11})E_2/\hbar$, while the sixth terms is due to the interaction of the first laser with the permanent dipoles. The last term describes the interaction of molecular subsystems with the environmental vacuum modes of the electromagnetic field reservoir. Further, $\vec{g} = \sqrt{2\pi\hbar\omega_k/V}\,\vec{e}_\lambda$ is the molecule–vacuum coupling strength with $\vec{e}_\lambda$ being the photon polarization vector and $\lambda \in \{1,2\}$, whereas V is the quantization volume; $\Delta = \omega_{21} - \omega_L$ is the laser field detuning from the molecular transition frequency ω_{21}. The molecule bare-state operators $S^+ = |2\rangle\langle 1|$ and $S^- = [S^+]^\dagger$ obey the commutation relations $[S^+, S^-] = 2S_z$ and $[S_z, S^\pm] = \pm S^\pm$. Here, $S_z = (|2\rangle\langle 2| - |1\rangle\langle 1|)/2$ is the bare-state inversion operator; $|2\rangle$ and $|1\rangle$ are the excited and ground state of the molecule, respectively, while $a_k^\dagger$ and a_k are the creation and annihilation operators of the k_{th} electromagnetic field mode and satisfy standard bosonic commutation relations, namely, $\left[a_k, a_k^\dagger\right] = \delta_{kk'}$ and $[a_k, a_{k'}] = \left[a_k^\dagger, a_{k'}^\dagger\right] = 0$. In the following, we will neglect the fast oscillating terms and consider a regime where the generalized Rabi frequency $\bar{\Omega} = \sqrt{\Omega^2 + (\Delta/2)^2}$ is larger than the single-molecule spontaneous decay rate, as well

as the coupling due to permanent dipoles, i.e., $\bar{\Omega} \gg \gamma$ and $\bar{\Omega} \gg G$. In this case, it is more convenient to describe our system in the semiclassical laser–molecule dressed state picture due to the first applied laser [2]:

$$|2\rangle = -\sin\theta\,|\bar{1}\rangle + \cos\theta\,|\bar{2}\rangle, \text{ and } |1\rangle = \cos\theta\,|\bar{1}\rangle + \sin\theta|\bar{2}\rangle, \quad (2)$$

with $\tan 2\theta = \frac{2\bar{\Omega}}{\Delta}$. Here, $|\bar{2}\rangle$ and $|\bar{1}\rangle$ are the corresponding upper and lower dressed states, respectively. Applying the dressed-state transformations in Hamiltonian (1), one arrives at the following Hamiltonian represented in a rotating frame also at the second laser field frequency, i.e., ω:

$$H = \sum_k \hbar(\omega_k - \omega_L)a_k^\dagger a_k + \hbar\bar{\Delta}R_z - \hbar\bar{G}(R^+ + R^-) +$$
$$+ i\sum_k (\vec{g}_k \cdot \vec{d})\left\{a_k^\dagger\left(\frac{1}{2}\sin 2\theta\, R_z + \cos^2\theta R^- e^{-i\omega t} - \sin^2\theta R^+ e^{i\omega t}\right) - H.C\right\}, \quad (3)$$

where $\bar{\Delta} \equiv \bar{\Omega} - \omega/2$, $\bar{G} = \frac{1}{4}G\sin 2\,\theta$, $R^+ = |\bar{2}\rangle\langle\bar{1}|$, $R^- = |\bar{1}\rangle\langle\bar{2}|$, $\bar{R}_z = |\bar{2}\rangle\langle\bar{2}| - |\bar{1}\rangle\langle\bar{1}|$. Here, we have assumed that $\omega \gg \bar{G}$ and performed the rotating wave approximation with respect to ω [10, 11]. Introducing Hamiltonian (3) in the Heisenberg equation describing the mean quantum evolution of any molecular operator Q, we obtain

$$\frac{d}{dt}\langle Q(t)\rangle = \frac{i}{\hbar}\langle[\hbar\bar{\Delta}R_z - \hbar\bar{G}(R^+ + R^-), Q]\rangle -$$

$$-\sum_k \frac{(\vec{g}_k \cdot \vec{d})}{\hbar}\left\{\langle a_k^\dagger\left[\frac{1}{2}\sin 2\,\theta\, R_z + \cos^2\theta R^- e^{-i\omega t} - \sin^2\theta R^+ e^{+i\omega t}\right], Q\rangle - H.C\right\}. \quad (4)$$

One can apply the double dressed-state formalism in order to obtain further information on our system, namely,

$$|\bar{2}\rangle = \sin\bar{\theta}\,|\tilde{1}\rangle + \cos\bar{\theta}|\tilde{2}\rangle\,,\ |\bar{1}\rangle = \cos\bar{\theta}\,|\tilde{1}\rangle - \sin\bar{\theta}|\tilde{2}\rangle. \quad (5)$$

Introducing (5) in Hamiltonian (4) and eliminating the degrees of freedom related with the environmental vacuum modes in the Born–Markov approximations, one arrives at the following double dressed master equation:

$$\frac{d}{dt}\langle Q(t)\rangle = i\bar{G}_R\langle[\tilde{R}_z, Q]\rangle - \bar{\Gamma}_0\{\langle\tilde{R}_z[\tilde{R}_z, Q]\rangle + \langle[Q, \tilde{R}_z]\tilde{R}_z\rangle\} -$$
$$-\bar{\Gamma}_+\{\langle\tilde{R}^+[\tilde{R}^-, Q]\rangle + \langle[Q, \tilde{R}^+]\tilde{R}^-\rangle\} - \bar{\Gamma}_-\{\langle\tilde{R}^-[\tilde{R}^+, Q]\rangle + \langle[Q, \tilde{R}^-]\tilde{R}^+\rangle\}. \quad (6)$$

here,

$$\bar{\Gamma}_0 = \frac{1}{4}\gamma(\omega_L)\sin^2 2\,\theta\cos^2 2\bar{\theta} + \frac{1}{4}\gamma(\omega_L + \omega)\sin^2 2\bar{\theta}\cos^4\theta + \frac{1}{4}\gamma(\omega_L - \omega)\sin^2 2\bar{\theta}\sin^4\theta,$$
$$\bar{\Gamma}_+ = \frac{1}{4}\gamma(\omega_L + 2\bar{G}_R)\sin^2 2\bar{\theta}\sin^2 2\,\theta +$$
$$+\frac{1}{4}\gamma(\omega_L + \omega + 2\bar{G}_R)\cos^4\bar{\theta}\cos^4\theta + \frac{1}{4}\gamma(\omega_L - \omega + 2\bar{G}_R)\sin^4\theta\sin^4\bar{\theta},$$
$$\bar{\Gamma}_- = \frac{1}{4}\gamma(\omega_L - 2\bar{G}_R)\sin^2 2\,\theta\sin^2 2\bar{\theta} +$$

$$+\frac{1}{4}\gamma(\omega_L+\ \omega-2\bar{G}_R)\cos^4\theta\sin^4\bar{\theta}+\frac{1}{4}\gamma(\omega_L-\ \omega-2\bar{G}_R)\sin^4\theta\cos^4\bar{\theta},$$

with $\gamma(x)=\frac{2d^2x^3}{3\,\hbar c^3}$, $\bar{G}_R=\sqrt{\bar{\Delta}^2+\bar{G}^2}$, $\bar{\Delta}=\bar{\Omega}-\omega/2$, $\cot 2\bar{\theta}=\frac{\bar{\Delta}}{\bar{G}}$. The new operators, i.e., $\tilde{R}^+=|\tilde{2}\rangle\langle\tilde{1}|$, $\tilde{R}^-=[\tilde{R}^+]^\dagger$ and $\tilde{R}_z=|\tilde{2}\rangle\langle\tilde{2}|-|\tilde{1}\rangle\langle\tilde{1}|$, are operating in the double dressed state picture obeying the following commutation relations: $[\tilde{R}^+,\tilde{R}^-]=2\tilde{R}_z$ and $[\tilde{R}_z,\tilde{R}^\pm]=\pm2\tilde{R}^\pm$. The master equation (6) contains slowly varying terms in the spontaneous emission damping; that is, we have assumed that $\bar{G}_R\gg\gamma(\omega_{21})$, with $\gamma(\omega_{21})=\frac{2d^2\omega_{21}^3}{3\,\hbar c^3}$ being the single-molecule spontaneous decay rate corresponding to the double dressed-state frequency ω_{21}.

With the help of the master equation (6), we obtain the Bloch system of differential equations, describing our sample, which is solved first in the stationary case, i.e., we consider that $\frac{d}{dt}\langle\tilde{R}^-(t)\rangle=0$; $\frac{d}{dt}\langle\tilde{R}^+(t)\rangle=0$; $\frac{d}{dt}\langle\tilde{R}_z(t)\rangle=0$ in

$$\begin{cases}\dfrac{d}{dt}\langle\tilde{R}_z(t)\rangle=-2(\bar{\Gamma}_++\bar{\Gamma}_-)\langle\tilde{R}_z\rangle+2(\bar{\Gamma}_--\bar{\Gamma}_+),\\ \dfrac{d}{dt}\langle\tilde{R}^+(t)\rangle=(2i\bar{G}_R-4\bar{\Gamma}_0-\bar{\Gamma}_+-\bar{\Gamma}_-)\langle\tilde{R}^+\rangle,\\ \dfrac{d}{dt}\langle\tilde{R}^-(t)\rangle=-(2i\bar{G}_R+4\bar{\Gamma}_0+\bar{\Gamma}_++\bar{\Gamma}_-)\langle\tilde{R}^-\rangle,\end{cases}\tag{7}$$

to arrive at: $\langle\tilde{R}_z\rangle_s=\frac{\bar{\Gamma}_--\bar{\Gamma}_+}{\bar{\Gamma}_-+\bar{\Gamma}_+}$, while $\langle\tilde{R}^+\rangle_s=\langle\tilde{R}^-\rangle_s=0$. Here, we took into account the relations: $\langle\tilde{R}^+\tilde{R}^-\rangle=\frac{1}{2}\left(1+\tilde{R}_z\right)$, $\langle\tilde{R}^-\tilde{R}^+\rangle=\frac{1}{2}\left(1-\tilde{R}_z\right)$. The time dependence of the mean-values of operators $\tilde{R}^\pm$ and $\tilde{R}_z$ in the "double dressed" state basis follows immediately from (7):

$$\begin{aligned}\langle\tilde{R}^+\rangle&=\langle\tilde{R}^+(0)\rangle e^{(2i\bar{G}_R-\bar{\Gamma}_s)\tau},\\ \langle\tilde{R}^-\rangle&=\langle\tilde{R}^-(0)\rangle e^{-(2i\bar{G}_R+\bar{\Gamma}_s)\tau},\\ \langle\tilde{R}_z\rangle&=\langle R_z(0)\rangle e^{-2(\bar{\Gamma}_-+\bar{\Gamma}_+)\tau}+\langle\tilde{R}_z\rangle_s\left(1-e^{-2(\bar{\Gamma}_-+\bar{\Gamma}_+)\tau}\right),\end{aligned}\tag{8}$$

where $\bar{\Gamma}_s=4\bar{\Gamma}_0+\bar{\Gamma}_++\bar{\Gamma}_-$.

3. Resonance Fluorescence

The phenomenon of resonance fluorescence is the process in which a laser-pumped two-level atom scatters photons both coherently and incoherently. If the driving field is monochromatic, at low excitement intensities, the atom absorbs a photon and reemits it at that frequency as a consequence of energy conservation. The spectral width of the fluorescent light is very narrow. The situation is considerably more complex when the laser intensity increases and the Rabi frequency associated with the laser field is comparable or greater than the width of the energy band of the quantum emitter. In this case, Rabi oscillations appear as a modulation of the dipolar quantum moment and side bands appear in the spectrum of the emitted radiation. The resonance fluorescence spectrum is represented via the terms of the double-correlated function of the emitted field [12]:

$$S(\omega) = \Phi(r) Re \int_0^\infty d\,\tau e^{i(\omega-\omega_L)\tau} \lim_{t\to\infty} \langle S^+(t) S^-(t-\tau)\rangle, \tag{9}$$

where $\Phi(r) = \frac{2d^2\omega_{21}^4}{3r^2c^4}$, r is the distance to the detector. In the double-dressed picture, we found the following expression for the correlation function entering in (9):

$$\begin{aligned}
&\lim_{t\to\infty}\langle S^+(t)S^-(t)\rangle = \\
&= \left(\frac{1}{4}\sin^2 2\,\theta\cos^2 2\bar{\theta} + \frac{1}{4}\sin^2 2\bar{\theta}\cos^4\theta e^{-i\,\omega\tau} + \frac{1}{4}\sin^2 2\bar{\theta}\sin^4\theta e^{i\,\omega\tau}\right)\langle \tilde{R}_z\tilde{R}_z(\tau)\rangle + \\
&+ \left(\frac{1}{4}\sin^2 2\,\theta\sin^2 2\bar{\theta} + \cos^4\theta\sin^4\bar{\theta} e^{-i\,\omega\tau} + \sin^4\theta\cos^4\bar{\theta} e^{i\,\omega\tau}\right)\langle \tilde{R}^-\tilde{R}^+(\tau)\rangle + \\
&+ \left(\tfrac{1}{4}\sin^2 2\bar{\theta}\sin^2 2\,\theta + \cos^4 4\bar{\theta}\cos^4\theta e^{-i\,\omega\tau} + \sin^4\theta\sin^4\bar{\theta} e^{i\,\omega\tau}\right)\langle \tilde{R}^+\tilde{R}^-(\tau)\rangle.
\end{aligned} \tag{10}$$

Using the time-dependence of the qubit operators in (10) and integrating the corresponding expressions, we obtain the final expression of resonance fluorescence spectra in the steady-state:

$$\begin{aligned}
S(\nu) = {} & \frac{1}{4}\sin^2 2\,\theta\cos^2 2\bar{\theta}\left\{\pi\langle\tilde{R}_z\rangle_s^2\delta(\nu-\omega_L) + \left(1-\langle\tilde{R}_z\rangle_s^2\right)\frac{\Gamma_\parallel}{\Gamma_\parallel^2+(\nu-\omega_L)^2}\right\} + \\
& + \frac{1}{4}\sin^2 2\bar{\theta}\cos^4\theta\left\{\pi\langle\tilde{R}_z\rangle_s^2\delta(\nu-\omega_L-\omega) + \left(1-\langle\tilde{R}_z\rangle_s^2\right)\frac{\Gamma_\parallel}{\Gamma_\parallel^2+(\nu-\omega_L-\omega)^2}\right\} + \\
& + \frac{1}{4}\sin^2 2\bar{\theta}\sin^4\theta\left\{\pi\langle\tilde{R}_z\rangle_s^2\delta(\nu-\omega_L+\omega) + \left(1-\langle\tilde{R}_z\rangle_s^2\right)\frac{\Gamma_\parallel}{\Gamma_\parallel^2+(\nu-\omega_L+\omega)^2}\right\} + \\
& + \langle\tilde{R}^-\tilde{R}^+\rangle_s\left[\frac{1}{4}\sin^2 2\,\theta\sin^2 2\bar{\theta}\frac{\bar{\Gamma}_s}{\bar{\Gamma}_s^2+(\nu-\omega_L+2\bar{G}_R)^2} + \right. \\
& + \cos^4\theta\sin^4\bar{\theta}\frac{\bar{\Gamma}_s}{\bar{\Gamma}_s^2+(\nu-\omega_L-\omega+2\bar{G}_R)^2} + \\
& \left. + \sin^4\theta\cos^4\bar{\theta}\frac{\bar{\Gamma}_s}{\bar{\Gamma}_s^2+(\nu-\omega_L+\omega+2\bar{G}_R)^2}\right] + \\
& + \langle\tilde{R}^+\tilde{R}^-\rangle_s\left[\frac{1}{4}\sin^2 2\bar{\theta}\sin^2 2\,\theta\frac{\bar{\Gamma}_s}{\bar{\Gamma}_s^2+(\nu-\omega_L-2\bar{G}_R)^2} + \right. \\
& + \cos^4\bar{\theta}\cos^4\theta\frac{\bar{\Gamma}_s}{\bar{\Gamma}_s^2+(\nu-\omega_L-\omega-2\bar{G}_R)^2} + \\
& \left. + \sin^4\theta\sin^4\bar{\theta}\frac{\bar{\Gamma}_s}{\bar{\Gamma}_s^2+(\nu-\omega_L+\omega-2\bar{G}_R)^2}\right],
\end{aligned} \tag{11}$$

note that: $\Gamma_\parallel = 2(\bar{\Gamma}_- + \bar{\Gamma}_+)$.

Analyzing the resonance fluorescence spectrum given in (11), one can observe that there are three coherently scattered spectral lines at ω_L, and $\omega_L \pm \omega$ nad up to nine incoherently scattered spectral bands, i.e., at $\nu-\omega_L=0$, $\nu-\omega_L-\omega=0$, $\nu-\omega_L+\omega=0$, etc., in agreement with the double-dressed state picture. Particularly, Fig. 1 depicts the resonance fluorescence spectrum for certain parameters. More specifically, one can observe the cancelation of the central spectral band due to interference effects among the induced double dressed-state transitions. Asymmetrical behaviors in the scattered light spectrum are observed as well. This is because of the population inversion in the bare state and it differs from the usual resonance fluorescence spectrum obtained in the absence of permanent dipoles [2, 13].

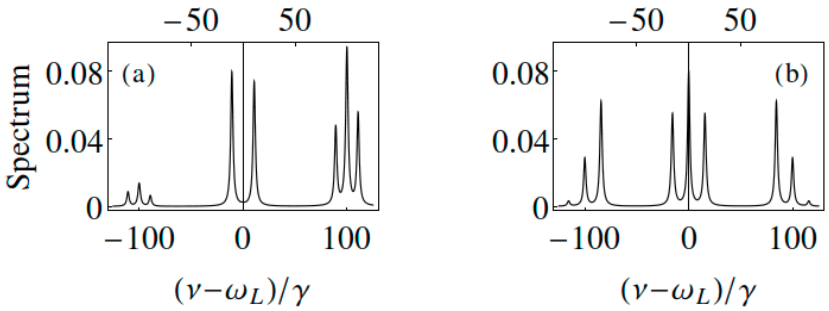

Fig. 1. Resonance fluorescence spectra. Here $\Omega/\gamma = 45$, $\omega/\gamma = 100$ and (a) $\Delta/(2\Omega) = 0{,}5$; (b) $\Delta/(2\Omega) = 0$

Finalizing this part, we have studied the resonance fluorescence properties of this system. In the following, we shall calculate the squeezing effects in the resonance fluorescence processes of laser-pumped molecules with permanent dipoles.

4. Squeezing Spectra and Quantum Fluctuations

The steady-state spectrum of squeezing can be determined as follows [14]:

$$S_\varphi(\nu) = (\gamma/|\mu|^2)\int_0^\infty [exp(i\nu\tau) + exp(-i\nu\tau)] \times \lim_{t\to\infty} \Gamma_\varphi(t+\tau, t)\, d\tau, \qquad (12)$$

where $\Gamma_\varphi(t+\tau, t) = \langle : \Delta E_\varphi(t+\tau)\Delta E_\varphi(t) : \rangle$. Reduced quantum fluctuations are phase dependent due to the weak oscillating terms of the field emitted to the detector:

$$E_\varphi(t) = \frac{E^{(+)}(t)exp(i\,\varphi) + E^{(-)}(t)exp(-i\,\varphi)}{2}, \qquad (13)$$

where φ is the phase angle and $E^{(\pm)}$ are the negative and positive amplitudes of the field. Particularly, one can show that

$$\Gamma_\varphi(t+\tau, t) =$$
$$\frac{1}{4}\times\langle : \left(E^{(+)}(t+\tau)e^{i\,\varphi} - E^{(-)}(t+\tau)e^{-i\,\varphi} - \langle E^{(+)}(t+\tau)\rangle e^{i\,\varphi} - \langle E^{(-)}(t+\tau)\rangle e^{-i\,\varphi}\right)$$
$$\times\left(E^{(+)}(t)e^{i\,\varphi} - E^{(-)}(t)e^{-i\,\varphi} - \langle E^{(+)}(t)\rangle e^{i\,\varphi} - \langle E^{(-)}(t)\rangle e^{-i\,\varphi}\right) : \rangle, \qquad (14)$$

or,

$$\Gamma_\varphi(t+\tau, t) =$$
$$\frac{1}{4}\times\{e^{2i\varphi}\langle E^{(+)}(t+\tau)E^{(+)}(t)\rangle + e^{-2i\varphi}\langle E^{(-)}(t+\tau)E^{(-)}(t)\rangle +$$
$$+\langle E^{(-)}(t+\tau)E^{(+)}(t)\rangle + \langle E^{(-)}(t)E^{(+)}(t+\tau)\rangle\}. \qquad (15)$$

In the strong field approximation and in the absence of the free field, the radiated field $E^{(+)}(t)$ can be substituted by $\mu S_{-}(t)$, where μ is a geometric factor. Since $E^{+} \sim a \sim S^{-}$; $E \sim a^{+} \sim S^{+}$, in this way, we obtain:

$$\Gamma_{\varphi}(t+\tau,t) = \frac{|\mu|^2}{4} \times \{e^{2i\varphi}(\langle S^{-}(t+\tau)S^{-}(t)\rangle - \langle S^{-}(t+\tau)\rangle\langle S^{-}(t)\rangle) + e^{-2i\varphi}(\langle S^{+}(t)S^{+}(t+\tau)\rangle - \langle S^{+}(t)\rangle\langle S^{+}(t+\tau)\rangle) + (\langle S^{+}(t+\tau)S^{-}(t)\rangle - \langle S^{+}(t+\tau)\rangle\langle S^{-}(t)\rangle) + (\langle S^{+}(t)S^{-}(t+\tau)\rangle - \langle S^{+}(t)\rangle\langle S^{-}(t+\tau)\rangle)\}. \quad (16)$$

Analytical expression for the spectrum of squeezing is computed according to (12)–(16) using the solutions of the equations of motion (8) [15]. Finally, we obtain

$$S_{\varphi}(\nu) = \frac{\gamma}{4} \times \{(\langle \tilde{R}_z^2\rangle_s - \langle \tilde{R}_z\rangle_s^2)[\sin^2 2\theta \cos^2 2\bar{\theta}\,(1+\cos 2\varphi)\chi_1(\nu) + \frac{1}{2}\sin^2 2\bar{\theta}\left(\cos^4\theta + \sin^4\theta + \frac{1}{2}\sin^2 2\theta\cos 2\varphi\right)\chi_2(\nu) + \frac{1}{2}\sin^2 2\theta \sin^2 2\bar{\theta}\,(1+\cos 2\varphi)\chi_3(\nu) + \sin^4\bar{\theta}\left(\cos^4\theta + \sin^4\theta - \langle \tilde{R}_z\rangle_s \cos 2\theta - \frac{1}{2}\sin^2 2\theta\cos 2\varphi\right)\chi_4(\nu) + \cos^4\bar{\theta}\left(\cos^4\theta + \sin^4\theta + \langle \tilde{R}_z\rangle_s \cos 2\theta - \frac{1}{2}\sin^2 2\theta\cos 2\varphi\right)\chi_5(\nu) + \frac{1}{2}\sin^2 2\theta \sin^2 2\bar{\theta}\sin 2\varphi\,\langle \tilde{R}_z\rangle_s\chi_6(\nu) + \frac{1}{2}\sin^2 2\theta \sin^4\bar{\theta}\sin 2\varphi\,\langle \tilde{R}_z\rangle_s\chi_7(\nu) + \frac{1}{2}\sin^2 2\theta\cos^4\bar{\theta}\sin 2\varphi\,\langle \tilde{R}_z\rangle_s\chi_8(\nu), \quad (17)$$

where

$\chi_1(\nu) = \frac{2\bar{\Gamma}_{\parallel}}{\bar{\Gamma}_{\parallel}^2+\nu^2}$, $\chi_2(\nu) = \frac{\bar{\Gamma}_s}{\bar{\Gamma}_s^2+(\nu-\omega)^2} + \frac{\bar{\Gamma}_s}{\bar{\Gamma}_s^2+(\nu+\omega)^2}$, $\chi_3(\nu) = \frac{\bar{\Gamma}_s}{\bar{\Gamma}_s^2+(\nu-2\bar{G}_R)^2} + \frac{\bar{\Gamma}_s}{\bar{\Gamma}_s^2+(\nu+2\bar{G}_R)^2}$, $\chi_4(\nu) = \frac{\bar{\Gamma}_s}{\bar{\Gamma}_s^2+(\nu-\omega+2\bar{G}_R)^2} + \frac{\bar{\Gamma}_s}{\bar{\Gamma}_s^2+(\nu+\omega-2\bar{G}_R)^2}$, $\chi_5(\nu) = \frac{\bar{\Gamma}_s}{\bar{\Gamma}_s^2+(\nu+\omega+2\bar{G}_R)^2} + \frac{\bar{\Gamma}_s}{\bar{\Gamma}_s^2+(\nu-\omega-2\bar{G}_R)^2}$, $\chi_6(\nu) = \frac{(\nu-2\bar{G}_R)}{\bar{\Gamma}_s^2+(\nu-2\bar{G}_R)^2} - \frac{(\nu+2\bar{G}_R)}{\bar{\Gamma}_s^2+(\nu+2\bar{G}_R)^2}$, $\chi_7(\nu) = \frac{(\nu-\omega+2\bar{G}_R)}{\bar{\Gamma}_s^2+(\nu-\omega+2\bar{G}_R)^2} - \frac{(\nu+\omega-2\bar{G}_R)}{\bar{\Gamma}_s^2+(\nu+\omega-2\bar{G}_R)^2}$, $\chi_8(\nu) = \frac{(\nu+\omega+2\bar{G}_R)}{\bar{\Gamma}_s^2+(\nu+\omega+2\bar{G}_R)^2} - \frac{(\nu-\omega-2\bar{G}_R)}{\bar{\Gamma}_s^2+(\nu-\omega-2\bar{G}_R)^2}$, $\langle \tilde{R}_z\rangle_s = \frac{\bar{\Gamma}_- - \bar{\Gamma}_+}{\bar{\Gamma}_- + \bar{\Gamma}_+}$.

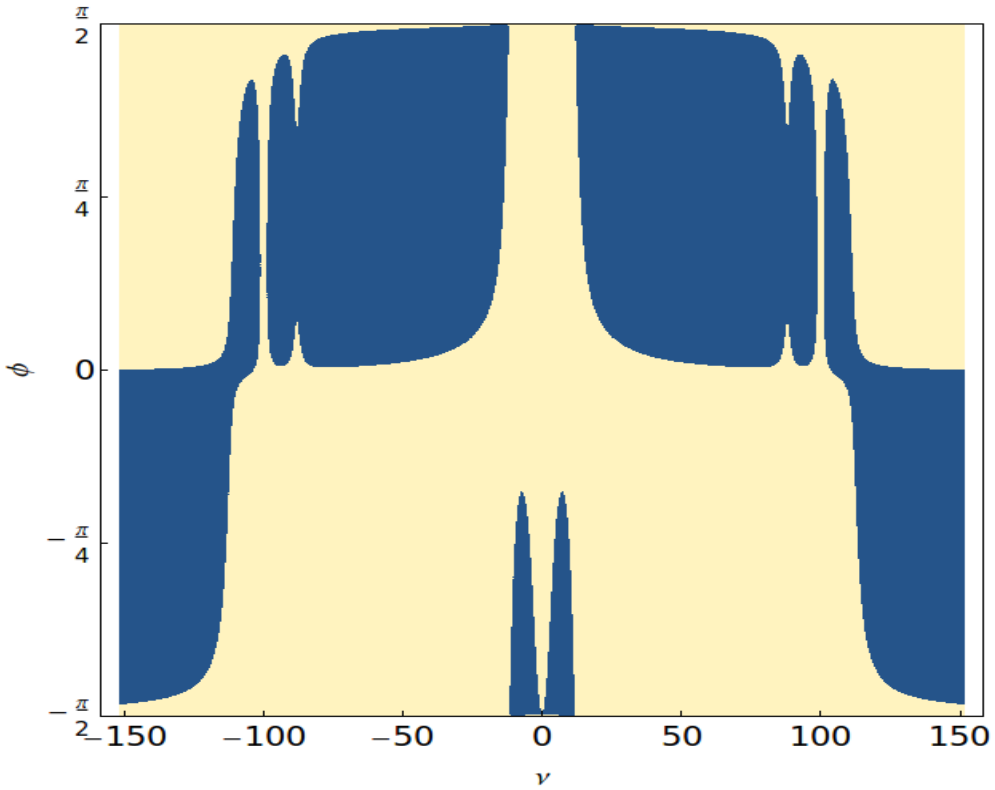

Fig. 2. Spectrum of squeezing in resonance fluorescence processes with permanent dipole systems. Parameters of interest are $\Omega/\gamma = 45$, $\omega/\gamma = 100$, $q = 0{,}7$.

In Fig. 2, we plot the squeezing spectrum for certain parameters of interest. Particularly, squeezing occurs for negative values (dark area in Fig. 2) and broader squeezing ranges take place because of permanent dipoles (see also [15]). Especially, squeezing around ν is due to permanent dipoles and will not be observed in the absence of it.

On the other hand, the total quantum fluctuation expression can be obtained after frequency integrating of (17), i.e.,

$$\langle{:}\left(\Delta E_{\varphi}\right)^{2}{:}\rangle = \pi\frac{d^{2}}{2\pi\gamma}\times$$
$$\left\{\left(\langle\tilde{R}_{z}^{2}\rangle_{s}-\langle\tilde{R}_{z}\rangle_{s}^{2}\right)[4\sin^{2}2\theta\cos^{2}2\bar{\theta}\cos^{2}\varphi+\right.$$
$$+\sin^{2}2\bar{\theta}\left(\cos^{4}\theta+\sin^{4}\theta+\frac{1}{2}\sin^{2}2\theta\cos 2\varphi\right)+\sin^{2}2\theta\sin^{2}2\bar{\theta}\,(1+\cos 2\varphi)+$$
$$+2\sin^{4}\bar{\theta}\left(\cos^{4}\theta+\sin^{4}\theta-\langle\tilde{R}_{z}\rangle_{s}\cos 2\theta-\frac{1}{2}\sin^{2}2\theta\cos 2\varphi\right)+$$
$$+2\cos^{4}\bar{\theta}\left(\cos^{4}\theta+\sin^{4}\theta+\langle\tilde{R}_{z}\rangle_{s}\cos 2\theta-\frac{1}{2}\sin^{2}2\theta\cos 2\varphi\right)+$$
$$+\sin^{2}2\theta\sin^{2}2\bar{\theta}\sin 2\varphi\,\langle\tilde{R}_{z}\rangle_{s}+\sin^{2}2\theta\sin^{4}\bar{\theta}\sin 2\varphi\,\langle\tilde{R}_{z}\rangle_{s}+$$
$$\left.+\sin^{2}2\theta\cos^{4}\bar{\theta}\sin 2\varphi\,\langle\tilde{R}_{z}\rangle_{s}.\right. \qquad (18)$$

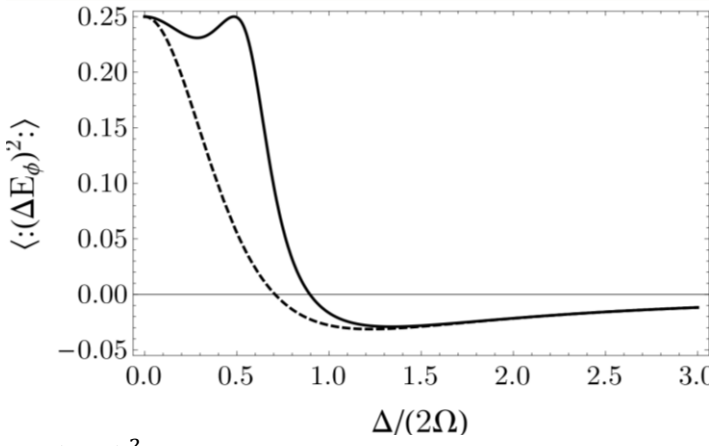

Fig. 3. The variance $\langle:\left(\Delta E_\phi\right)^2:\rangle$ in units of $|d|^2$ as a function of $\Delta/2\Omega$ for $G/\gamma = 0$ (dashed line) $G/\gamma = 16$ (solid line). Other parameters are $\varphi = -\frac{\pi}{4}$, $\omega/\gamma = 100$, $q = 0.7$, $\Omega/\gamma = 45$.

In Fig. 3, we depict variance $\langle:\left(\Delta E_\phi\right)^2:\rangle$ proceeding from the resonance fluorescence processes of laser-pumped two-level systems possessing permanent dipoles. We have found distinct quantum fluctuations features, which are due to permanent dipoles (compare the solid and dashed curves in Fig. 3, see also [16]).

5. Summary

We have studied the resonanse fluorescence spectrum of spontaenously emitted photons during the laser pumping processes of two-level molecules with permanent dipoles. Features differing from those in the case of similar processes yet in the absence of permanent dipoles have been found. In particular, additional spectral lines are emitted and extra squeezed frequency domains are observed.

Acknowledgements. We acknowledge the financial support of the Academy of Sciences of Moldova via grant no. 15.817.02.09F.

References

[1] D.F.Walls and P.Zoller, Phys. Rev. Lett. 47, 709 (1981).
[2] M.O.Scully and M.S.Zubairy, Quantum Optics, Cambridge University Press, Cambridge, UK, 1997.
[3] P. Michler, A. Kiraz, C. Becher, W. V. Schoenfeld, P. M. Petroff, Lidong Zhang, E. Hu, and A. Imamoğlu, Science, 290 (5500), 2282 (2000).
[4] N. Gisin, G. Ribordy, W. Tittel, and H. Zbinden, Rev. Mod. Phys. 74, 145 (2002).
[5] E. Knill, R. Laflamme, and G. J. Milburn, Nature 409, 46 (2001).
[6] A. J. Ramsay, Semicond. Sci. Technol. 25 (10), 103001 (2010).
[7] S. Haroche, Rev. Mod. Phys. 85, 1083 (2013).
[8] J. M. Gérard, B. Sermage, B. Gayral, B. Legrand, E. Costard, and V. Thierry-Mieg, Phys. Rev. Lett. 81 (5), 1110 (1998).

[9] K. Müller, A. Rundquist, K. A. Fischer, T. Sarmiento, K. G. Lagoudakis, Y. A. Kelaita, C. Sánchez, Muñoz, E. del Valle, F. P. Laussy, and J. Vučković, Phys. Rev. Lett. 114, 233601 (2015).
[10] M. Macovei, M. Mishra, and C. H. Keitel, Phys. Rev. A 92, 013846-1 (2015).
[11] F. Oster, C. Keitel, and M. Macovei, Phys. Rev. A 85, 063814-1 (2012).
[12] Q. V. Lawande and S. V. Lawande, Phys. Rev. A 38, 800 (1988).
[13] A. Mirzac, Proc. VI Sci. Conf. of Post-Graduate Students (with international participation) Tendinte Contemporane ale Dezvoltarii Stiintei: Viziuni ale Tinerilor Cercetatori, vol. I, pp. 79–84, Chisinau, 2017.
[14] M. A. Anton, S. Maede-Razavi, F.Carreno, I.Thanopulos, and E.Paspalakis, Phys.Rev. A 96, 063812-1 (2017).
[15] A. Mirzac, V. Ciornea, and M. A. Macovei, in Proc. 6th Int. Conf. on Telecommunications, Electronics, and Informatics, pp. 89–91, 2018.
[16] A. Mirzac, Proc. VI Sci. Conf. of Post-Graduate Students (with international participation) Tendinte Contemporane ale Dezvoltarii Stiintei: Viziuni ale Tinerilor Cercetatori, vol. I, pp. 59–64, Chisinau, 2018.

POLYNOMIAL INEQUALITIES FOR MULTIPARTITE QUANTUM SYSTEMS IN MIXED STATES

Yu. Palii[1,2]

[1]*Institute of Applied Physics, str. Academiei 5, Chisinau, MD-2028 Republic of Moldova*

[2]*Laboratory of Information Technologies, Joint Institute for Nuclear Research, Joliot-Curie 6, Dubna, 141980 Russia*

E-mail: palii@jinr.ru

(Received July 31, 2018)

Abstract

Entanglement in a multipartite quantum system represents non-local correlations between the system parts. This phenomenon is not affected by the action of a symmetry group, which acts separately on each part of the multipartite composite system. The space of the invariants of the action is a natural domain of the definition for all possible measures of the entanglement. Allowed values of the invariants are restricted by a set of inequalities, which is analyzed in this paper. The inequalities ensue from the semipositivity and Hermicity of the density matrix for the system as well as from the orbit space description in terms of the invariant theory.

1. Introduction

An extraordinary phenomenon—entanglement—is the cornerstone of the modern theory of quantum computing and quantum information [1, 2]. Basically, the term entanglement is understood as an exposition of diverse nonlocal correlations between parts of a composite multipartite quantum system, which have no classical analogue. From both theoretical and experimental points of view, the major problem consists in the definition of entanglement measures.

It is shown [3] that, from the mathematical point of view, characteristics of entanglement can be understood in terms of the classical theory of invariants [4, 5]. The key observation is that there exists a special group G consisting of the so-called *local unitary transformations* [3]. It means that G acts separately on every part of the multipartite composite system and does not affect the nonlocal correlations. For example, consider a binary quantum system composed of two subsystems of dimensions n_1 and n_2. The local unitary group $G = SU(n_1) \times SU(n_2)$ acts on density matrix ϱ adjointly,

$$(\mathrm{Ad}\, g)\varrho = g\, \varrho\, g^{-1}, \quad g \in G \subset SU(n_1 \times n_2).$$

Therefore, any characteristic of the entanglement is a function on the quotient space ϱ/G and, consequently, a function of G-invariant polynomials $p(\varrho)$ in the elements of the density matrix ϱ. Suppose that we know the integrity basis $\mathcal{P} = \{p_1, p_2, \ldots, p_q\}$ for the invariant ring[1]

[1] Basically, there are algebraic relations between the elements of the basis called syzigies.

$$\mathbb{R}[\varrho]^{\mathrm{G}}=\mathbb{R}[p_1, p_2, \dots, p_q], \tag{1.2}$$

which means that any G-invariant polynomial $P(\varrho)$ is a polynomial in p_k from the basis. So, the domain of definition of all possible entanglement measures is the image of the map from ϱ/G into a submanifold X in the real space $\mathbb{R}^q$, where p_k take their values.

In this paper, we present a complete set of polynomial inequalities defining the semi-algebraic structure of X and show that they stem from two sources:

(i) positive semi-definiteness and Hermicity of the density matrix ϱ,

(ii) positive semi-definiteness of the Gram matrix [6] of gradient vectors to level surfaces $p_k(\varrho) = const$ for each p_k from the integrity basis $\mathcal{P}$ for $\mathbb{R}[\varrho]^{\mathrm{G}}$ [7].

Their formulation is given in Sections 2 and 3, respectively. In Section 4, we illustrate them using the example of a two-qubit system described by a 5-parameter density matrix.

2. Inequalities from the Properties of Density Matrices

•Density matrices

Following the ideas of John von Neuman [8] and Lev Landau [9], a quantum system is described by the self-adjoint, positive semi-definite *density operator* acting in the Hilbert space of the system. Given a non-relativistic *n*–dimensional quantum system, Hilbert space $\mathcal{H}$ is the *n*–dimensional complex space $\mathbb{C}^n$ and the density operator can be identified with n×n Hermitian, unit trace, positive semi-definite matrix ϱ, which is referred to as the *density matrix*.

Constraints to the density operator due to semi-positive definiteness have been imposed in the sixtieth of the last century in studying the production and decay of resonant states in strong interaction processes [10]. Nowadays, the quantum computing and the theory of quantum information reveal a new role of these constraints; recently, they have been derived once again [11, 12][2].

To formulate the semi-definiteness property, let us choose the Bloch representation of a density matrix [15] for *n*-level quantum system:

$$\varrho = \frac{1}{n}\left(\mathbb{I}_n + \sqrt{\frac{n(n-1)}{2}}\sum_{i=1}^{n^2-1}\xi_i\,\lambda_i\right) \tag{2.1}$$

where (n^2-1) is the dimensional Bloch vector $\xi \in \mathbb{R}^{(n^2-1)}$ is contracted with elements $\lambda_i, i = 1, \dots, (n^2-1)$ of the Hermitian basis of $\mathfrak{su}(n)$ Lie algebra.

•Positivity of density matrices

A necessary and sufficient condition for the Hermitian matrix to be positive is that coefficients S_k of the characteristic equation

$$|\mathbb{I}_n x - \varrho| = x^n - S_1 x^{n-1} + S_2 x^{n-2} - \dots + (-1)^n S_n = 0 \tag{2.2}$$

should be non-negative [10]:

$$\varrho \geq 0 \quad \Leftrightarrow \quad S_k \geq 0 \quad k = 1, \dots, n \tag{2.3}$$

[2] In our publication [13] the positivity conditions for density operators was analyzed in the context of their consequences for integrity basis of SU(2)⊗SU(2) polynomial invariants ring as well as for entanglement characteristics of mixed qubit states [14].

This statement is based on the Descartes theorem [16] about the number of positive roots of a polynomial equation. The expressions for coefficients S_k in terms of the traces

$$t_k = tr(\varrho^k) \tag{2.4}$$

are given by the determinants

$$S_k = \frac{1}{k!}\begin{vmatrix} t_1 & 1 & 0 & 0 & \cdots & 0 \\ t_2 & t_1 & 2 & 0 & \cdots & 0 \\ t_3 & t_2 & t_1 & 3 & \cdots & 0 \\ \vdots & \vdots & \vdots & \vdots & \cdots & \vdots \\ t_{k-1} & t_{k-2} & t_{k-3} & t_{k-4} & \ddots & k-1 \\ t_k & t_{k-1} & t_{k-2} & t_{k-3} & \cdots & t_1 \end{vmatrix} \tag{2.5}$$

In addition, from restrictions (2.3), there are upper bounds on S_k due to the normalization condition $\mathrm{tr}(\varrho) = 1$, $\mathrm{tr}(\varrho^k) \leq 1$ for $k \geq 2$. Note that the equality fulfils for pure states and the maximal values of S_k are achieved for the equal eigenvalues of density matrices.

Finally, the positive semi-definiteness and normalizability conditions for density matrices of *n*-level system can be written as the following set of inequalities

$$0 \leq \frac{k! n^{k-1} S_k}{(n-1)(n-2)\cdots(n-k+1)} \leq 1, \quad k = 2, \cdots, n. \tag{2.6}$$

•Hermicity of density matrices

Since matrix ϱ is Hermitian, all its eigenvalues are real numbers. However, conditions (2.3) for coefficients S_k do not explicitly recognize that the characteristic equation (2.2) should not have any complex roots . For the case of all distinct roots, the necessary and sufficient condition providing reality of the roots λ_i is the positivity of the discriminant

$$\mathrm{Discr} = \prod_{i<j} (\lambda_i - \lambda_j)^2$$

which is considered as a function of traces (2.4)

$$\mathrm{Discr} = \begin{vmatrix} \mathrm{d} & \mathrm{t}_1 & \mathrm{t}_2 & \cdots & \mathrm{t}_{n-1} \\ \mathrm{t}_1 & \mathrm{t}_2 & \mathrm{t}_3 & \cdots & \mathrm{t}_{n-2} \\ \mathrm{t}_2 & \mathrm{t}_3 & \mathrm{t}_4 & \cdots & \mathrm{t}_{n+1} \\ \vdots & \vdots & \vdots & \ddots & \vdots \\ \mathrm{t}_{n-1} & \mathrm{t}_{n-2} & \mathrm{t}_{n+1} & \cdots & \mathrm{t}_{2n-2} \end{vmatrix} \geq 0. \tag{2.7}$$

To take into account the case of the multiple roots, we should demand the positivity of all principal minors of Discr. Dependence of the discriminant on the trace invariants up to order 2*n*-2 as pointed in the left side of (2.7) assumes that all the higher trace invariants t_k with *k*>*n* are expressed via polynomials in $t_1, t_2, \ldots, t_n$ using the Cayley-Hamilton theorem.

The summary of this section is as follows. The set of inequalities originating from Hermicity (2.7) and semi-positivity (2.6) requirements on density matrices can be formulated in terms of traces t_k. Note that t_k are the invariants of the group SU(n) acting globally on the entire system.

3. Inequalities from the Invariant Theory

The inequalities stemming from the invariant theory should be formulated in terms of the invariants relative to the group G⊂SU(n) of local unitary transformations. Again, consider a binary quantum system composed from two subsystems of dimensions n_1 and n_2 with local group G = SU(n_1)×SU(n_2), $n_1 \times n_2 = n$. The adjoint action (1.1) of the local group can be linearized [17] if we represent density matrix ϱ as vector $\vec{\varrho}$ in the real space $\mathbb{R}^{(n^2-1)}$ and consider the linear transformation

$$\vec{\varrho} \to \overrightarrow{\varrho'} = L\vec{\varrho}$$

with the linear operator $L \in G \otimes \bar{G}$, where the overlined $\bar{G}$ denotes the complex conjugate of G. The property being linear of the adjoint action makes possible application of the invariant theory and, in particular, application of algorithmic methods for construction of the integrity basis. The local invariant ring $\mathbb{R}[\varrho]^G$ has a much more complicated structure than the invariant ring $\mathbb{R}[\varrho]^{SU(n)}$. A complete description of it has been given up to now only for the simplest case G = SU(2)×SU(2) [18]. Note that traces t_k (2.4), being invariants of group SU(*n*), are polynomials in terms of G-invariants. Consequently, conditions (2.6) and (2.7) restrict the possible values of G-invariants.

Let us discuss additional inequalities that follow from the invariant theory. Let *K* be a compact Lie group acting on a *n*-dimensional linear space *V*. Assume that

$$\mathcal{P} = \{p_1, p_2, \dots, p_q\}, \tag{3.1}$$

is a set of real homogeneous polynomials that forms the integrity basis invariant ring

$$\mathbb{R}[x_1, x_2, \dots, x_n]^K = \mathbb{R}[p_1, p_2, \dots, p_q], \tag{3.2}$$

The elements of $\mathcal{P}$ define the polynomial mapping:

$$\text{P: } V \to \mathbb{R}^q, \qquad (x_1, x_2, \dots, x_n) \longrightarrow (p_1, p_2, \dots, p_q). \tag{3.3}$$

Since the integrity basis elements p_k are constants along the orbits of *K*, the P map induces a homeomorphism of the orbit space *V*/G and its image *X*, i.e., *V*/G ≃ X [7]. Generally speaking, there are polynomial relations $h(p_1, p_2, \dots, p_q)$ between p_k forming the syzygy ideal $I_{\mathcal{P}}$ of $\mathcal{P}$ (3.1):

$$I_{\mathcal{P}}(p_1, p_2, \dots, p_q) = \{h \in \mathbb{R}[p_1, p_2, \dots, p_q] : \ h(p_1, p_2, \dots, p_q) = 0 \ \text{ in } \mathbb{R}[x_1, x_2, \dots, x_n]\}. \tag{3.4}$$

This means that all $h(p_1, p_2, \dots, p_q)$ are identically zero when $p_k$are considered as functions of coordinates $x_1, x_2, \dots, x_n$ in *V*. The syzygies define a submanifold $Z \subset \mathbb{R}^q$ consisting of the locus of common zeros of all elements in $I_{\mathcal{P}}$. Finally, we should introduce a symmetric q×q-matrix Grad whose elements are the inner products of the gradients $\text{grad}(p_i)$ to the level surfaces $p_i = const_i$ in *V*:

$$\text{Grad}_{ij} = (\text{grad}(p_i), \text{grad}(p_j)\,). \tag{3.4}$$

The elements of the Grad-matrix can be written as polynomials on generators p_i of the integrity basis [7].

A theorem due to Procesi and Schwarz [19] states that image X of orbit space V/K is a subset of Z and is defined by the set of inequalities expressing semipositivity of the matrix Grad:

$$\text{Grad} \geq 0. \tag{3.5}$$

The rigorous proof of the theorem is rather involved; however, the key point is quite simple. Gradients $\text{grad}(p_i)$ form the basis of the normal space to tangent space $T\mathcal{O}$ of the K-orbit $\mathcal{O}$. They should be linearly independent in order the normal space has right dimension[3] equal to the difference $dim\, V - dim\, \mathcal{O}$. Note that this difference is just the number of algebraically independent invariants among the integrity basis elements. Since matrix Grad is the Gram matrix for the set of the vectors $\text{grad}(p_i)$, its positivity ensure us that these vectors are linearly independent according to the well-known theorem of linear algebra (see, for example, [6] chapter IX, §3).

The Grad-matrix can be represented as a product $Grad = J \cdot J^T$ where $J = (\partial p_i/\partial x_j)$ is the Jacobian of polynomial map P. It is shown [19] that J generalizes Vandermonde matrix Δ for the roots of a polynomial equation. Therefore, if we consider the ring of SU(n) invariants of density matrix ϱ, then the Grad-matrix is similar to the discriminant $\text{Discr} = \Delta \cdot \Delta^{\text{T}}$, as shown by explicit calculations in [20].

4. Illustrative Example

4.1 Invariant Ring of a Two-Qubit System

We consider a composite system which consists of two qubits; that is, each subsystem has two quantum levels. It is useful to represent the density matrix of the system in the so-called Fano form:

$$\varrho = \frac{1}{4}\left(\mathbb{I}_2 \otimes \mathbb{I}_2 + \sum_{i=1}^{3} a_i\, \sigma_i \otimes \mathbb{I}_2 + \sum_{i=1}^{3} b_i\, \mathbb{I}_2 \otimes \sigma_i + \sum_{i,j=1}^{3} c_{ij}\, \sigma_i \otimes \sigma_j\right) \tag{4.1}$$

where 3-component vectors $\vec{a} = (a_1, a_2, a_3)$ and $\vec{b} = (b_1, b_2, b_3)$ are Bloch vectors of constituent qubits, $\sigma_i, i = 1,2,3$, are the Pauli matrices making up the basis of the Lie algebra $\mathfrak{su}(2)$:

$$\sigma_1 = \begin{pmatrix} 0 & 1 \\ 1 & 0 \end{pmatrix},\ \sigma_2 = \begin{pmatrix} 0 & -i \\ i & 0 \end{pmatrix},\ \sigma_3 = \begin{pmatrix} 1 & 0 \\ 0 & -1 \end{pmatrix} \tag{4.2}$$

Information about the correlations between qubits is encoded in the matrix $C = (c_{ij}), i, j = 1,2,3$.

The G group of the local unitary transformations for this system is the tensor product $SU(2) \otimes SU(2) \subset SU(4)$ and acts in the following way:

$$\varrho \mapsto (SU(2) \otimes SU(2)) \cdot \varrho \cdot (SU(2) \otimes SU(2))^{\dagger},$$

where the dagger states for the Hermitian conjugate.

The local invariant ring $\mathbb{R}[\varrho]^G$ consists of real homogeneous polynomials in fifteen variables a_i, b_j, c_{ij}. The homogeneity holds separately for each set of variables a_i, b_j, c_{ij} and every invariant can be labeled by degrees of variables from this three sets. So, an invariant

[3] Here, we consider only the special case of the regular orbits of the adjoint action.

$C_{(s\,t\,q)}$ is a sum of monomials containing s variables a_i, t variables b_j, and q variables c_{ij}. The number of algebraically independent invariants is as follows:

$$15 - 2\dim SU(2) = 9.$$

The integrity basis of the ring $\mathbb{R}[\varrho]^G$ contains 15 additional invariants required for the Hironaka representation of $\mathbb{R}[\varrho]^G$ [18]. Below, we list the invariants of lowest orders relevant for our simple example given in the following subsections. The completely antisymmetric symbol ϵ_{ijk} represents the structure constant tensor of $SU(2)$ group. We use the Einstein index summation convention.

Degree Invariants

2 $C_{200} = a_i\, a_i, \quad C_{020} = b_j\, b_j, \quad C_{002} = c_{ij}\, c_{ij}$

3 $C_{111} = a_i\, b_j\, c_{ij}, \quad C_{003} = \frac{1}{3}\epsilon_{ijk}\epsilon_{pqr}\, c_{ip}\, c_{jq} c_{kr}$

4 $C_{202} = a_i\, a_j\, c_{ip}\, c_{jp} \quad C_{022} = b_i\, b_j\, c_{pi}\, c_{pj} \quad C_{004} = c_{ip}\, c_{iq} c_{jp}\, c_{jq}$

$C_{112} = \frac{1}{2}\epsilon_{ijk}\epsilon_{pqr}\, a_i\, b_p\, c_{jq}\, c_{kr}$

5 $C_{113} = a_i\, b_p\, c_{ij}\, c_{kj}\, c_{kp}$

6 $C_{204} = a_i\, a_p\, c_{ij}\, c_{kj}\, c_{kq}\, c_{pq} \quad C_{024} = b_i\, b_p\, c_{ji}\, c_{jk}\, c_{qk}\, c_{qp}$

4.2 5-Parameter Subset of Density Matrices

Let us denote five Fano parameters

$$a_3 = \alpha, \quad b_3 = \beta, \quad c_{11} = \gamma_1, \quad c_{22} = \gamma_2, \quad c_{33} = \gamma_3,$$

and equate all others to zero. We get the following density matrix

$$\varrho = \frac{1}{4}\begin{pmatrix} 1+\alpha+\beta+\gamma_3 & 0 & 0 & \gamma_1-\gamma_2 \\ 0 & 1+\alpha+\beta+\gamma_3 & \gamma_1+\gamma_2 & 0 \\ 0 & \gamma_1+\gamma_2 & 1+\alpha+\beta+\gamma_3 & 0 \\ \gamma_1-\gamma_2 & 0 & 0 & 1+\alpha+\beta+\gamma_3 \end{pmatrix} \tag{4.3}$$

which belongs to the class of the so-called X-states because nonzero elements are placed only on the diagonals. The invariant ring for these states is studied in [21]. There are only 12 non-zero local invariants in this case:

Degree Invariants

2 $C_{200} = \alpha^2, \quad C_{020} = \beta^2, \quad C_{002} = \gamma_1^2 + \gamma_2^2 + \gamma_3^2$

3 $C_{111} = \alpha\,\beta\,\gamma_3, \quad C_{003} = \gamma_1\,\gamma_2\,\gamma_3$

4 $C_{202} = \alpha^2\,\gamma_3^2 \quad C_{022} = \beta^2\,\gamma_3^2 \quad C_{004} = \gamma_1^4 + \gamma_2^4 + \gamma_3^4 \quad C_{112} = \alpha\,\beta\,\gamma_1\,\gamma_2$

5 $C_{113} = \alpha\,\beta\,\gamma_3^3$

6 $C_{204} = \alpha^2\,\gamma_3^4 \quad C_{024} = \beta^2\,\gamma_3^4$

There are only five algebraically independent invariants among them. We choose the lowest order invariants

$$C_{200}, C_{020}, C_{002}, C_{111}, C_{003}$$

and introduce special notations for the following combinations of them to simplify the representation of the inequalities in terms of these invariants:

$$C_2 \coloneqq C_{200} + C_{020} + C_{002}, \quad C_3 \coloneqq C_{111} - C_{003}, \quad D \coloneqq \frac{C_{200}\, C_{020}}{{C_{111}}^2}\,.$$

The complete set of the inequalities is as follows:

- Semipositivity of density matrix ϱ:

$$0 \le C_2 \le 3, \quad 0 \le C_2 - 2C_3 \le 1\,, \tag{4.4}$$

$$0 \le D^2((1-C_2)^2 + 8C_3) - 4(C_2 D + {C_3}^2 D^3 - 1) \le 1\ . \tag{4.5}$$

- Semipositivity of discriminant Disc:

$$0 \le C_2(C_2 D - 1) + {C_3}^2 D^2 (C_2 D - 9)\ , \tag{4.6}$$

$$0 \le (C_2 D - 1)^2 - 4{C_3}^2 D^3. \tag{4.7}$$

- Semipositivity of matrix Grad:

$$0 \le (C_{002} D - 1)^2 - 4{C_{003}}^2 D^3\ . \tag{4.8}$$

To visualize the solution of these inequalities, let us fix the values of the invariants $C_{111} = 1/2$, $C_{003} = 1/128$. The solution domain in the plane $C_{200} = C_{020}$ is presented in Fig. 1. The possible values of the invariants lie in the red domain near the vertex B of the curvilinear triangle ABC. The blue A–B and B–C lines are defined from (4.5) when the middle expression is equal to zero. Analogously, the green A–C line is defined from (4.7). The purple line separates the domain where the Grad matrix is positive (right upper part of the plane) from one where the Grad matrix is negative.

4.3 Peres-Horodecki Separability Criterion

If we transpose the second factors in the tensor products in the definition of density matrix ϱ (4.1), we get so-called partially transposed density matrix ϱ^{T_b} [22]. For our example (4.3), it reads as follows:

$$\varrho^{\mathrm{T}_b} = \frac{1}{4}\begin{pmatrix} 1+\alpha+\beta+\gamma_3 & 0 & 0 & \gamma_1+\gamma_2 \\ 0 & 1+\alpha+\beta+\gamma_3 & \gamma_1-\gamma_2 & 0 \\ 0 & \gamma_1-\gamma_2 & 1+\alpha+\beta+\gamma_3 & 0 \\ \gamma_1+\gamma_2 & 0 & 0 & 1+\alpha+\beta+\gamma_3 \end{pmatrix}$$

Using ϱ^{T_b} and the derived system of the inequalities (4.4)–(4.8), we can formulate the separability criterion for two-qubit systems due to Peres–Horodecki [23, 24]:

The two-qubit the system is in a separable state if and only if the partially transposed density matrix ϱ^{T_b} satisfies the conditions for the density matrix.

The semipositivity domain for ϱ^{T_b} is defined by inequalities (4.4)–(4.8) up to a minor correction: the sign of $C_{003} = \gamma_1\,\gamma_2\,\gamma_3$ changes, because ϱ^{T_b} differs from ϱ only in the sign of γ_2. The separability area (red domain) is shown in Fig. 2, where the A'B'C' curvilinear triangle corresponds to ϱ^{T_b}. Let us note that invariant C_{003} is nothing than the determinant of correlation

matrix C in the Fano form (4.1) of ϱ. If C_{003} is zero, then correlation matrix C vanishes, while the ABC and A'B'C' triangles coincide. This means that all states are separable. With an increase in C_{003} , the correlations in the system become stronger and the separability area shrinks to zero.

5. Conclusions

The orbit space ϱ/G of the local group action on an entangled system is an appropriate space for the definition of the entanglement measures. In a general case, ϱ/G has a lower dimension than the state space of the system described by density matrix ϱ. The semi-algebraic structure of the orbit space is completely determined by two kinds of inequalities in the elements of the integrity basis for the invariant ring $\mathbb{R}[\varrho]^G$. The first kind originates from the Hermicity and semi-positivity requirements on density matrices, while the second one follows from the orbit space description in the invariant theory. The Peres–Horodecki separability criterion for the two-qubit mixed states is consider as an example of application of the inequalities.

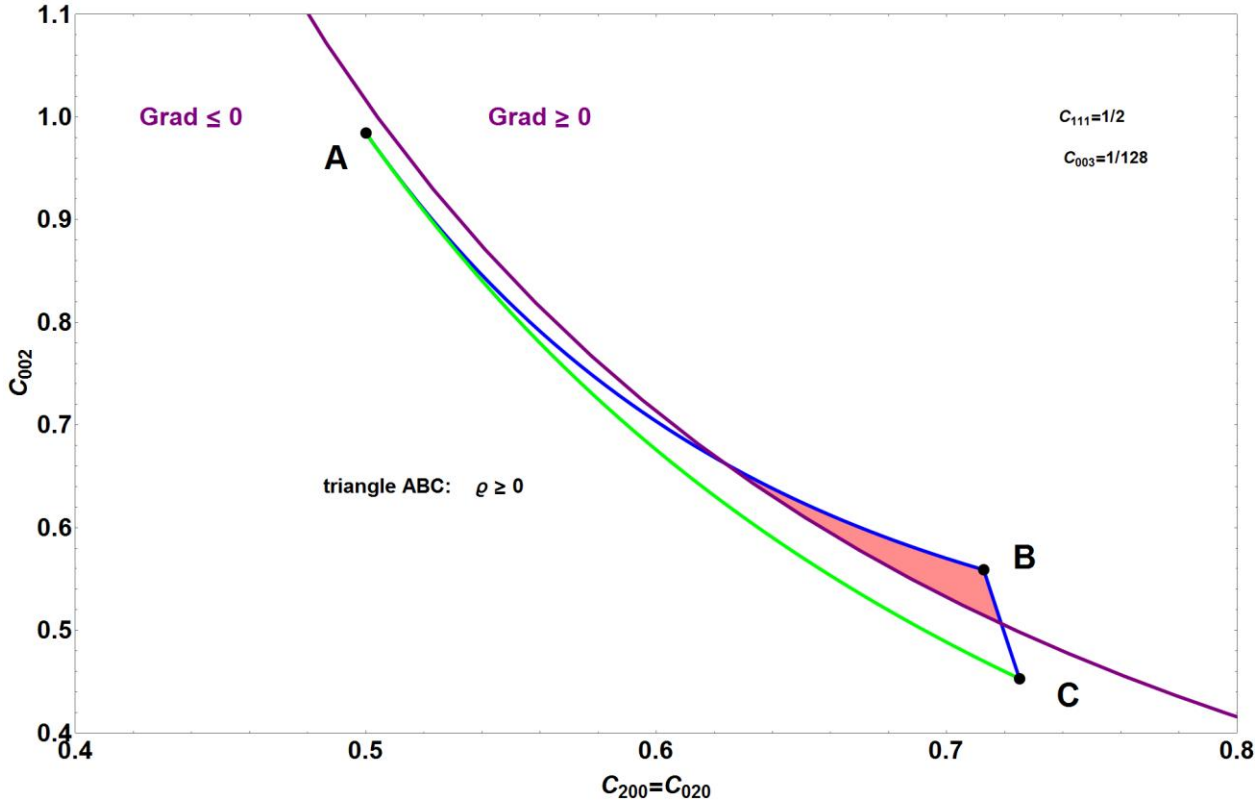

Fig. 1. Solution of Inequalities.

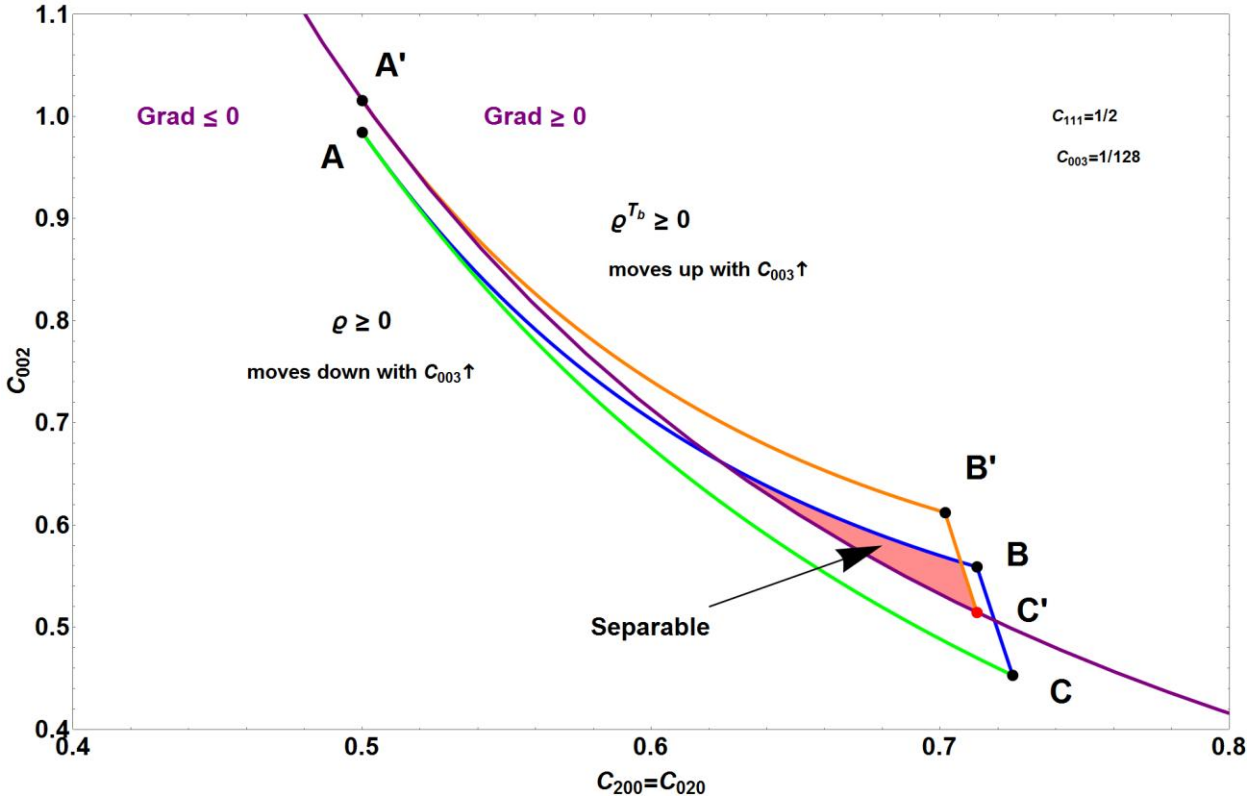

Fig. 2. Separability area.

References

[1] M.A. Nielsen and I.L. Chuang, Quantum Computation and Quantum Information, Cambridge University Press, Cambridge, 2000.
[2] V. Vedral, Introduction to Quantum Information Science, Oxford University Press, New York, 2006.
[3] N. Linden and S. Popescu, Fortschr. Phys. 46, 567 (1998).
[4] H. Weyl, The Classical Groups: Their Invariants and Representations, Princeton University Press, Princeton, 1939.
[5] V.L. Popov and E.B. Vinberg, Invariant theory in Algebraic Geometry IV, Encycl. Math. Sci., Springer-Verlag, 1994, vol. 55, p. 123.
[6] F.G. Gantmacher, The Theory of Matrices, American Mathematical Society, 2000.
[7] M. Abud and G. Sartori, Phys. Lett. B 104, 147 (1981)
[8] J. von Neumann, Nachr. Ges. Wiss. Gött., Math.–Phys. Kl. 1927, 245 (1927).
[9] L.D. Landau, Zeitschrift Phys. 45, 430 (1927).
[10] S.M. Deen, P.K. Kabir, and G. Karl, Phys. Rev. D 4, 1662 (1971).
[11] G. Kimura, Phys. Lett. A 314, 339 (2003).
[12] M. S. Byrd and N. Khaneja, Phys. Rev. A 68, 062322 (2003).
[13] V. Gerdt, A. Khvedelidze, and Yu. Palii, J. Math. Sci. 168, 368 (2010).
[14] V. Gerdt, A. Khvedelidze, and Yu. Palii, Phys. Atom. Nucl. 74 (6), 893 (2011).

[15] F.T. Hioe and J.H. Eberly, Phys. Rev. Lett. 47, 838 (1981).
[16] A.G. Kurosh, Course of Higher Algebra. 5th ed., Gos. Izdat., Moscow, 1956.
[17] M. Grassl, M. Rötteler, and T. Beth, Phys. Rev. A 58, 1833 (1998).
[18] R.C. King, T.A. Welsh and P. D. Jarvis, J. Phys. A: Math. Theor. 40, 10083 (2007).
[19] C. Procesi and G. Schwarz, Invent. Math., 81, 539 (1985).
[20] V. Gerdt, A. Khvedelidze, and Yu. Palii, J. Math. Sci., 200(6), 682 (2014).
[21] V. Gerdt, A. Khvedelidze, and Yu. Palii, J. Math. Sci., 224(2), 228 (2017).
[22] I. Bengtsson and K. Życzkowski, Geometry of Quantum States: An Introduction to Quantum Entanglement, 2nd ed., Cambridge University Press, Cambridge, 2017.
[23] A. Peres, Phys. Rev. Lett. 77, 1433 (1996).
[24] M.Horodecki, P. Horodecki, and R. Horodecki, Phys. Lett. A 223, 1 (1996).

CONTENTS